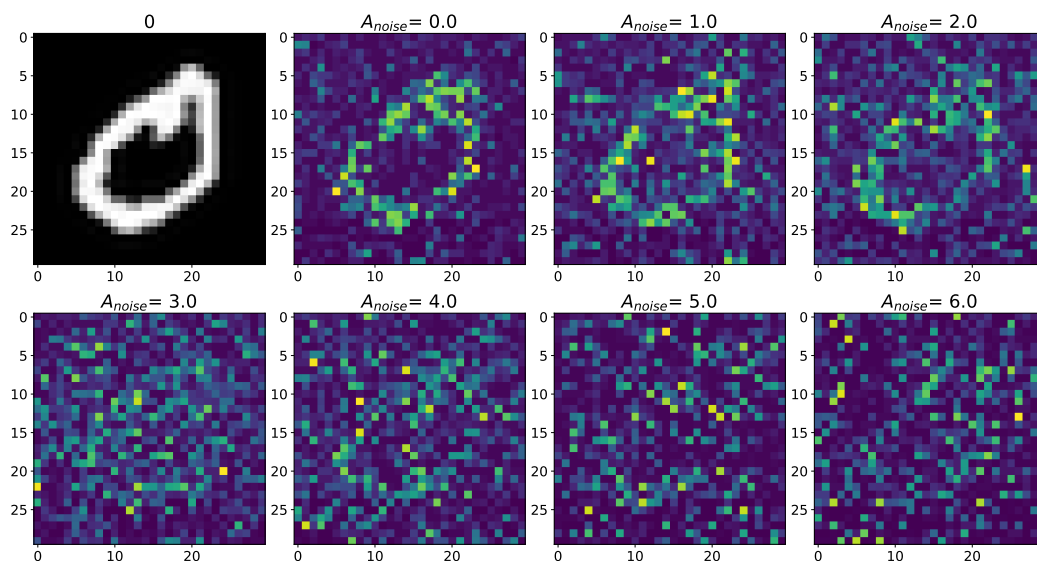


# Supplementary Materials: Dynamic Image Representation in a Spiking Neural Network Supplied by Astrocytes

Sergey V. Stasenko \*  and Victor B. Kazantsev 

## S1. Cases with numbers from database MNIST

### S1.1. Number 0 from database MNIST



**Figure S1.** Changes in the spatial sweep of the spike neural network during the representation of the supplied image 0 from handwritten database MNIST [1] when the amplitude,  $A_{noise}$ , of the noise current,  $I_{noise}$ , changes from 0 to 6 without modulation of neuronal activity by astrocytes.

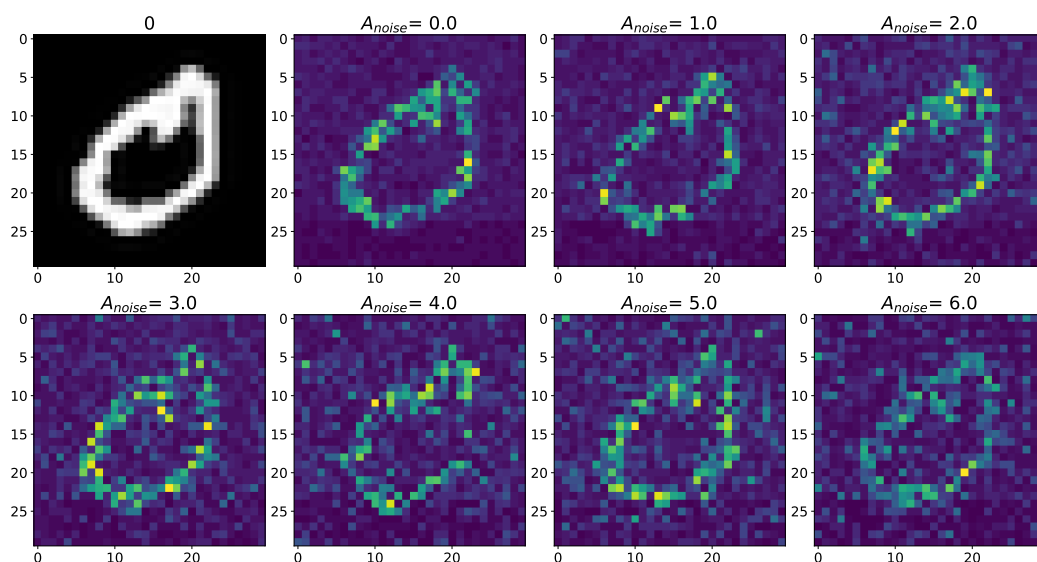


**Figure S2.** Changes in the spatial sweep of the spike neural network during the representation of the supplied image 0 from handwritten database MNIST [1] when the amplitude,  $A_{noise}$ , of the noise current,  $I_{noise}$ , changes from 0 to 6 with modulation of neuronal activity by astrocytes.

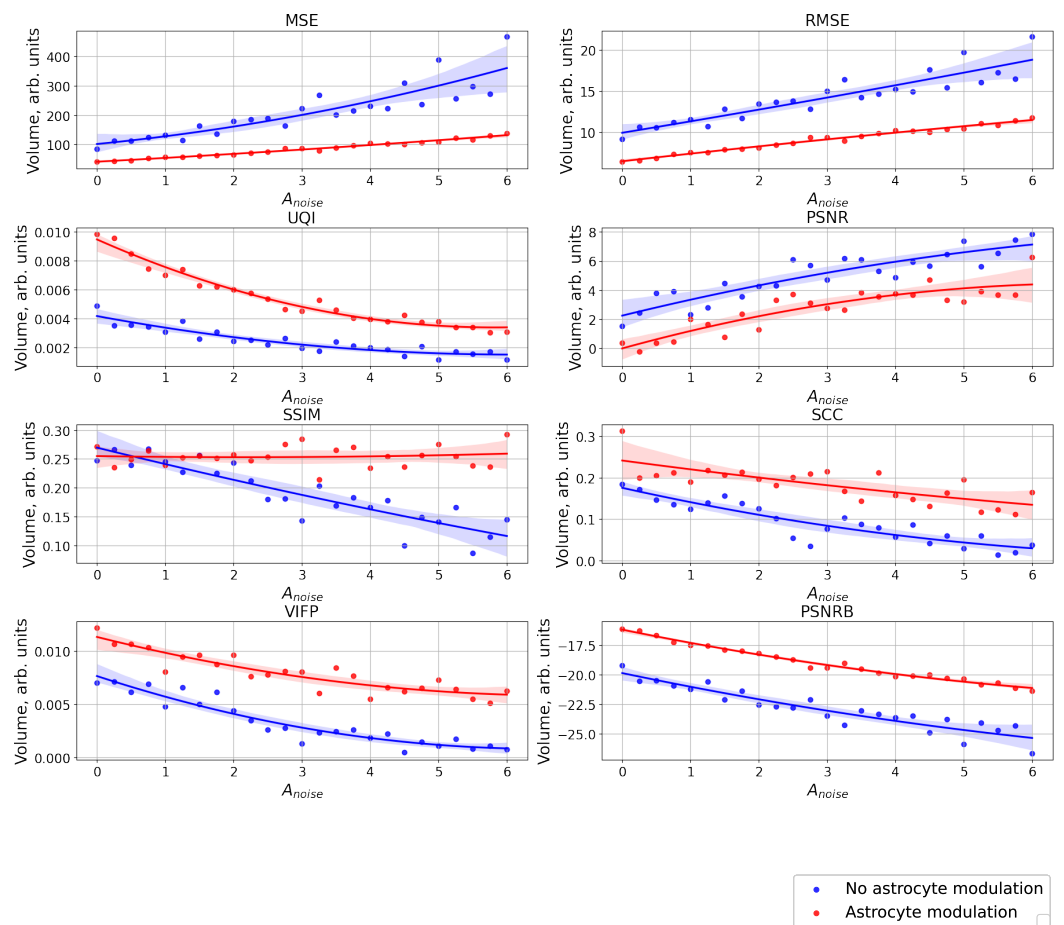


**Figure S3.** The case of using a quality metrics (MSE, RMSE, UQI, PSNR, SSIM, SCC, VIFP, PSNRB) for comparing raster diagrams of neural activity from Figure S1 and Figure S2 with an image 0 from handwritten database MNIST [1] fed to a spike neural network with an increase in the amplitude,  $A_{noise}$ , of the noise signal from 0 to 6 supplied to the neurons of the neural network without astrocytic modulation (blue dots and curve) and with astrocytic modulation (red dots and curve).

S1.2. Number 1 from database MNIST

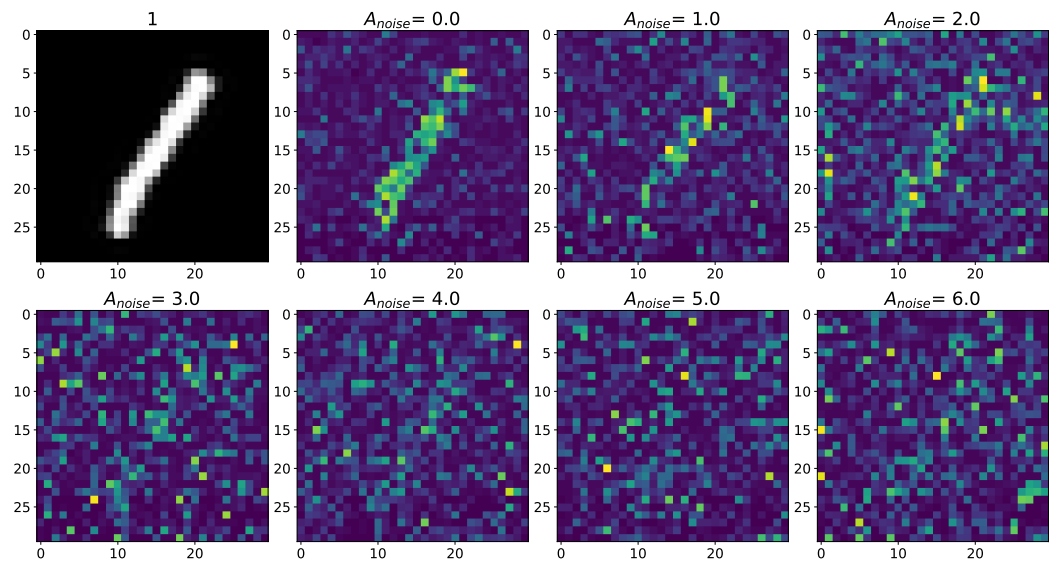


**Figure S4.** Changes in the spatial sweep of the spike neural network during the representation of the supplied image 1 from handwritten database MNIST [1] when the amplitude,  $A_{noise}$ , of the noise current,  $I_{noise}$ , changes from 0 to 6 without modulation of neuronal activity by astrocytes.

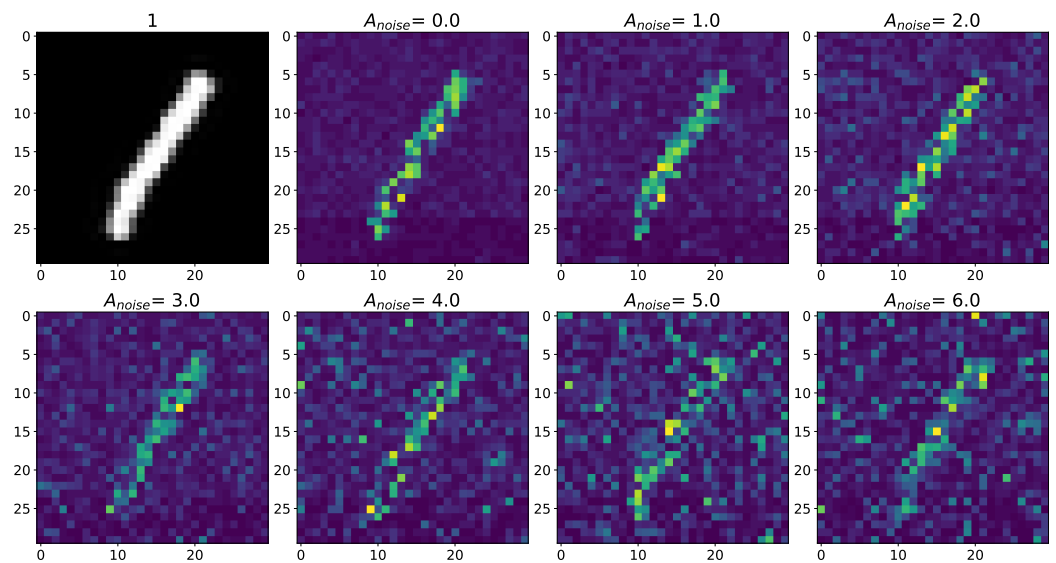


**Figure S5.** Changes in the spatial sweep of the spike neural network during the representation of the supplied image 1 from handwritten database MNIST [1] when the amplitude,  $A_{noise}$ , of the noise current,  $I_{noise}$ , changes from 0 to 6 with modulation of neuronal activity by astrocytes.

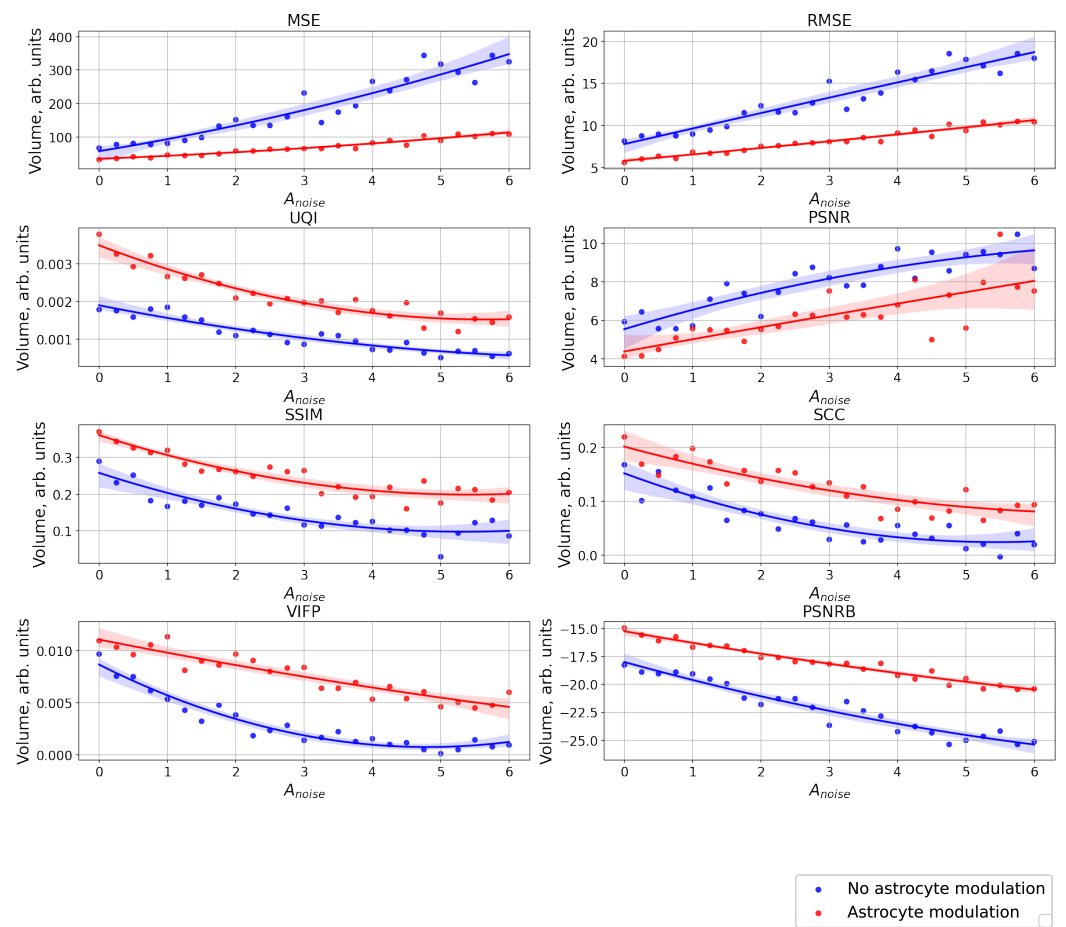


**Figure S6.** The case of using a quality metrics (MSE, RMSE, UQI, PSNR, SSIM, SCC, VIFP, PSNRB) for comparing raster diagrams of neural activity from Figure S4 and Figure S5 with an image 1 from handwritten database MNIST [1] fed to a spike neural network with an increase in the amplitude,  $A_{noise}$ , of the noise signal from 0 to 6 supplied to the neurons of the neural network without astrocytic modulation (blue dots and curve) and with astrocytic modulation (red dots and curve).

S1.3. Number 2 from database MNIST

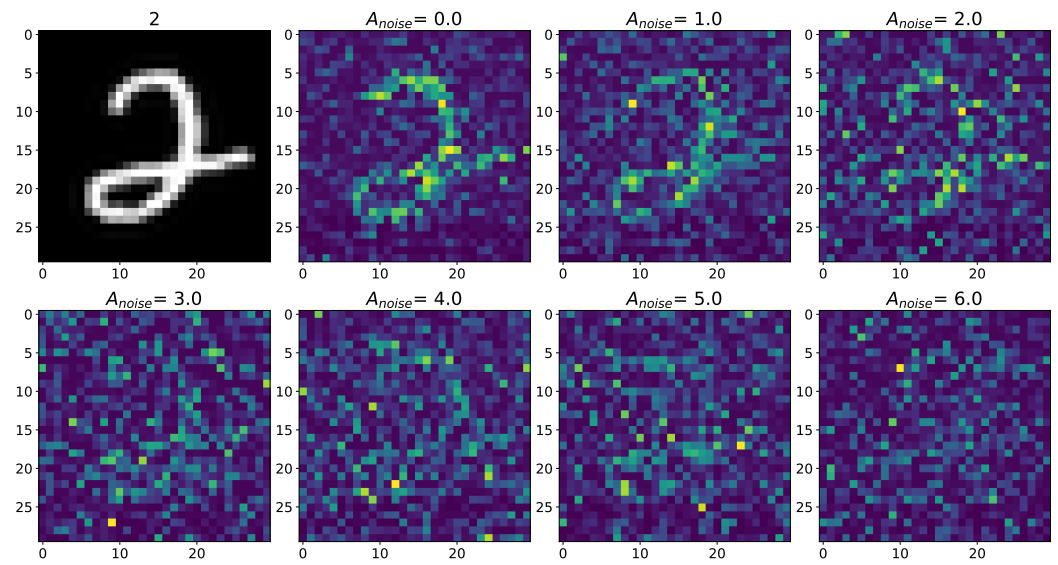


**Figure S7.** Changes in the spatial sweep of the spike neural network during the representation of the supplied image 2 from handwritten database MNIST [1] when the amplitude,  $A_{noise}$ , of the noise current,  $I_{noise}$ , changes from 0 to 6 without modulation of neuronal activity by astrocytes.

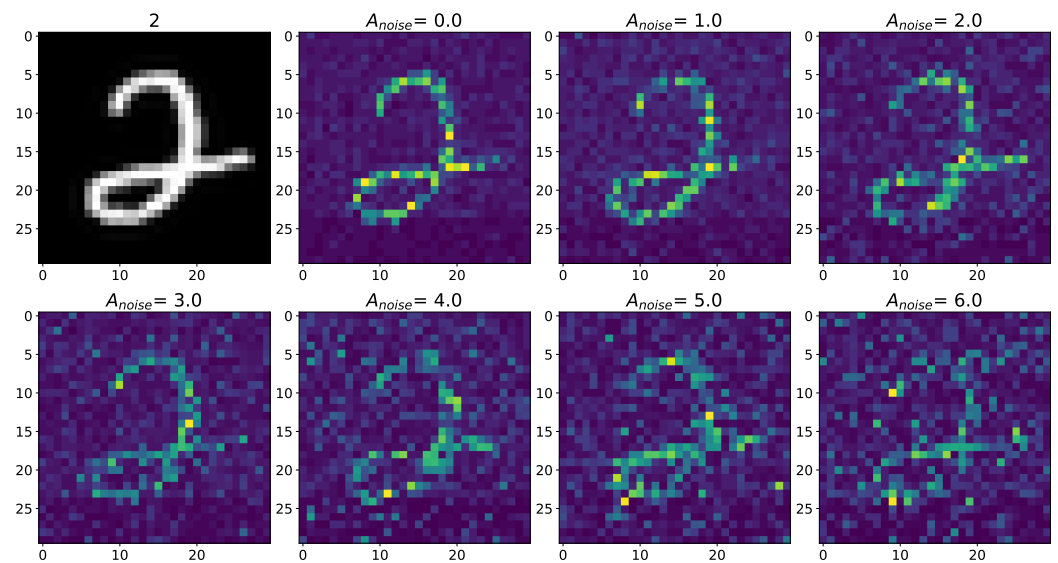


**Figure S8.** Changes in the spatial sweep of the spike neural network during the representation of the supplied image 2 from handwritten database MNIST [1] when the amplitude,  $A_{noise}$ , of the noise current,  $I_{noise}$ , changes from 0 to 6 with modulation of neuronal activity by astrocytes.

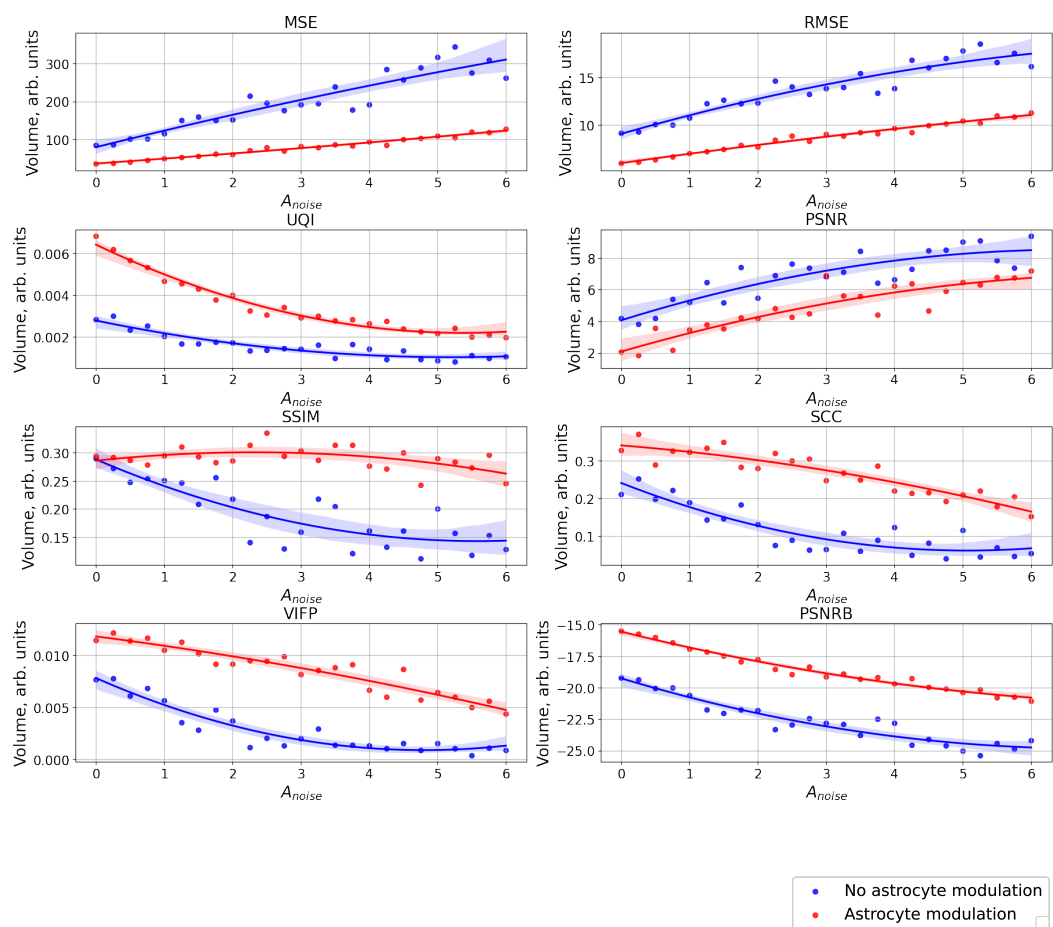


**Figure S9.** The case of using a quality metrics (MSE, RMSE, UQI, PSNR, SSIM, SCC, VIFP, PSNRB) for comparing raster diagrams of neural activity from Figure S7 and Figure S8 with an image 2 from handwritten database MNIST [1] fed to a spike neural network with an increase in the amplitude,  $A_{noise}$ , of the noise signal from 0 to 6 supplied to the neurons of the neural network without astrocytic modulation (blue dots and curve) and with astrocytic modulation (red dots and curve).

S1.4. Number 4 from database MNIST

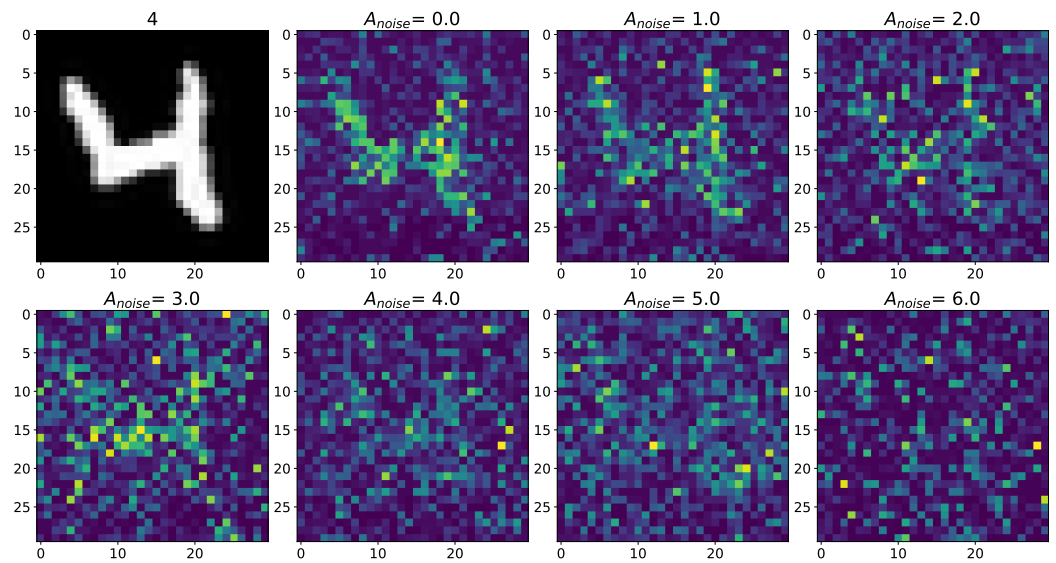


**Figure S10.** Changes in the spatial sweep of the spike neural network during the representation of the supplied image 4 from handwritten database MNIST [1] when the amplitude,  $A_{noise}$ , of the noise current,  $I_{noise}$ , changes from 0 to 6 without modulation of neuronal activity by astrocytes.

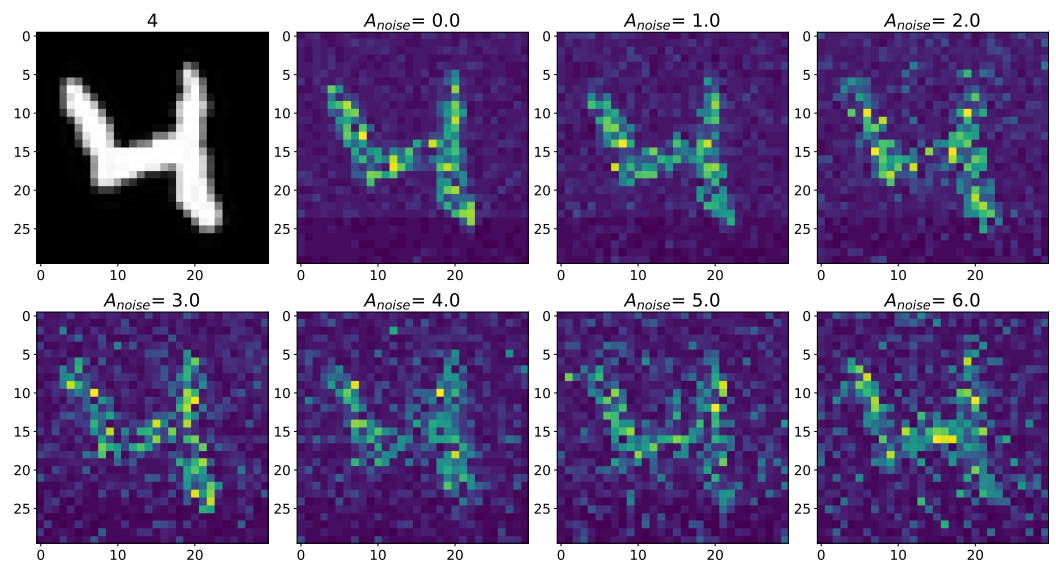


**Figure S11.** Changes in the spatial sweep of the spike neural network during the representation of the supplied image 4 from handwritten database MNIST [1] when the amplitude,  $A_{noise}$ , of the noise current,  $I_{noise}$ , changes from 0 to 6 with modulation of neuronal activity by astrocytes.

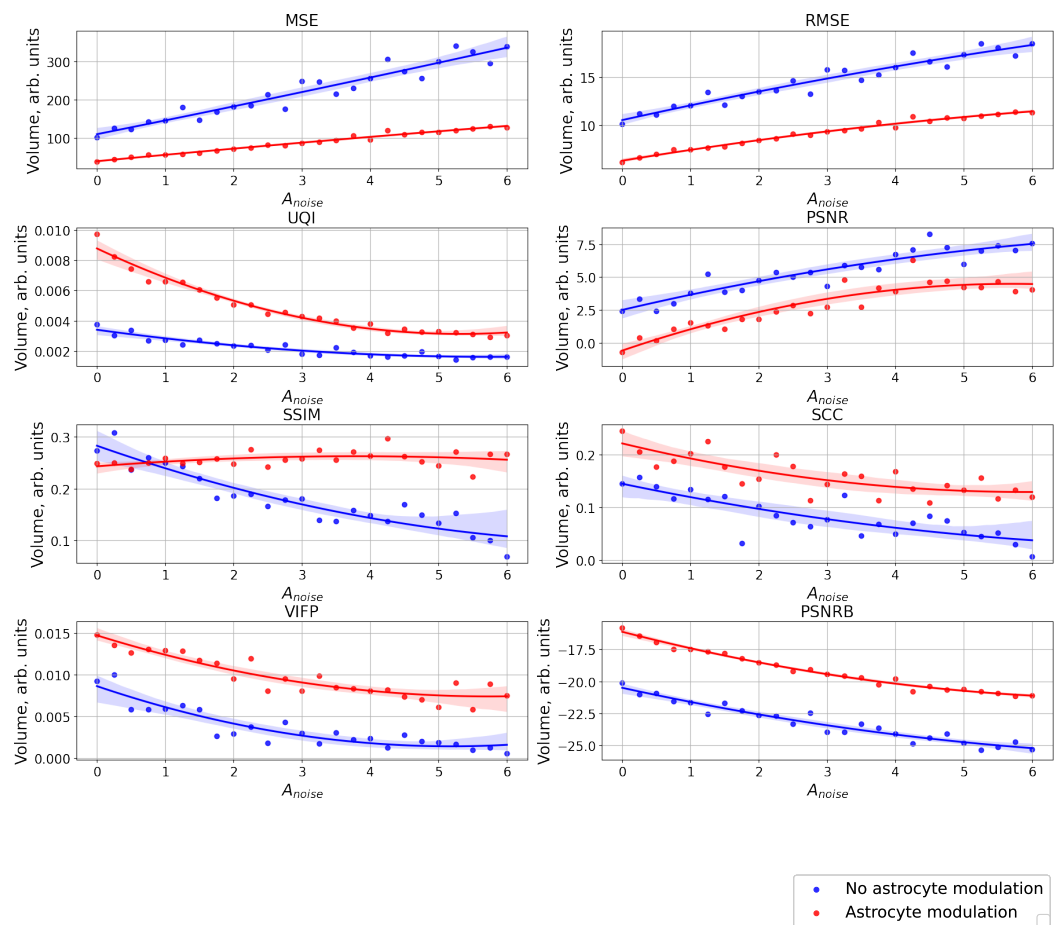


**Figure S12.** The case of using a quality metrics (MSE, RMSE, UQI, PSNR, SSIM, SCC, VIFP, PSNRB) for comparing raster diagrams of neural activity from Figure S10 and Figure S11 with an image 4 from handwritten database MNIST [1] fed to a spike neural network with an increase in the amplitude,  $A_{noise}$ , of the noise signal from 0 to 6 supplied to the neurons of the neural network without astrocytic modulation (blue dots and curve) and with astrocytic modulation (red dots and curve).

S1.5. Number 6 from database MNIST

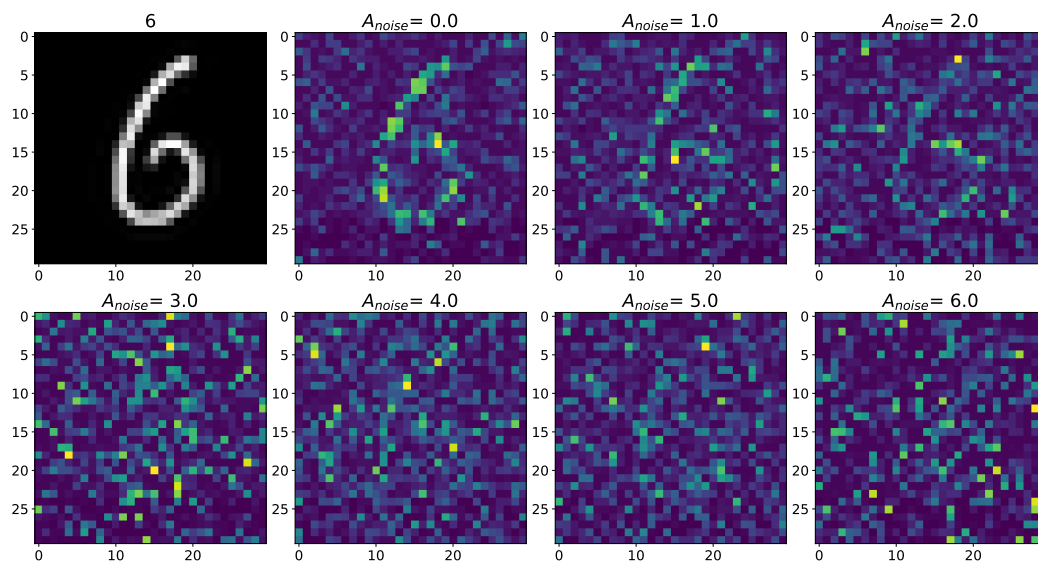


**Figure S13.** Changes in the spatial sweep of the spike neural network during the representation of the supplied image 6 from handwritten database MNIST [1] when the amplitude,  $A_{noise}$ , of the noise current,  $I_{noise}$ , changes from 0 to 6 without modulation of neuronal activity by astrocytes.

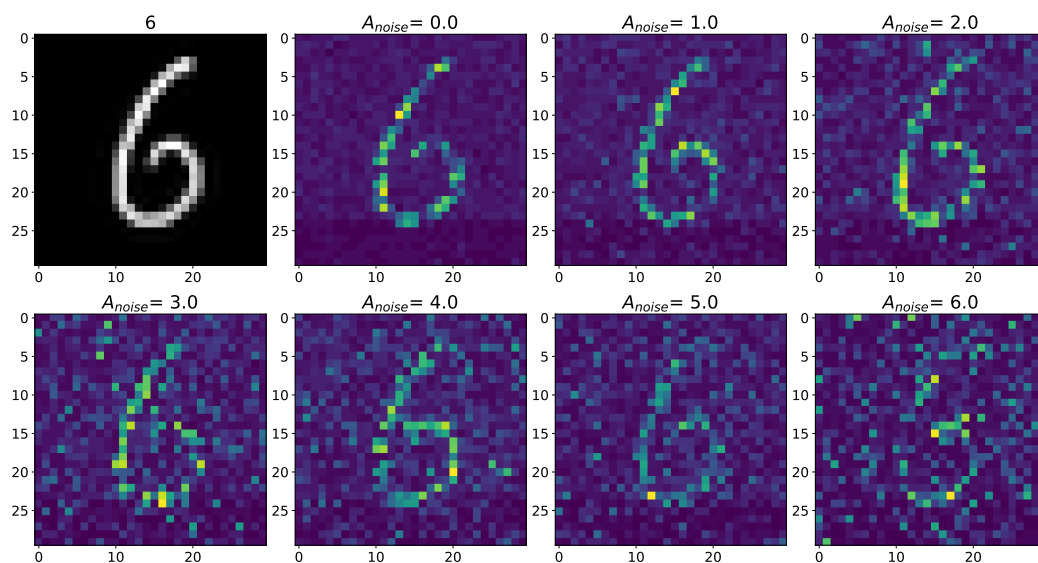


**Figure S14.** Changes in the spatial sweep of the spike neural network during the representation of the supplied image 6 from handwritten database MNIST [1] when the amplitude,  $A_{noise}$ , of the noise current,  $I_{noise}$ , changes from 0 to 6 with modulation of neuronal activity by astrocytes.

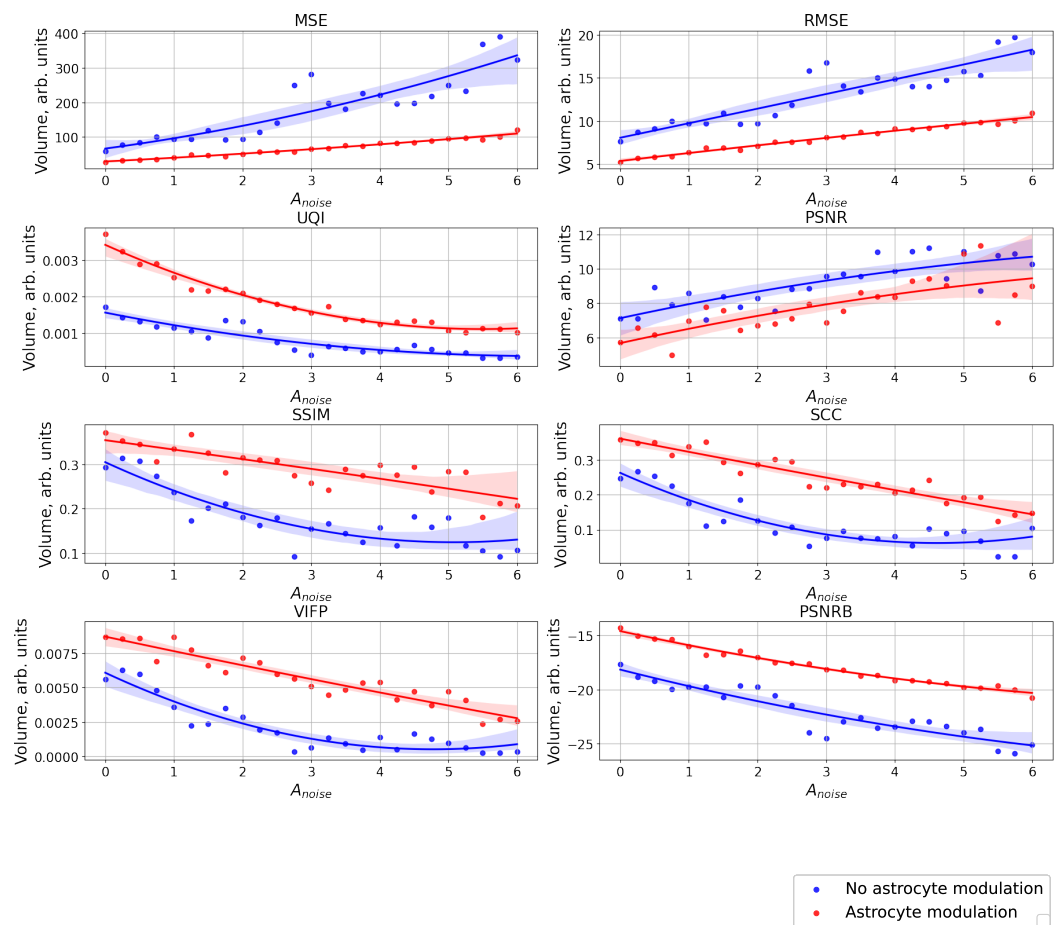


**Figure S15.** The case of using a quality metrics (MSE, RMSE, UQI, PSNR, SSIM, SCC, VIFP, PSNRB) for comparing raster diagrams of neural activity from Figure S13 and Figure S14 with an image 6 from handwritten database MNIST [1] fed to a spike neural network with an increase in the amplitude,  $A_{noise}$ , of the noise signal from 0 to 6 supplied to the neurons of the neural network without astrocytic modulation (blue dots and curve) and with astrocytic modulation (red dots and curve).

S1.6. Number 7 from database MNIST

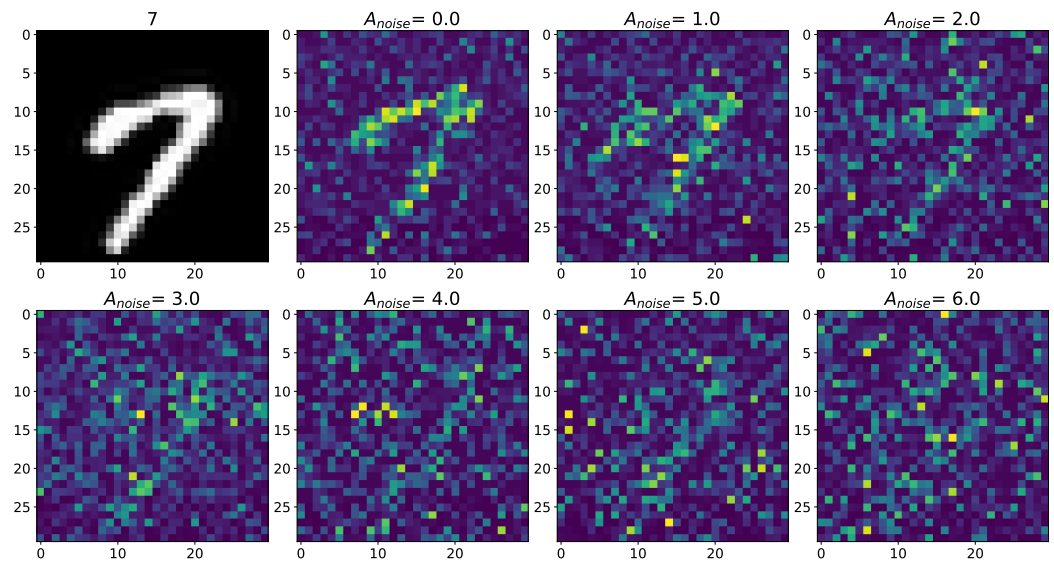


**Figure S16.** Changes in the spatial sweep of the spike neural network during the representation of the supplied image 7 from handwritten database MNIST [1] when the amplitude,  $A_{noise}$ , of the noise current,  $I_{noise}$ , changes from 0 to 6 without modulation of neuronal activity by astrocytes.

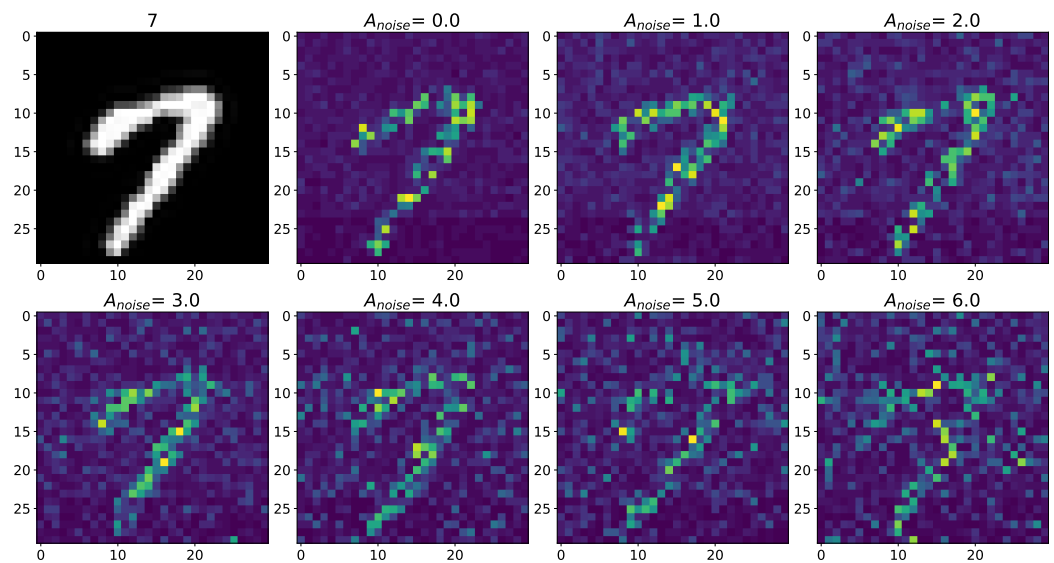


**Figure S17.** Changes in the spatial sweep of the spike neural network during the representation of the supplied image 7 from handwritten database MNIST [1] when the amplitude,  $A_{noise}$ , of the noise current,  $I_{noise}$ , changes from 0 to 6 with modulation of neuronal activity by astrocytes.

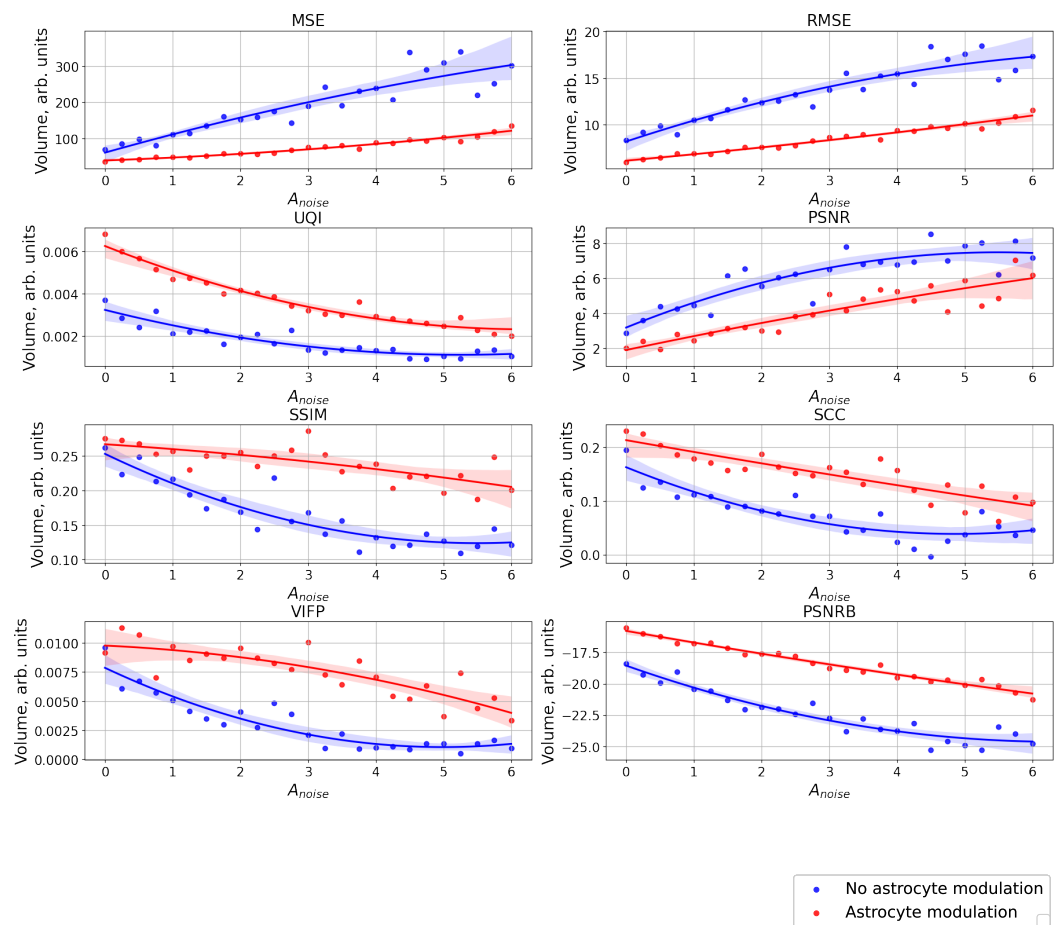


**Figure S18.** The case of using a quality metrics (MSE, RMSE, UQI, PSNR, SSIM, SCC, VIFP, PSNRB) for comparing raster diagrams of neural activity from Figure S16 and Figure S17 with an image 7 from handwritten database MNIST [1] fed to a spike neural network with an increase in the amplitude,  $A_{noise}$ , of the noise signal from 0 to 6 supplied to the neurons of the neural network without astrocytic modulation (blue dots and curve) and with astrocytic modulation (red dots and curve).

S1.7. Number 8 from database MNIST

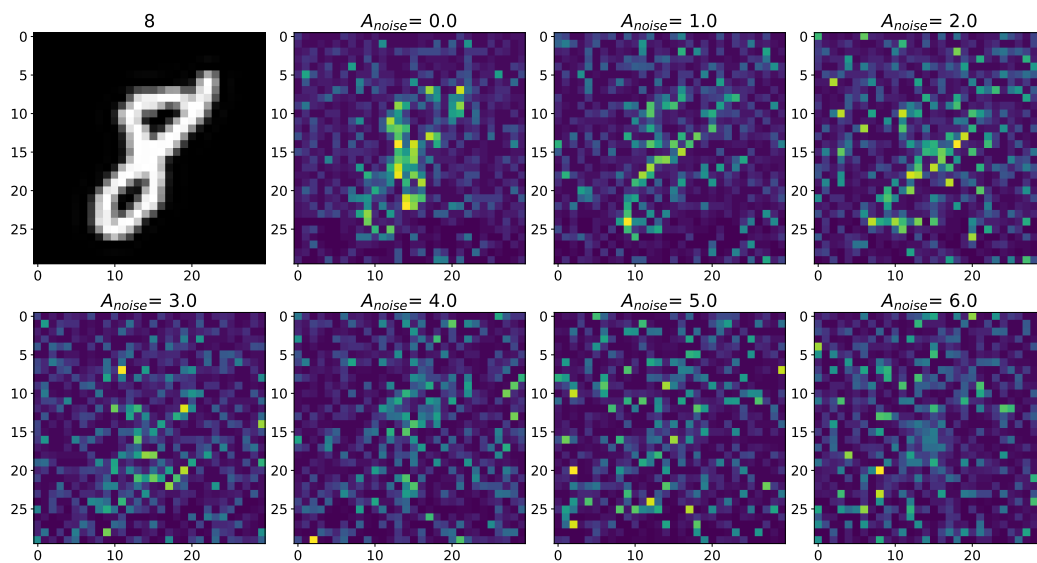


**Figure S19.** Changes in the spatial sweep of the spike neural network during the representation of the supplied image 8 from handwritten database MNIST [1] when the amplitude,  $A_{noise}$ , of the noise current,  $I_{noise}$ , changes from 0 to 6 without modulation of neuronal activity by astrocytes.

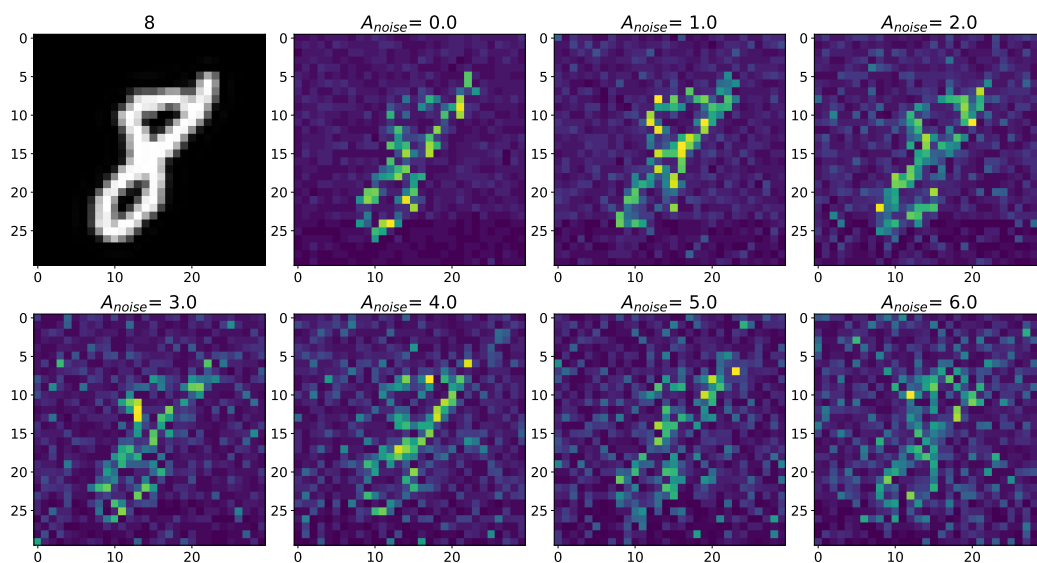


**Figure S20.** Changes in the spatial sweep of the spike neural network during the representation of the supplied image 8 from handwritten database MNIST [1] when the amplitude,  $A_{noise}$ , of the noise current,  $I_{noise}$ , changes from 0 to 6 with modulation of neuronal activity by astrocytes.

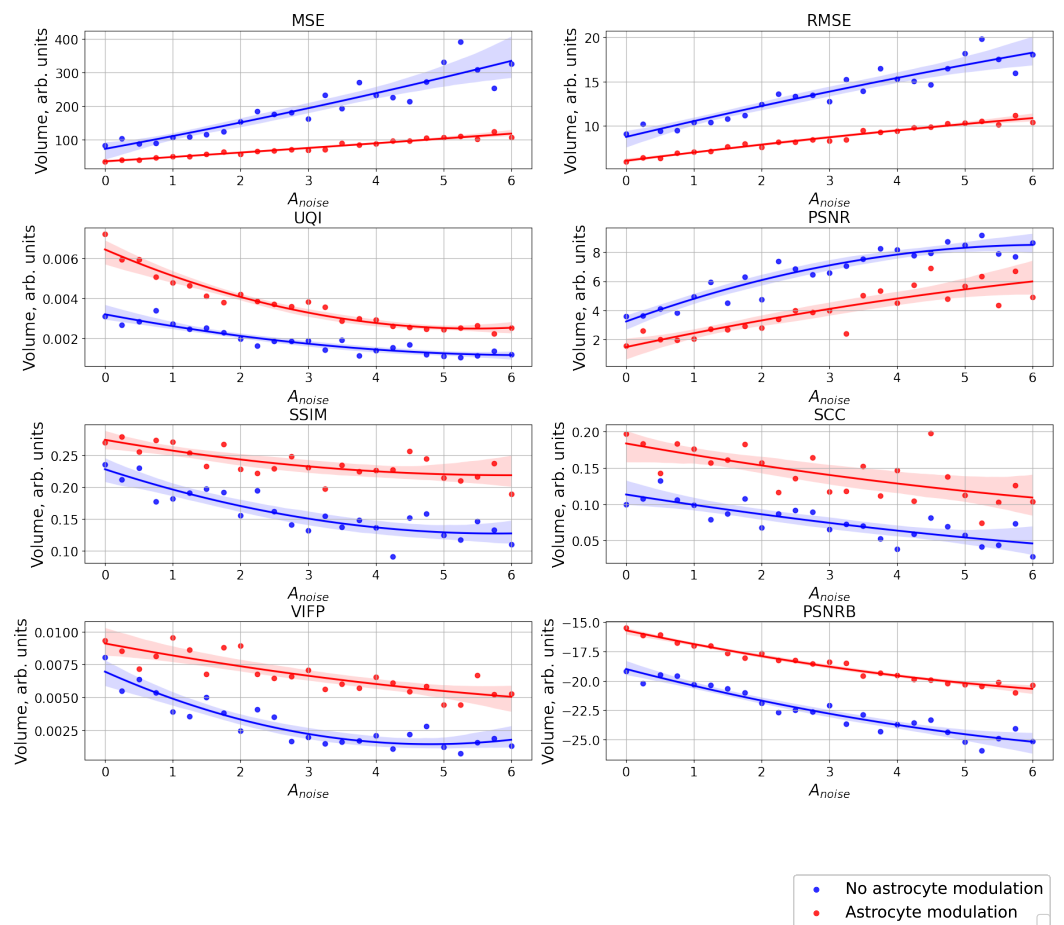


**Figure S21.** The case of using a quality metrics (MSE, RMSE, UQI, PSNR, SSIM, SCC, VIFP, PSNRB) for comparing raster diagrams of neural activity from Figure S19 and Figure S20 with an image 8 from handwritten database MNIST [1] fed to a spike neural network with an increase in the amplitude,  $A_{noise}$ , of the noise signal from 0 to 6 supplied to the neurons of the neural network without astrocytic modulation (blue dots and curve) and with astrocytic modulation (red dots and curve).

S1.8. Number 9 from database MNIST

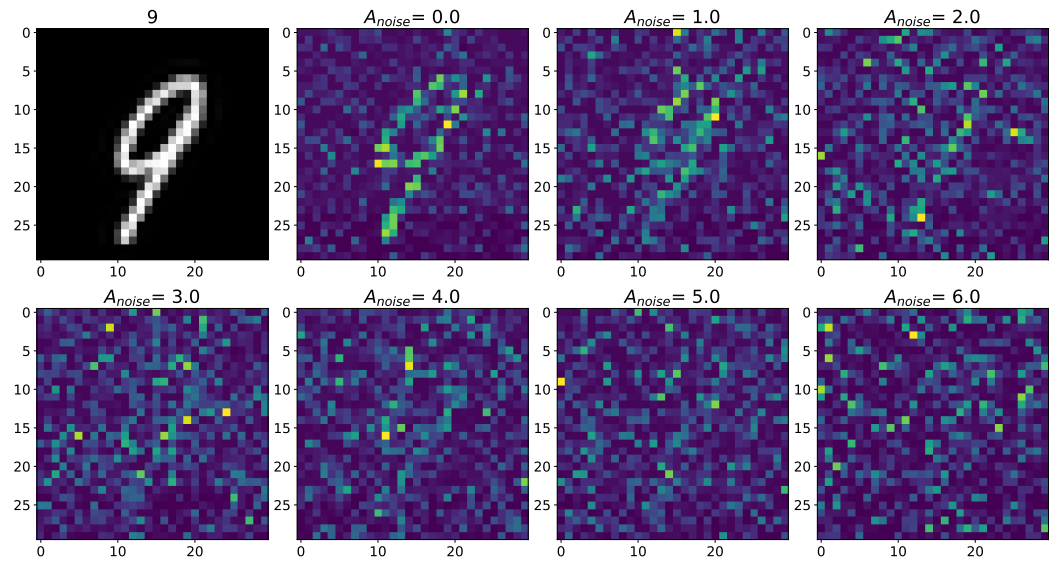


**Figure S22.** Changes in the spatial sweep of the spike neural network during the representation of the supplied image 9 from handwritten database MNIST [1] when the amplitude,  $A_{noise}$ , of the noise current,  $I_{noise}$ , changes from 0 to 6 without modulation of neuronal activity by astrocytes.

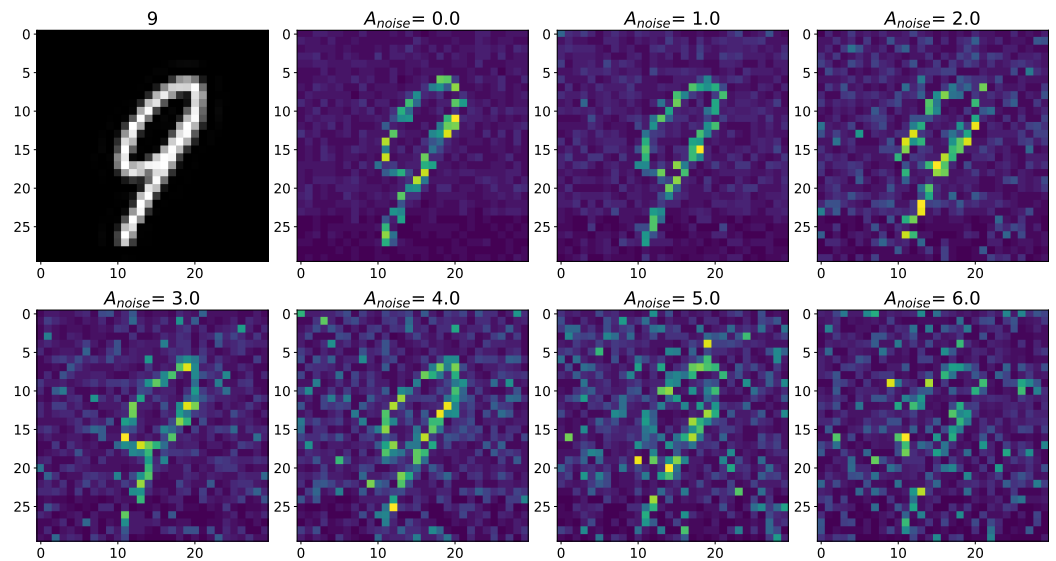


**Figure S23.** Changes in the spatial sweep of the spike neural network during the representation of the supplied image 9 from handwritten database MNIST [1] when the amplitude,  $A_{noise}$ , of the noise current,  $I_{noise}$ , changes from 0 to 6 with modulation of neuronal activity by astrocytes.

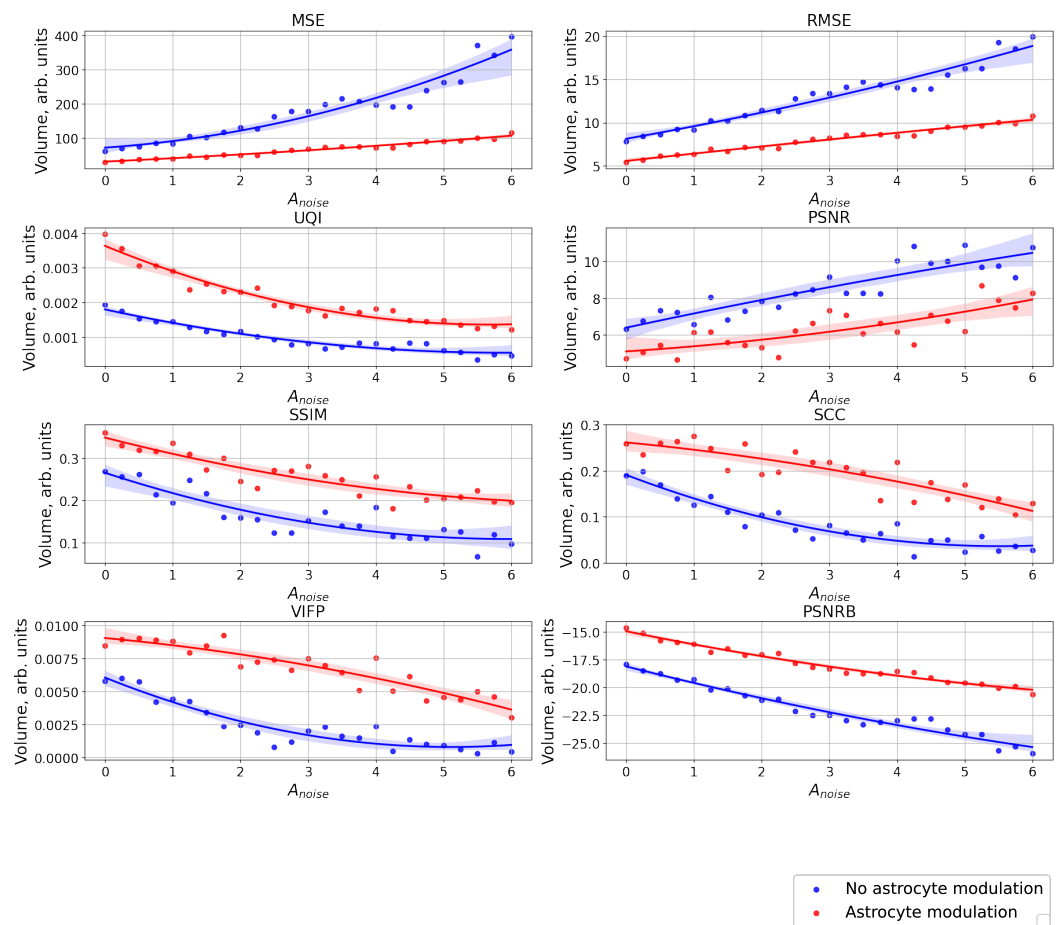


**Figure S24.** The case of using a quality metrics (MSE, RMSE, UQI, PSNR, SSIM, SCC, VIFP, PSNRB) for comparing raster diagrams of neural activity from Figure S22 and Figure S23 with an image 9 from handwritten database MNIST [1] fed to a spike neural network with an increase in the amplitude,  $A_{noise}$ , of the noise signal from 0 to 6 supplied to the neurons of the neural network without astrocytic modulation (blue dots and curve) and with astrocytic modulation (red dots and curve).

## S2. Cases with category from database Fashion-MNIST

### S2.1. Category 0 from database Fashion-MNIST

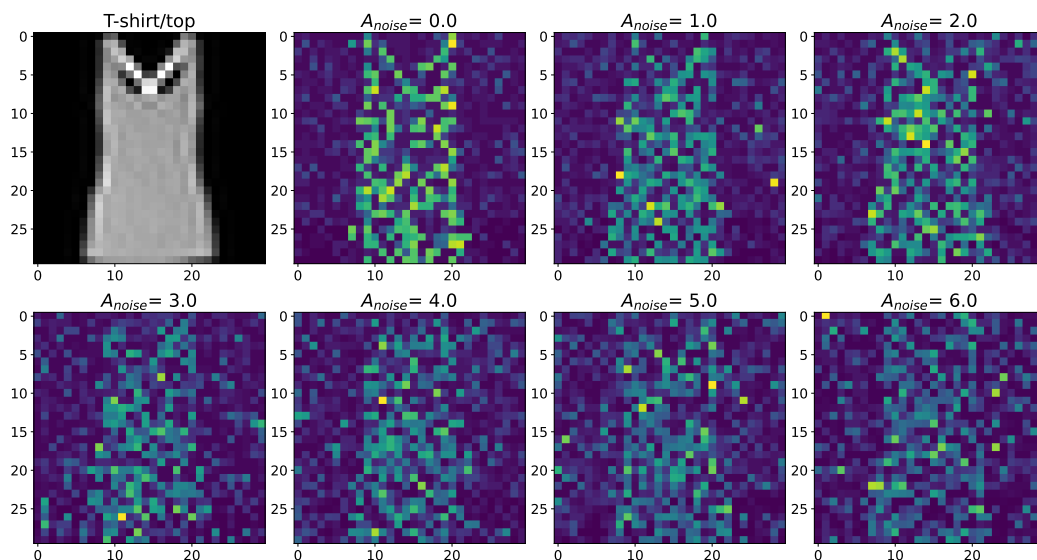


**Figure S25.** Changes in the spatial sweep of the spike neural network during the representation of the supplied image category 0 from database Fashion-MNIST [2] when the amplitude,  $A_{noise}$ , of the noise current,  $I_{noise}$ , changes from 0 to 6 without modulation of neuronal activity by astrocytes.

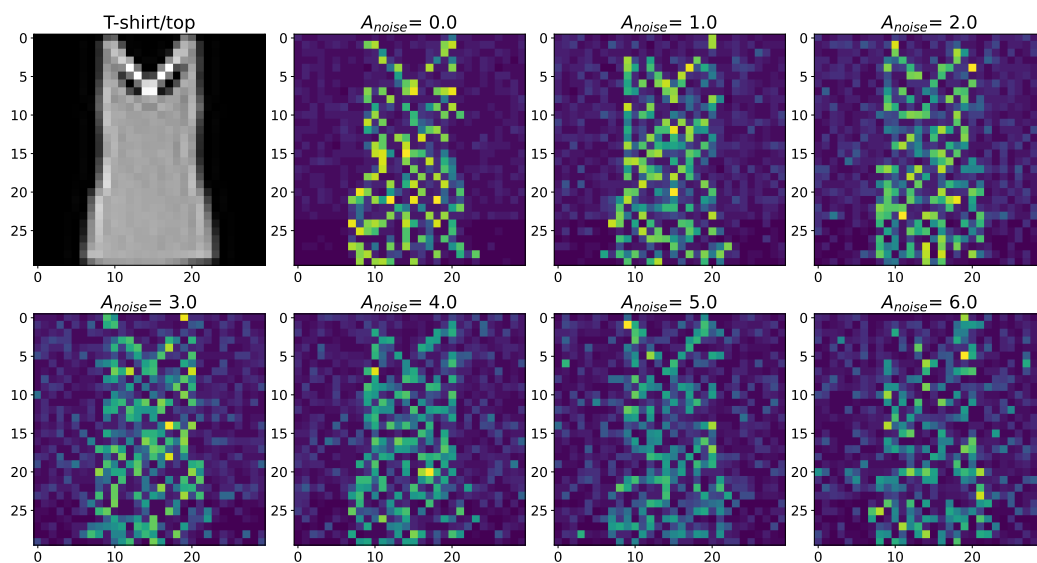


**Figure S26.** Changes in the spatial sweep of the spike neural network during the representation of the supplied image category 0 from database Fashion-MNIST [2] when the amplitude,  $A_{noise}$ , of the noise current,  $I_{noise}$ , changes from 0 to 6 with modulation of neuronal activity by astrocytes.

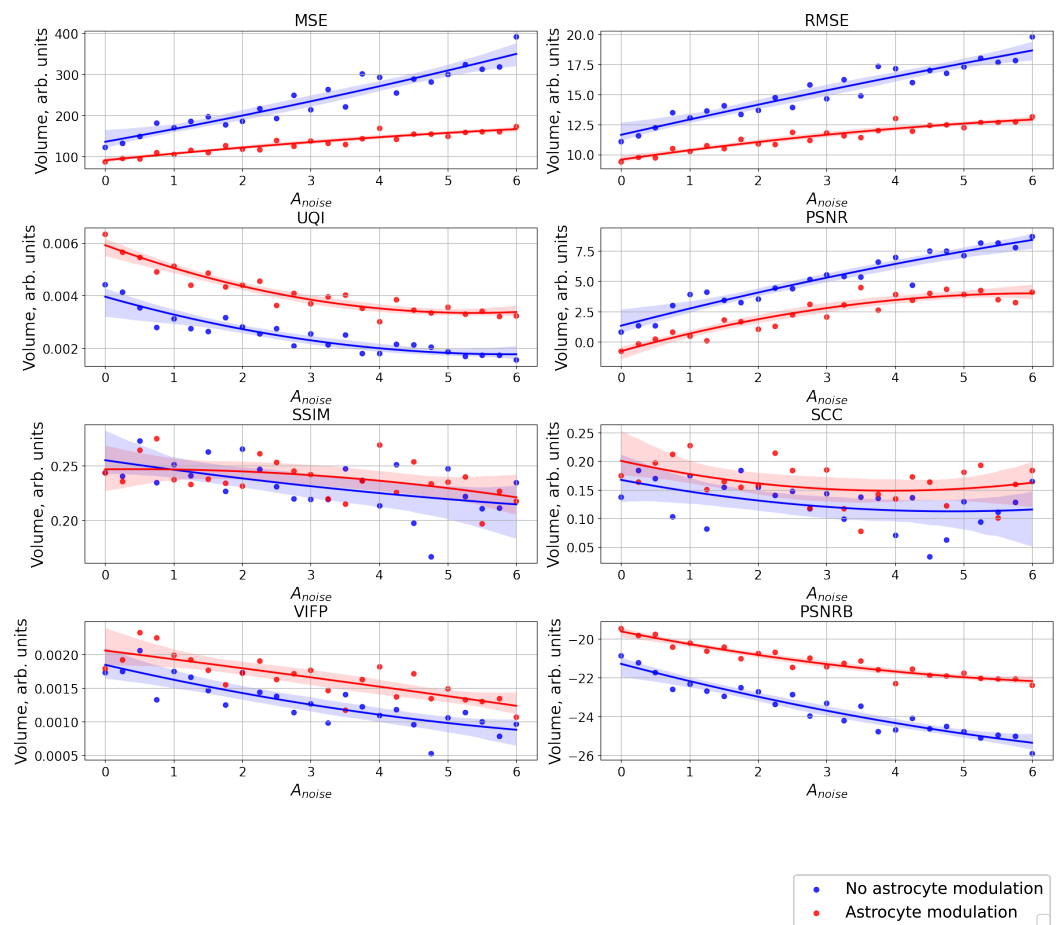


**Figure S27.** The case of using a quality metrics (MSE, RMSE, UQI, PSNR, SSIM, SCC, VIFP, PSNRB) for comparing raster diagrams of neural activity from Figure S25 and Figure S26 with an image category 0 from database Fashion-MNIST [2] fed to a spike neural network with an increase in the amplitude,  $A_{noise}$ , of the noise signal from 0 to 6 supplied to the neurons of the neural network without astrocytic modulation (blue dots and curve) and with astrocytic modulation (red dots and curve).

S2.2. Category 1 from database Fashion-MNIST

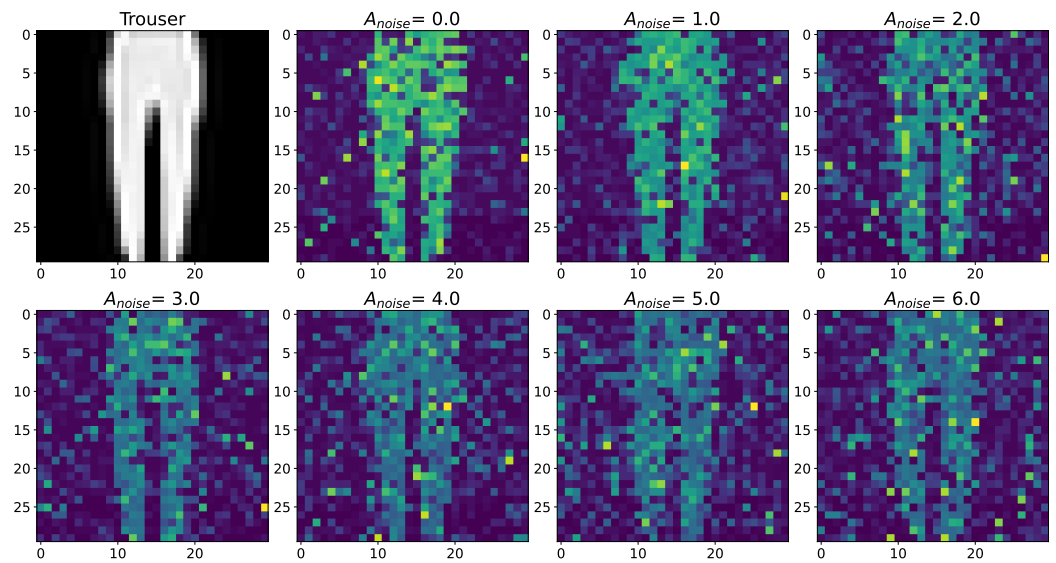


**Figure S28.** Changes in the spatial sweep of the spike neural network during the representation of the supplied image category 1 from database Fashion-MNIST [2] when the amplitude,  $A_{noise}$ , of the noise current,  $I_{noise}$ , changes from 0 to 6 without modulation of neuronal activity by astrocytes.

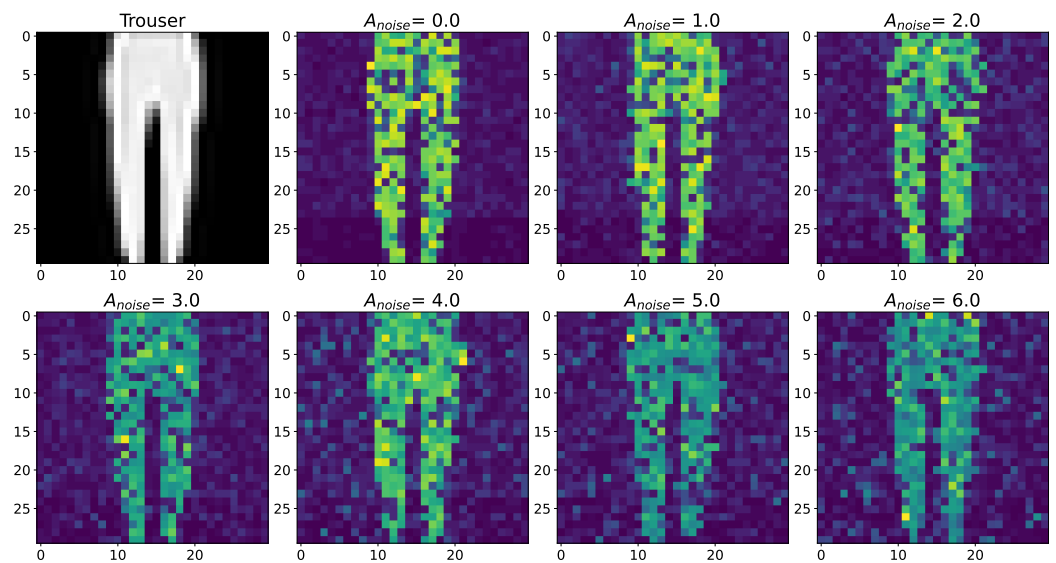


**Figure S29.** Changes in the spatial sweep of the spike neural network during the representation of the supplied image category 1 from database Fashion-MNIST [2] when the amplitude,  $A_{noise}$ , of the noise current,  $I_{noise}$ , changes from 0 to 6 with modulation of neuronal activity by astrocytes.

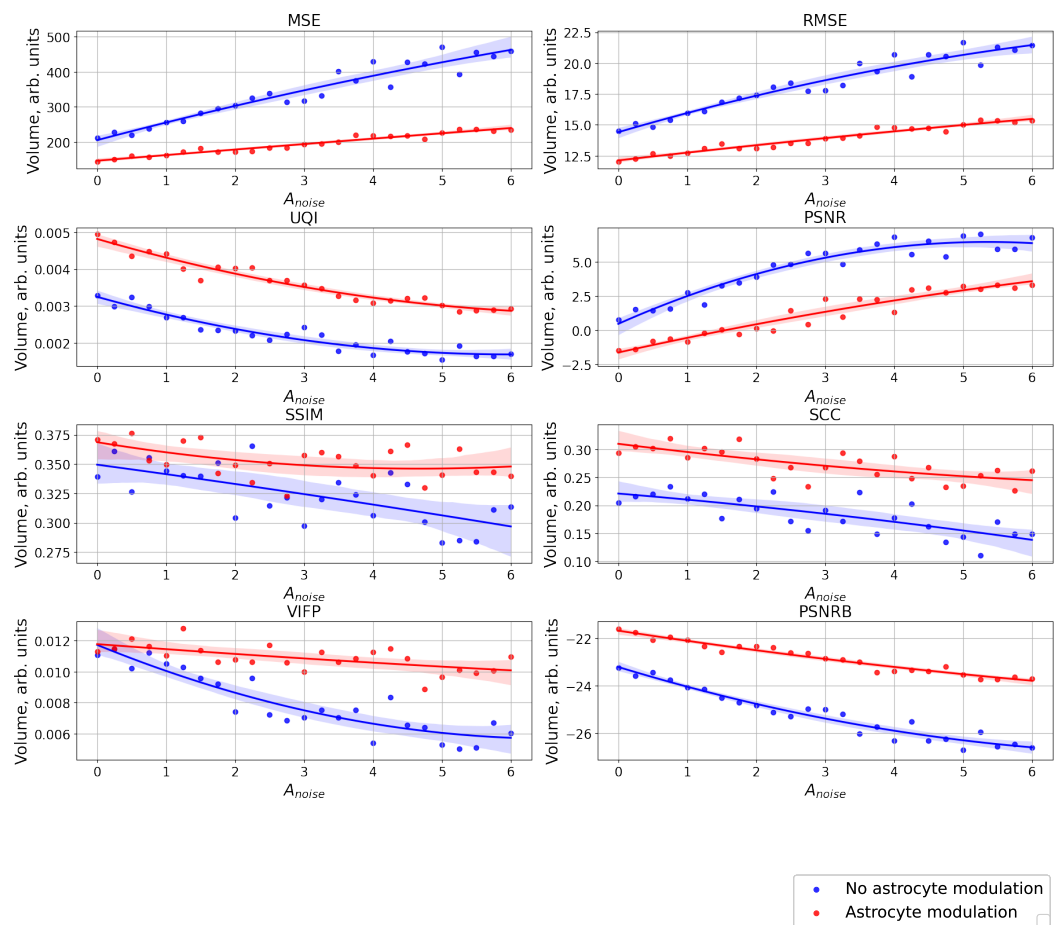


**Figure S30.** The case of using a quality metrics (MSE, RMSE, UQI, PSNR, SSIM, SCC, VIFP, PSNRB) for comparing raster diagrams of neural activity from Figure S28 and Figure S29 with an image category 1 from database Fashion-MNIST [2] fed to a spike neural network with an increase in the amplitude,  $A_{noise}$ , of the noise signal from 0 to 6 supplied to the neurons of the neural network without astrocytic modulation (blue dots and curve) and with astrocytic modulation (red dots and curve).

S2.3. Category 2 from database Fashion-MNIST

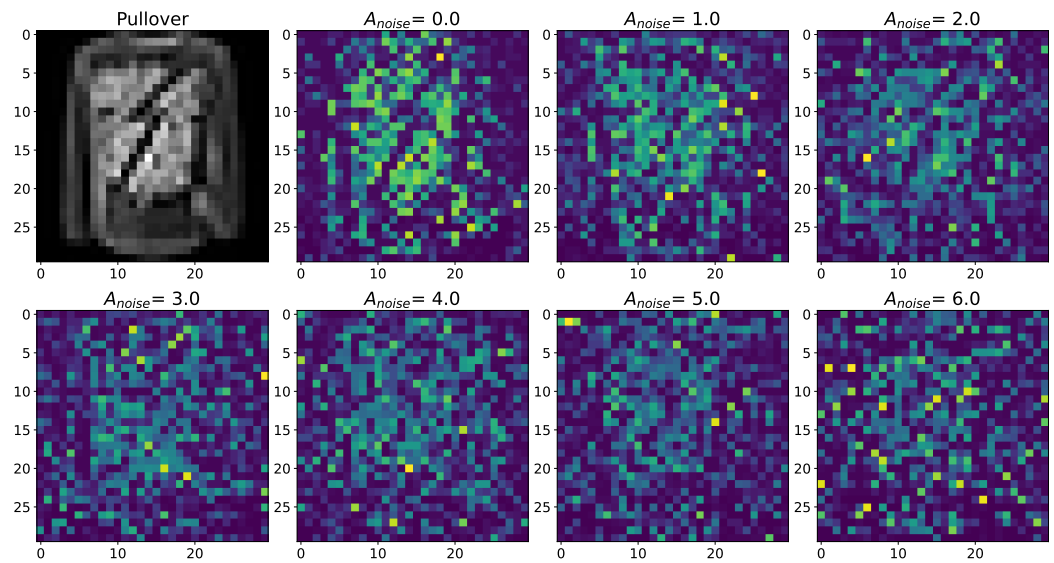


**Figure S31.** Changes in the spatial sweep of the spike neural network during the representation of the supplied image category 2 from database Fashion-MNIST [2] when the amplitude,  $A_{noise}$ , of the noise current,  $I_{noise}$ , changes from 0 to 6 without modulation of neuronal activity by astrocytes.

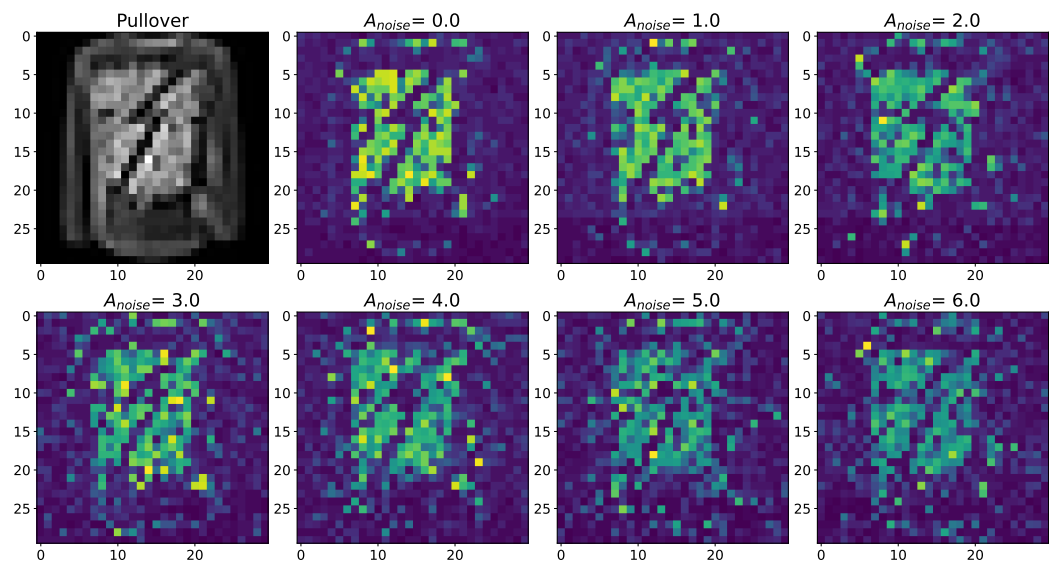


**Figure S32.** Changes in the spatial sweep of the spike neural network during the representation of the supplied image category 2 from database Fashion-MNIST [2] when the amplitude,  $A_{noise}$ , of the noise current,  $I_{noise}$ , changes from 0 to 6 with modulation of neuronal activity by astrocytes.

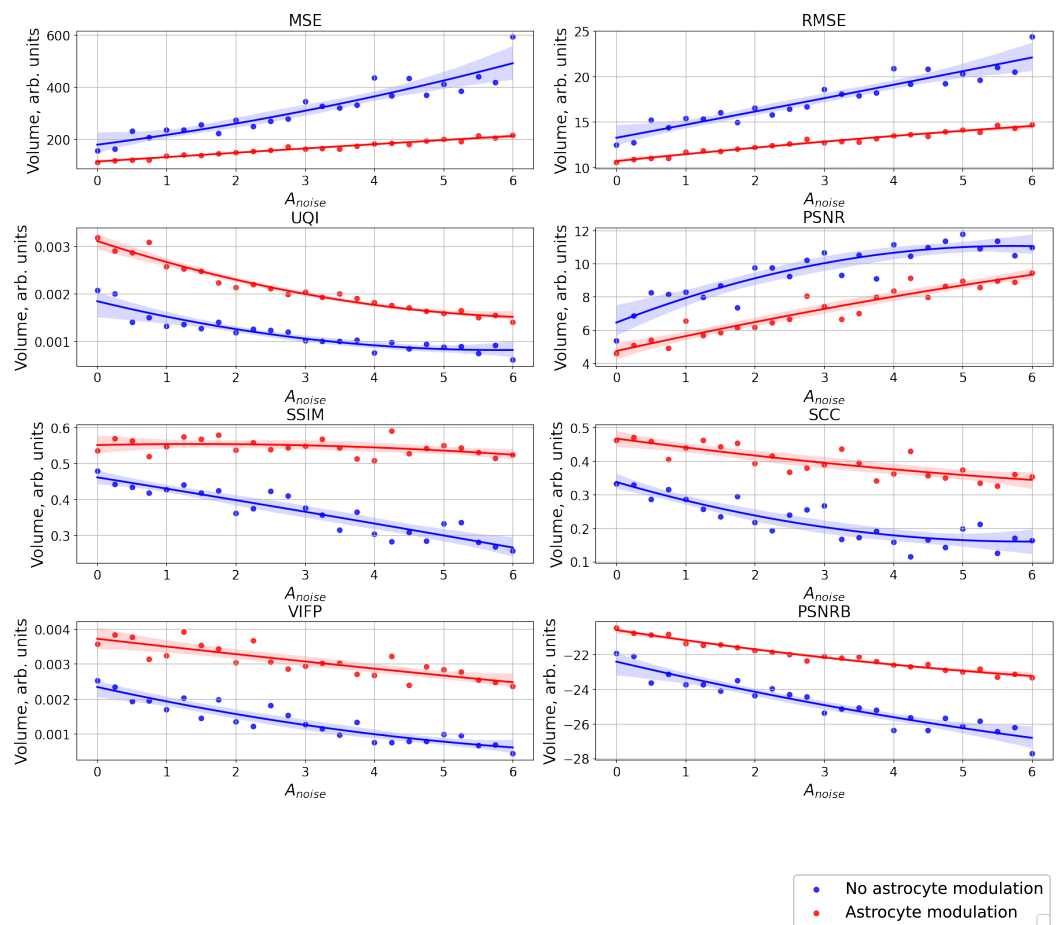


**Figure S33.** The case of using a quality metrics (MSE, RMSE, UQI, PSNR, SSIM, SCC, VIFP, PSNRB) for comparing raster diagrams of neural activity from Figure S31 and Figure S32 with an image category 2 from database Fashion-MNIST [2] fed to a spike neural network with an increase in the amplitude,  $A_{noise}$ , of the noise signal from 0 to 6 supplied to the neurons of the neural network without astrocytic modulation (blue dots and curve) and with astrocytic modulation (red dots and curve).

S2.4. Category 3 from database Fashion-MNIST

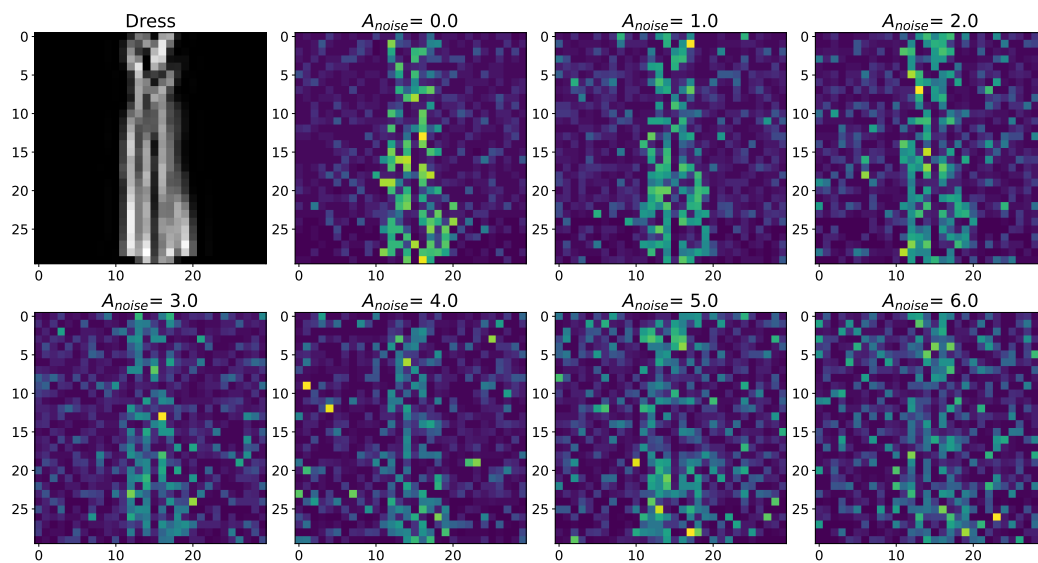


**Figure S34.** Changes in the spatial sweep of the spike neural network during the representation of the supplied image category 3 from database Fashion-MNIST [2] when the amplitude,  $A_{noise}$ , of the noise current,  $I_{noise}$ , changes from 0 to 6 without modulation of neuronal activity by astrocytes.

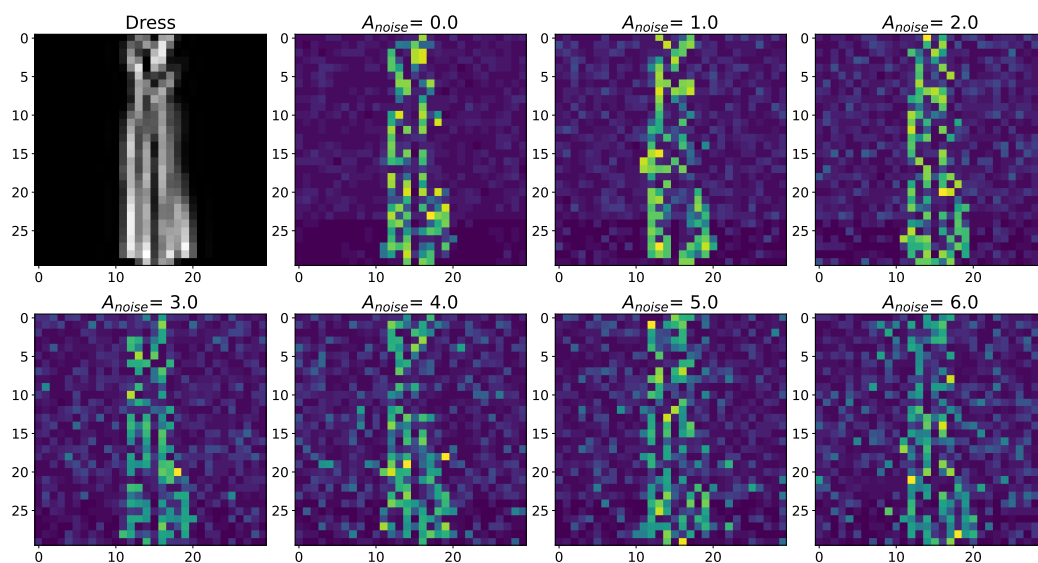


**Figure S35.** Changes in the spatial sweep of the spike neural network during the representation of the supplied image category 3 from database Fashion-MNIST [2] when the amplitude,  $A_{noise}$ , of the noise current,  $I_{noise}$ , changes from 0 to 6 with modulation of neuronal activity by astrocytes.

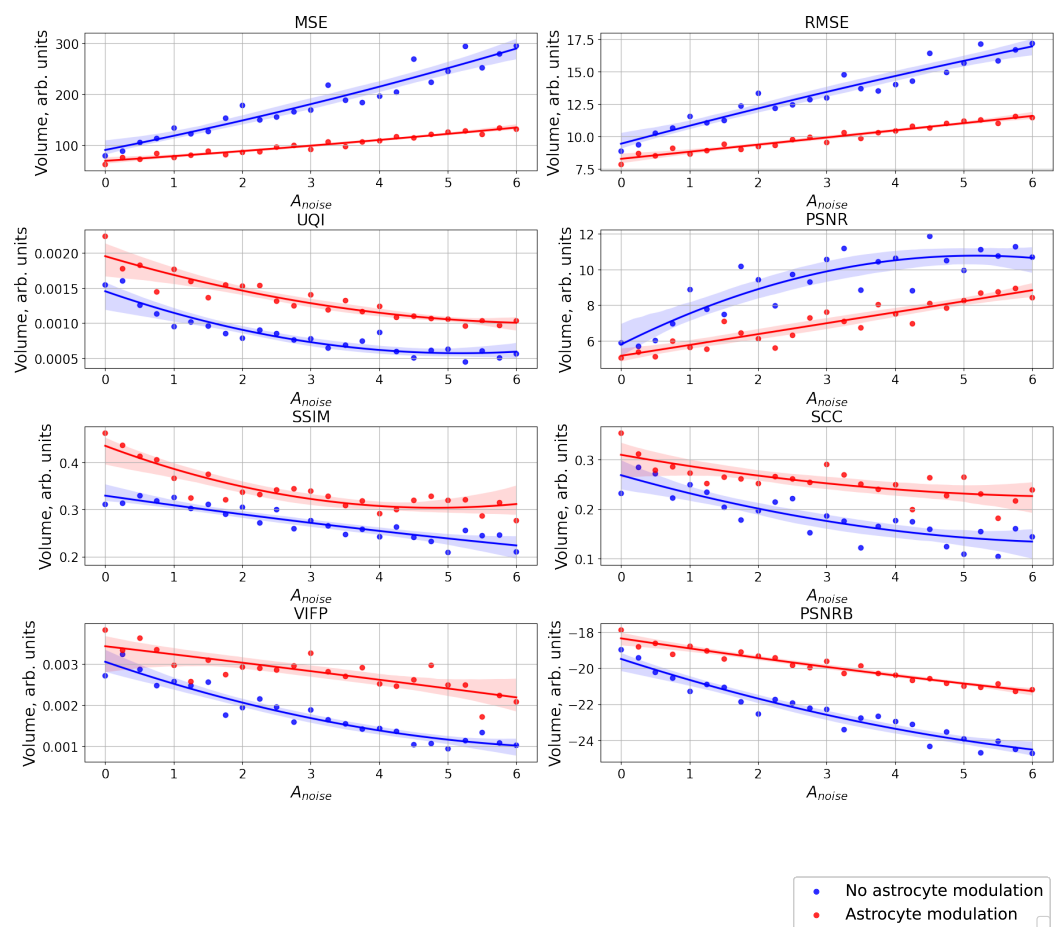


**Figure S36.** The case of using a quality metrics (MSE, RMSE, UQI, PSNR, SSIM, SCC, VIFP, PSNRB) for comparing raster diagrams of neural activity from Figure S34 and Figure S35 with an image category 3 from database Fashion-MNIST [2] fed to a spike neural network with an increase in the amplitude,  $A_{noise}$ , of the noise signal from 0 to 6 supplied to the neurons of the neural network without astrocytic modulation (blue dots and curve) and with astrocytic modulation (red dots and curve).

S2.5. Category 4 from database Fashion-MNIST

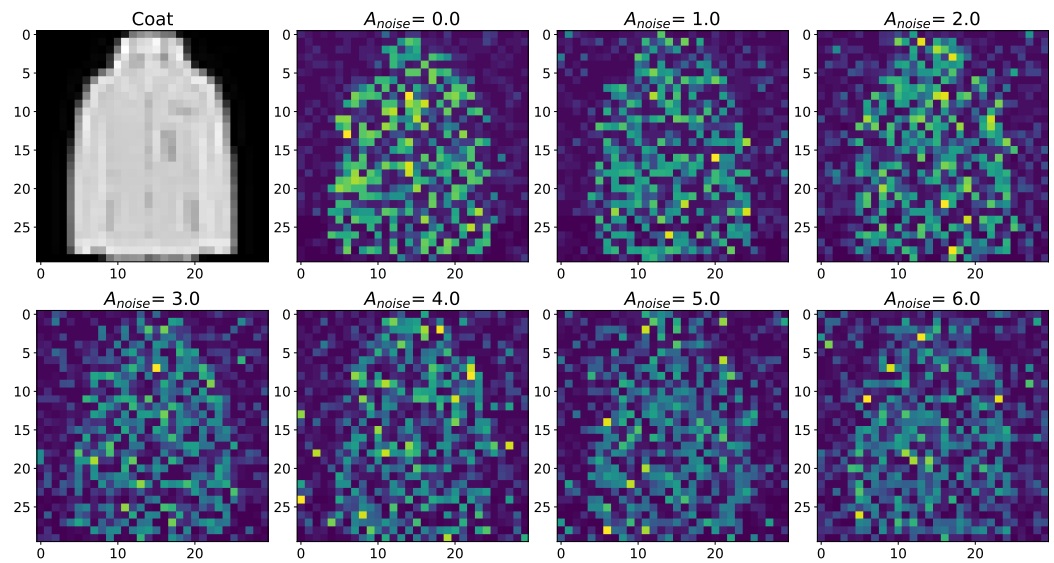


**Figure S37.** Changes in the spatial sweep of the spike neural network during the representation of the supplied image category 4 from database Fashion-MNIST [2] when the amplitude,  $A_{noise}$ , of the noise current,  $I_{noise}$ , changes from 0 to 6 without modulation of neuronal activity by astrocytes.

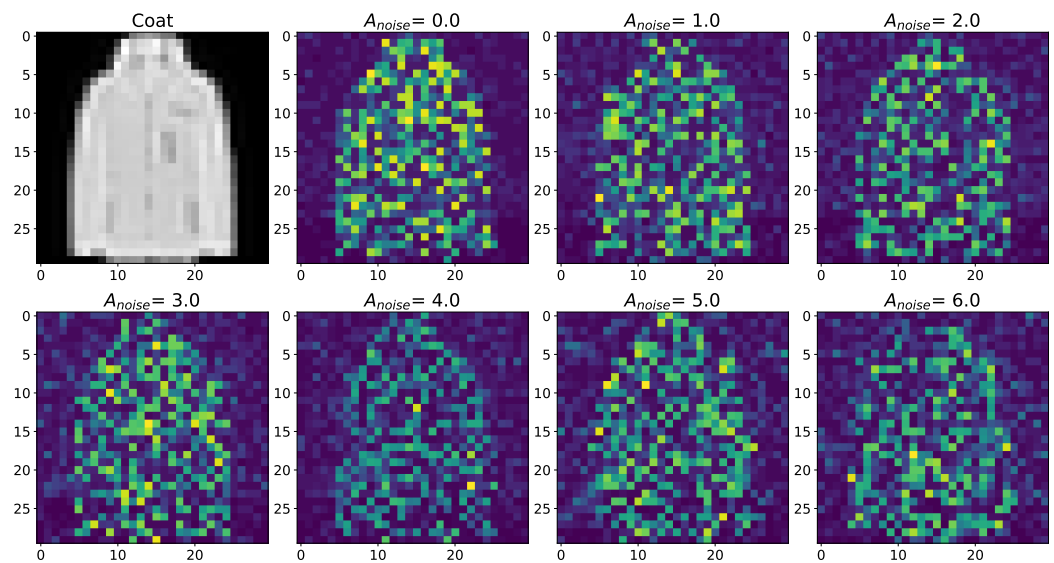


**Figure S38.** Changes in the spatial sweep of the spike neural network during the representation of the supplied image category 4 from database Fashion-MNIST [2] when the amplitude,  $A_{noise}$ , of the noise current,  $I_{noise}$ , changes from 0 to 6 with modulation of neuronal activity by astrocytes.

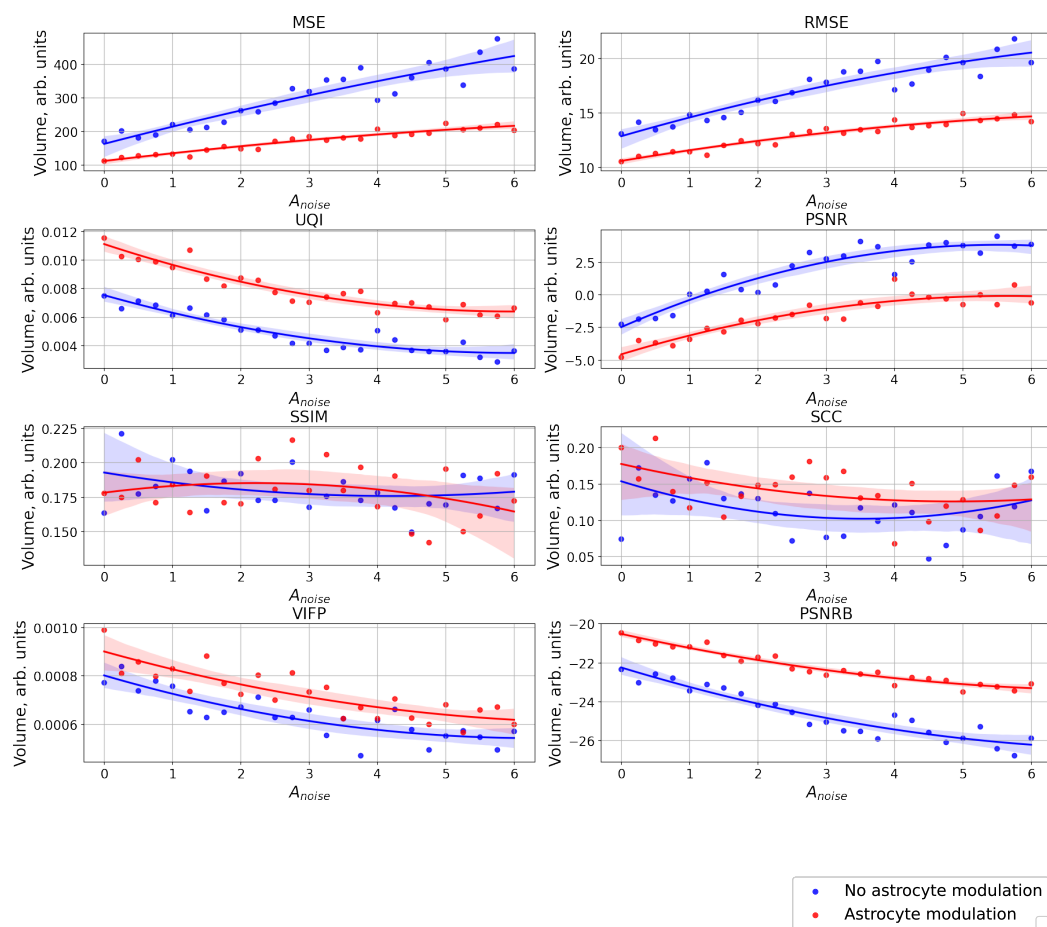


**Figure S39.** The case of using a quality metrics (MSE, RMSE, UQI, PSNR, SSIM, SCC, VIFP, PSNRB) for comparing raster diagrams of neural activity from Figure S37 and Figure S38 with an image category 4 from database Fashion-MNIST [2] fed to a spike neural network with an increase in the amplitude,  $A_{noise}$ , of the noise signal from 0 to 6 supplied to the neurons of the neural network without astrocytic modulation (blue dots and curve) and with astrocytic modulation (red dots and curve).

S2.6. Category 5 from database Fashion-MNIST

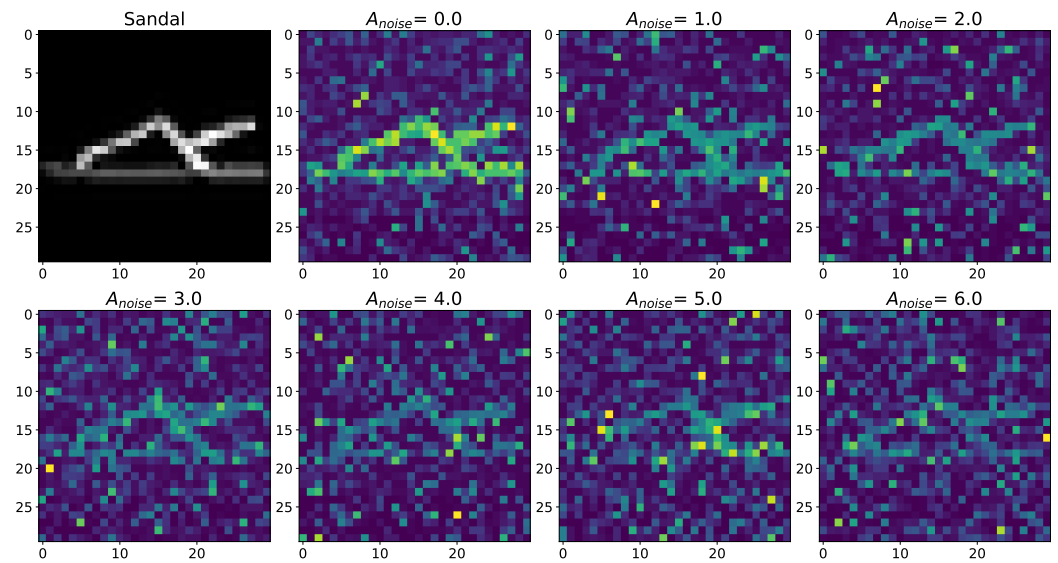


**Figure S40.** Changes in the spatial sweep of the spike neural network during the representation of the supplied image category 5 from database Fashion-MNIST [2] when the amplitude,  $A_{noise}$ , of the noise current,  $I_{noise}$ , changes from 0 to 6 without modulation of neuronal activity by astrocytes.

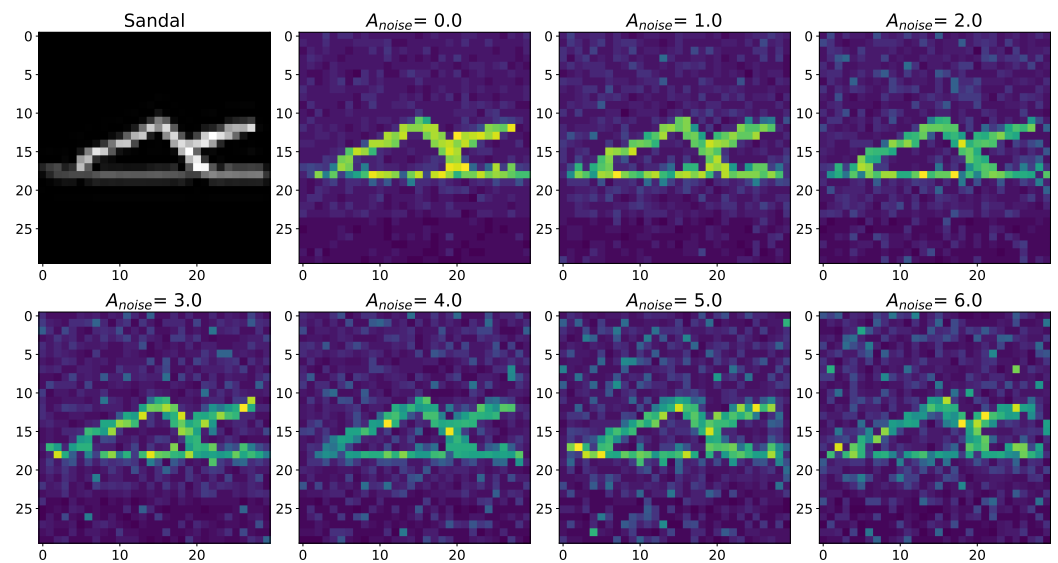


**Figure S41.** Changes in the spatial sweep of the spike neural network during the representation of the supplied image category 5 from database Fashion-MNIST [2] when the amplitude,  $A_{noise}$ , of the noise current,  $I_{noise}$ , changes from 0 to 6 with modulation of neuronal activity by astrocytes.

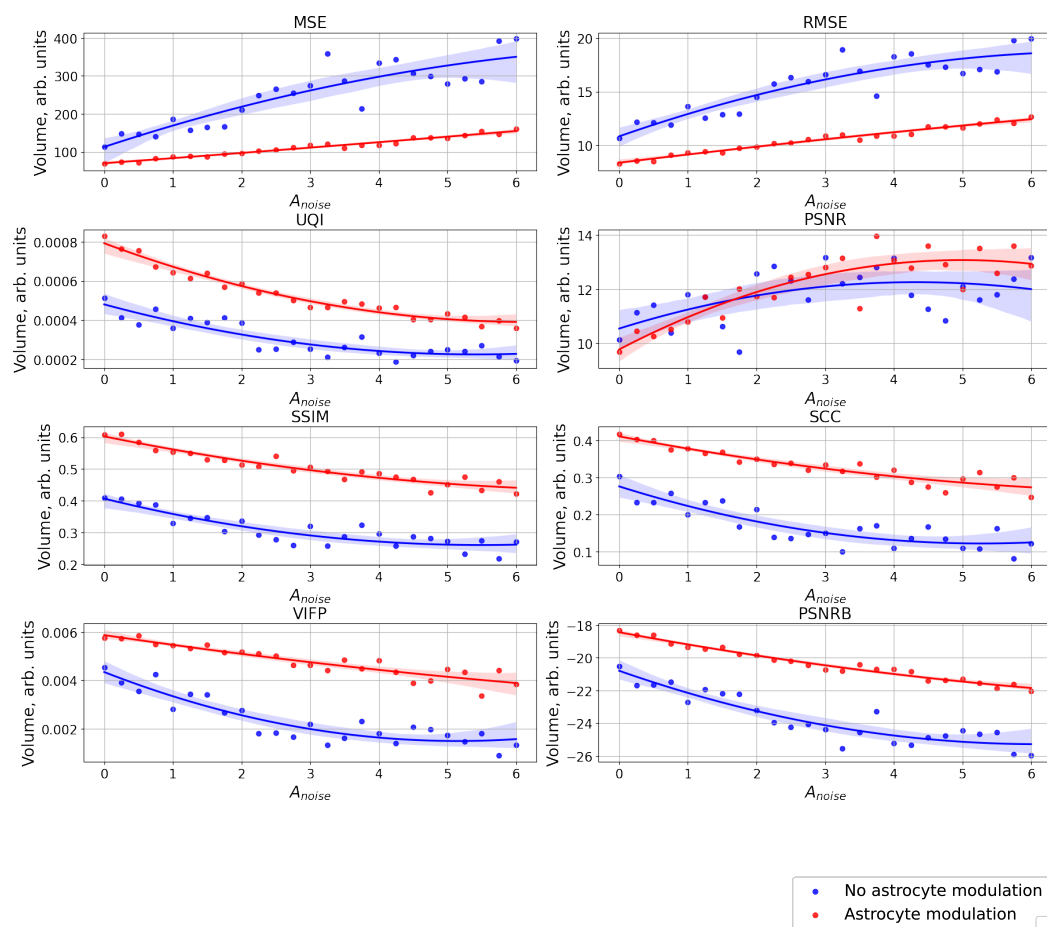


**Figure S42.** The case of using a quality metrics (MSE, RMSE, UQI, PSNR, SSIM, SCC, VIFP, PSNRB) for comparing raster diagrams of neural activity from Figure S40 and Figure S41 with an image category 5 from database Fashion-MNIST [2] fed to a spike neural network with an increase in the amplitude,  $A_{noise}$ , of the noise signal from 0 to 6 supplied to the neurons of the neural network without astrocytic modulation (blue dots and curve) and with astrocytic modulation (red dots and curve).

S2.7. Category 6 from database Fashion-MNIST

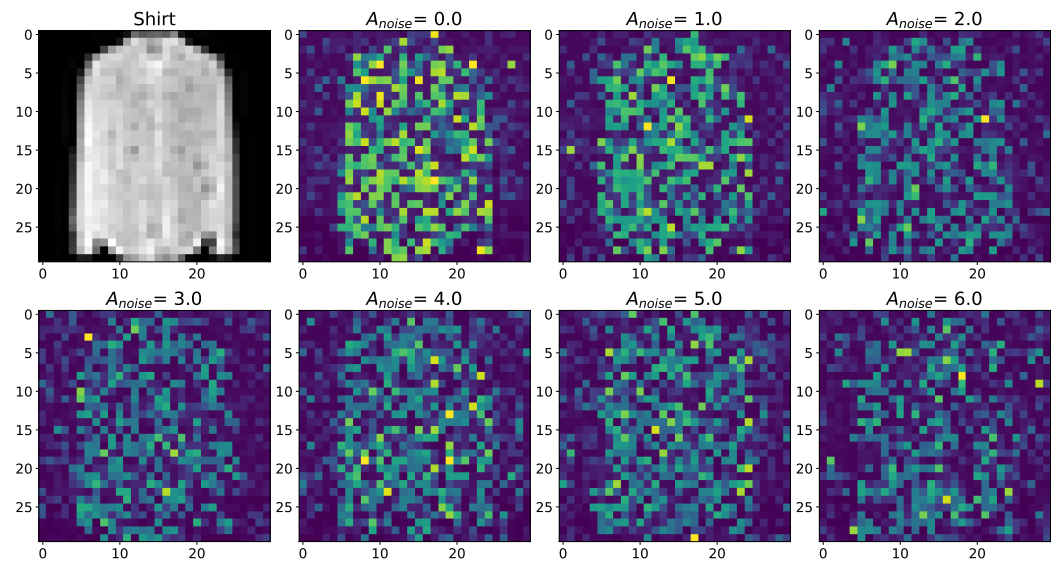


**Figure S43.** Changes in the spatial sweep of the spike neural network during the representation of the supplied image category 6 from database Fashion-MNIST [2] when the amplitude,  $A_{noise}$ , of the noise current,  $I_{noise}$ , changes from 0 to 6 without modulation of neuronal activity by astrocytes.

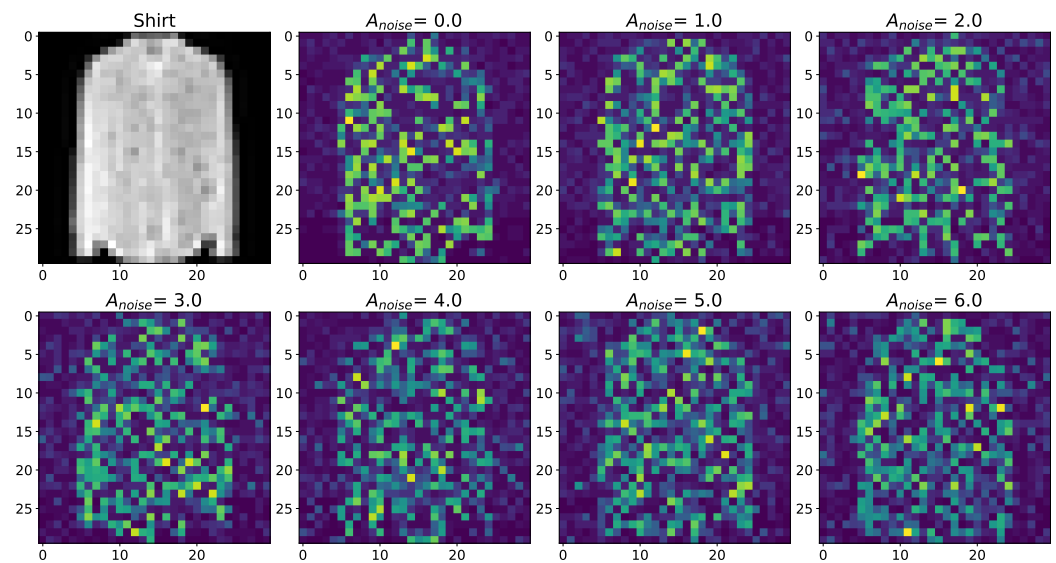


**Figure S44.** Changes in the spatial sweep of the spike neural network during the representation of the supplied image category 6 from database Fashion-MNIST [2] when the amplitude,  $A_{noise}$ , of the noise current,  $I_{noise}$ , changes from 0 to 6 with modulation of neuronal activity by astrocytes.

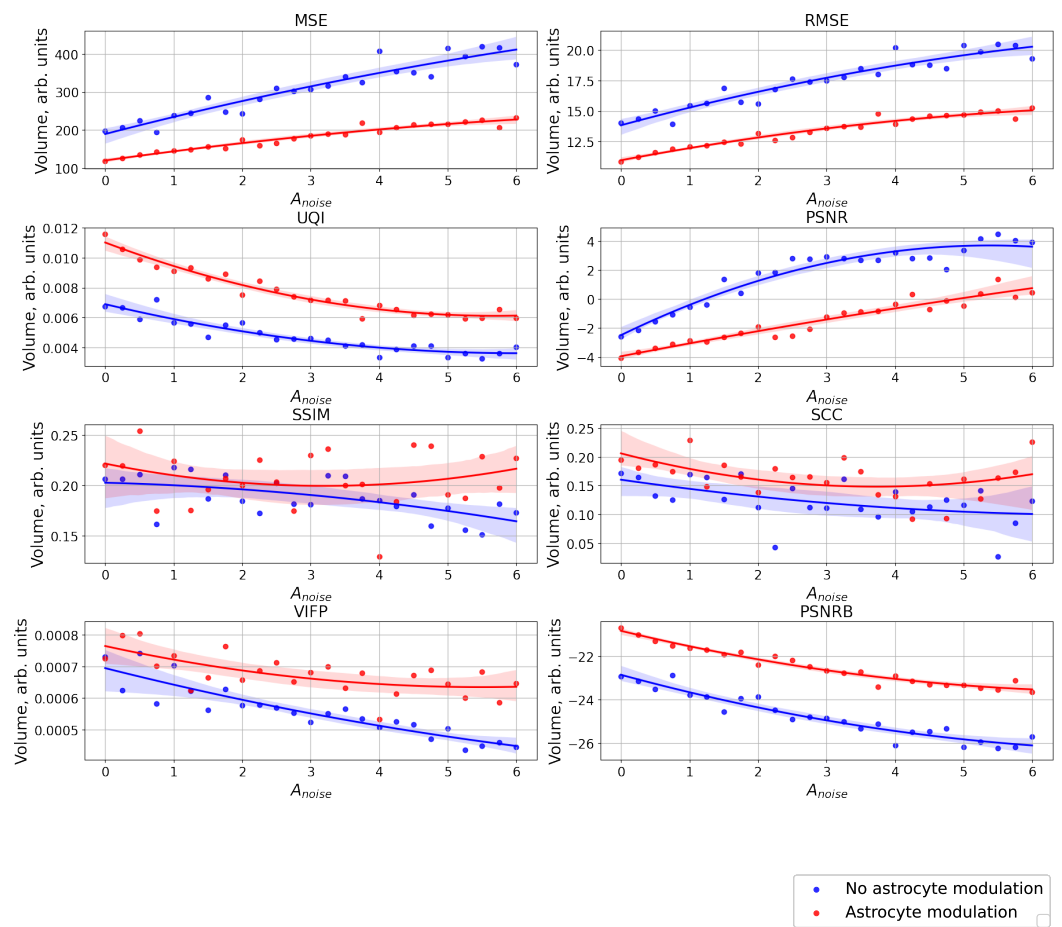


**Figure S45.** The case of using a quality metrics (MSE, RMSE, UQI, PSNR, SSIM, SCC, VIFP, PSNRB) for comparing raster diagrams of neural activity from Figure S43 and Figure S44 with an image category 6 from database Fashion-MNIST [2] fed to a spike neural network with an increase in the amplitude,  $A_{noise}$ , of the noise signal from 0 to 6 supplied to the neurons of the neural network without astrocytic modulation (blue dots and curve) and with astrocytic modulation (red dots and curve).

S2.8. Category 7 from database Fashion-MNIST

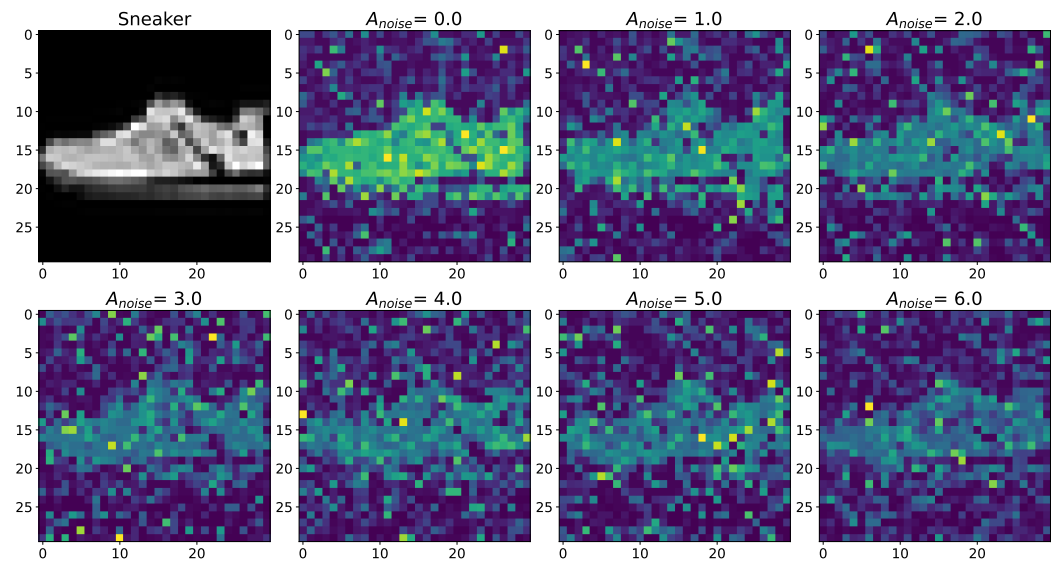


**Figure S46.** Changes in the spatial sweep of the spike neural network during the representation of the supplied image category 7 from database Fashion-MNIST [2] when the amplitude,  $A_{noise}$ , of the noise current,  $I_{noise}$ , changes from 0 to 6 without modulation of neuronal activity by astrocytes.

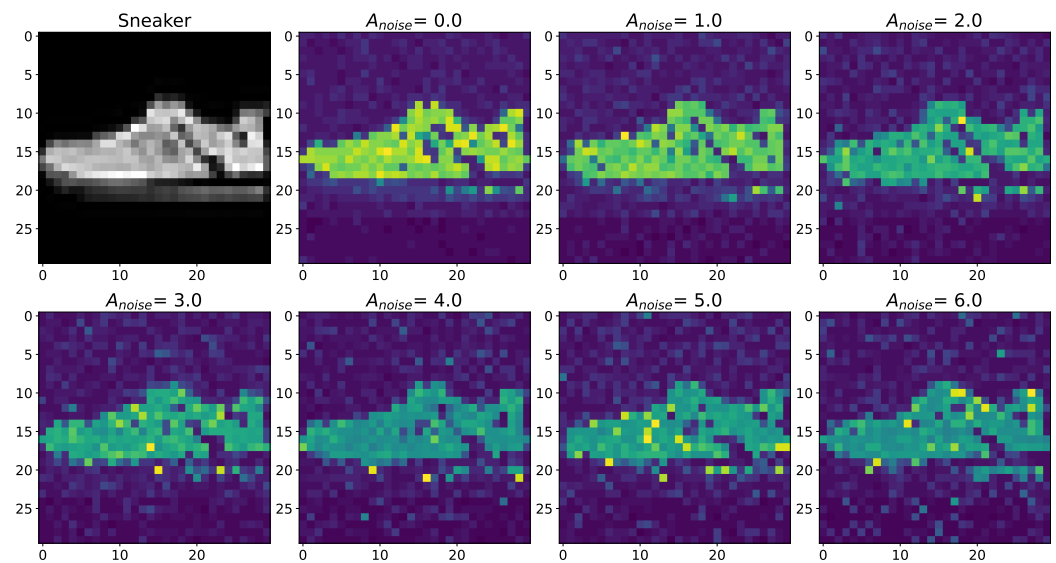


**Figure S47.** Changes in the spatial sweep of the spike neural network during the representation of the supplied image category 7 from database Fashion-MNIST [2] when the amplitude,  $A_{noise}$ , of the noise current,  $I_{noise}$ , changes from 0 to 6 with modulation of neuronal activity by astrocytes.

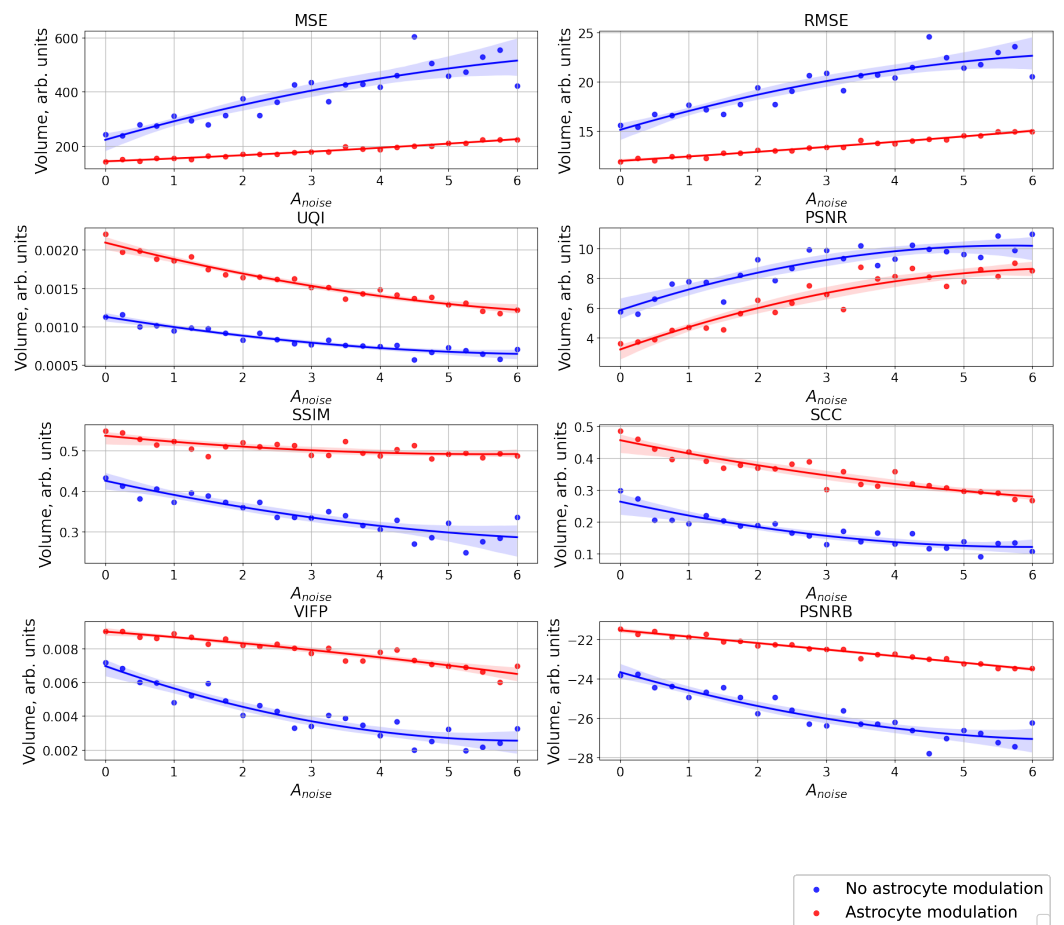


**Figure S48.** The case of using a quality metrics (MSE, RMSE, UQI, PSNR, SSIM, SCC, VIFP, PSNRB) for comparing raster diagrams of neural activity from Figure S46 and Figure S47 with an image category 7 from database Fashion-MNIST [2] fed to a spike neural network with an increase in the amplitude,  $A_{noise}$ , of the noise signal from 0 to 6 supplied to the neurons of the neural network without astrocytic modulation (blue dots and curve) and with astrocytic modulation (red dots and curve).

S2.9. Category 8 from database Fashion-MNIST

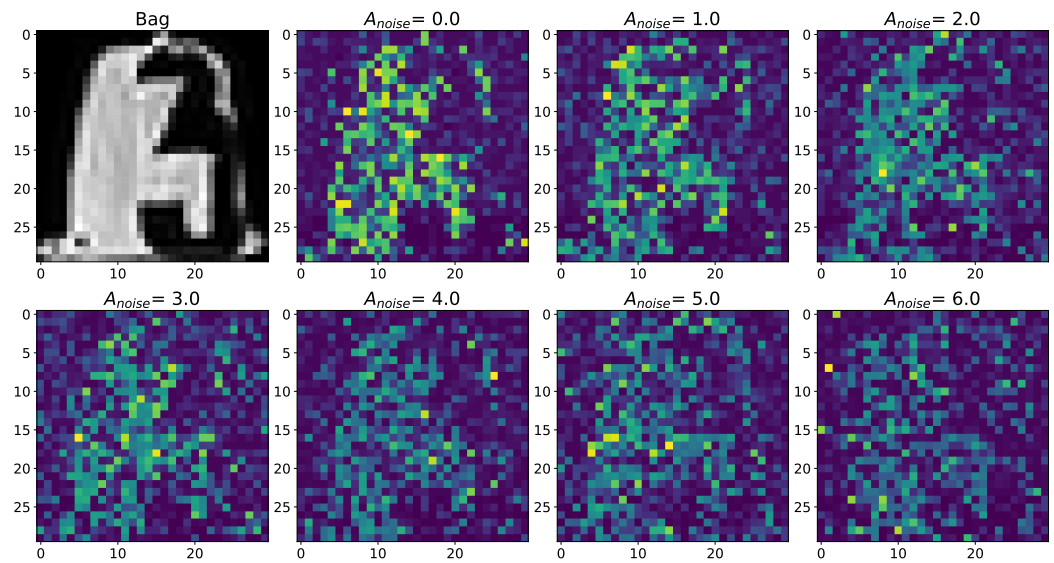


**Figure S49.** Changes in the spatial sweep of the spike neural network during the representation of the supplied image category 8 from database Fashion-MNIST [2] when the amplitude,  $A_{noise}$ , of the noise current,  $I_{noise}$ , changes from 0 to 6 without modulation of neuronal activity by astrocytes.

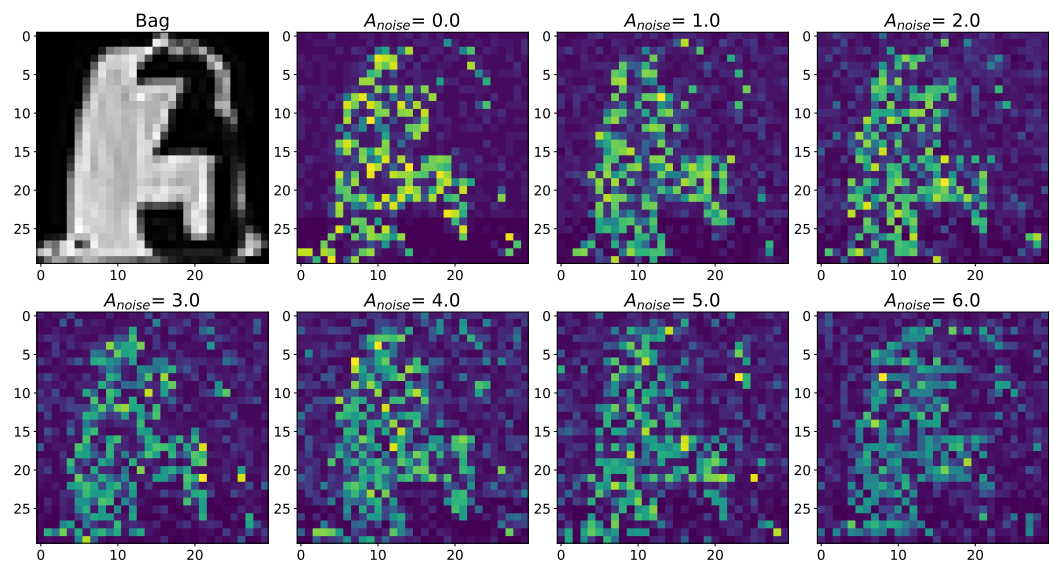


**Figure S50.** Changes in the spatial sweep of the spike neural network during the representation of the supplied image category 8 from database Fashion-MNIST [2] when the amplitude,  $A_{noise}$ , of the noise current,  $I_{noise}$ , changes from 0 to 6 with modulation of neuronal activity by astrocytes.

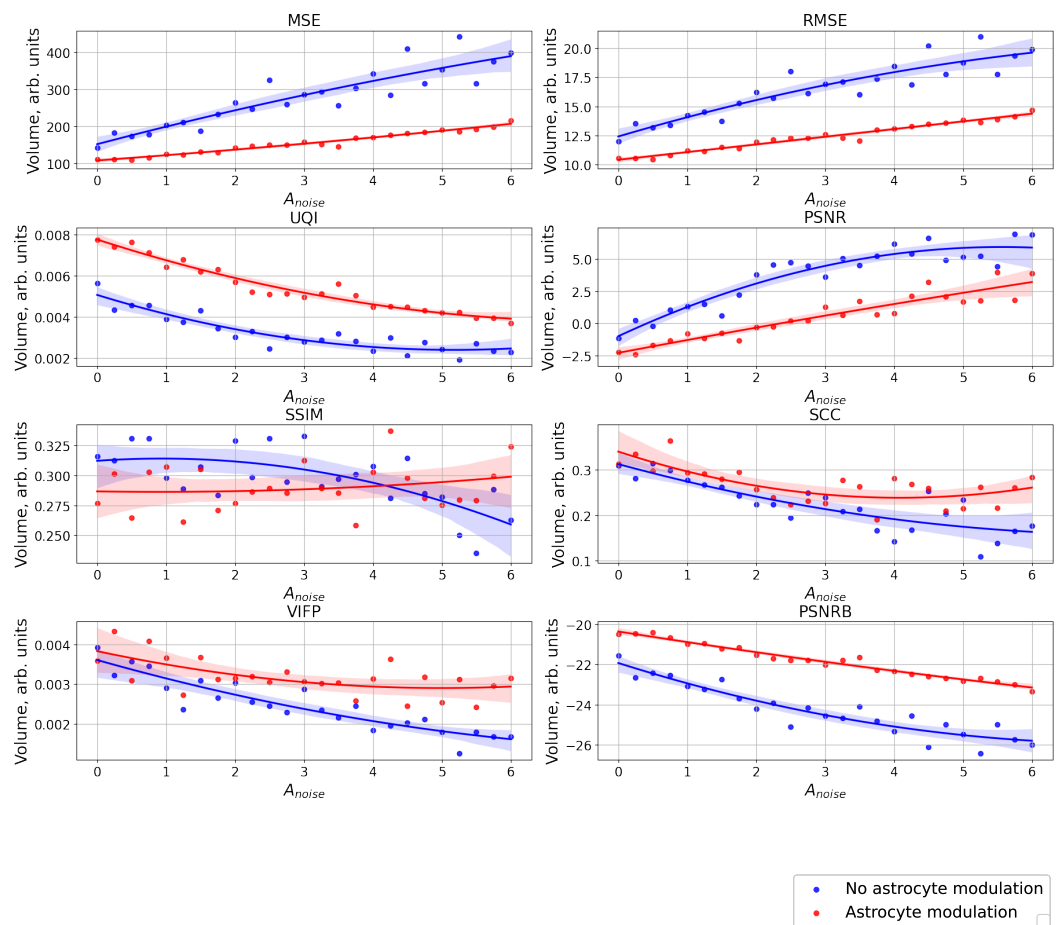


**Figure S51.** The case of using a quality metrics (MSE, RMSE, UQI, PSNR, SSIM, SCC, VIFP, PSNRB) for comparing raster diagrams of neural activity from Figure S49 and Figure S50 with an image category 8 from database Fashion-MNIST [2] fed to a spike neural network with an increase in the amplitude,  $A_{noise}$ , of the noise signal from 0 to 6 supplied to the neurons of the neural network without astrocytic modulation (blue dots and curve) and with astrocytic modulation (red dots and curve).

S2.10. Category 9 from database Fashion-MNIST

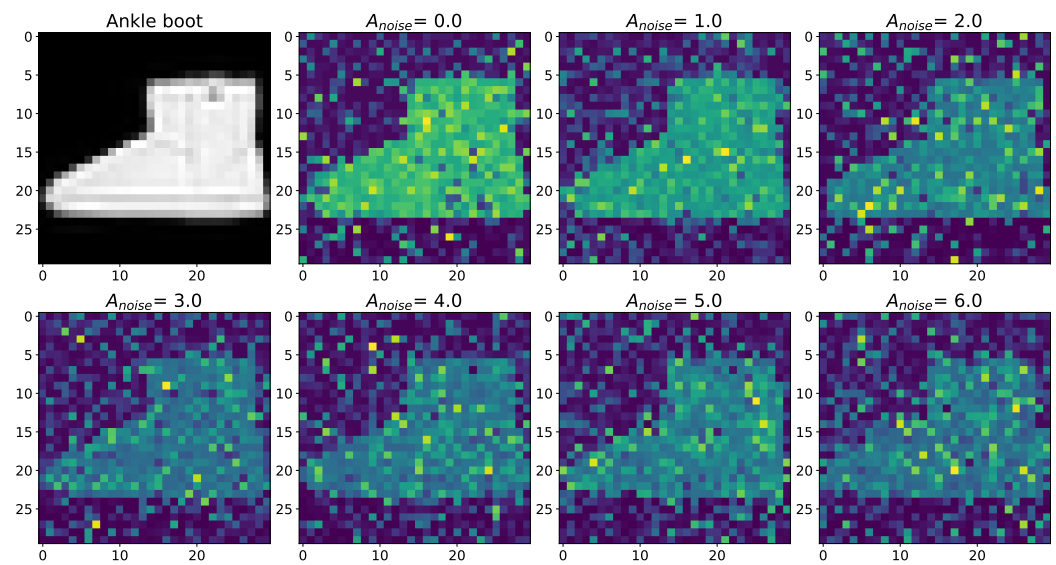


**Figure S52.** Changes in the spatial sweep of the spike neural network during the representation of the supplied image category 9 from database Fashion-MNIST [2] when the amplitude,  $A_{noise}$ , of the noise current,  $I_{noise}$ , changes from 0 to 6 without modulation of neuronal activity by astrocytes.

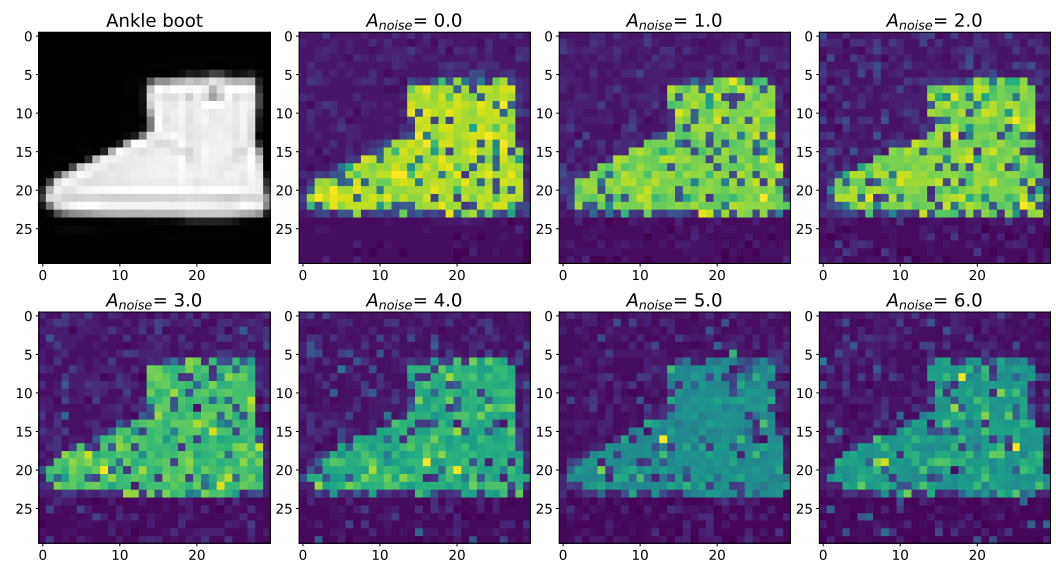


**Figure S53.** Changes in the spatial sweep of the spike neural network during the representation of the supplied image category 9 from database Fashion-MNIST [2] when the amplitude,  $A_{noise}$ , of the noise current,  $I_{noise}$ , changes from 0 to 6 with modulation of neuronal activity by astrocytes.

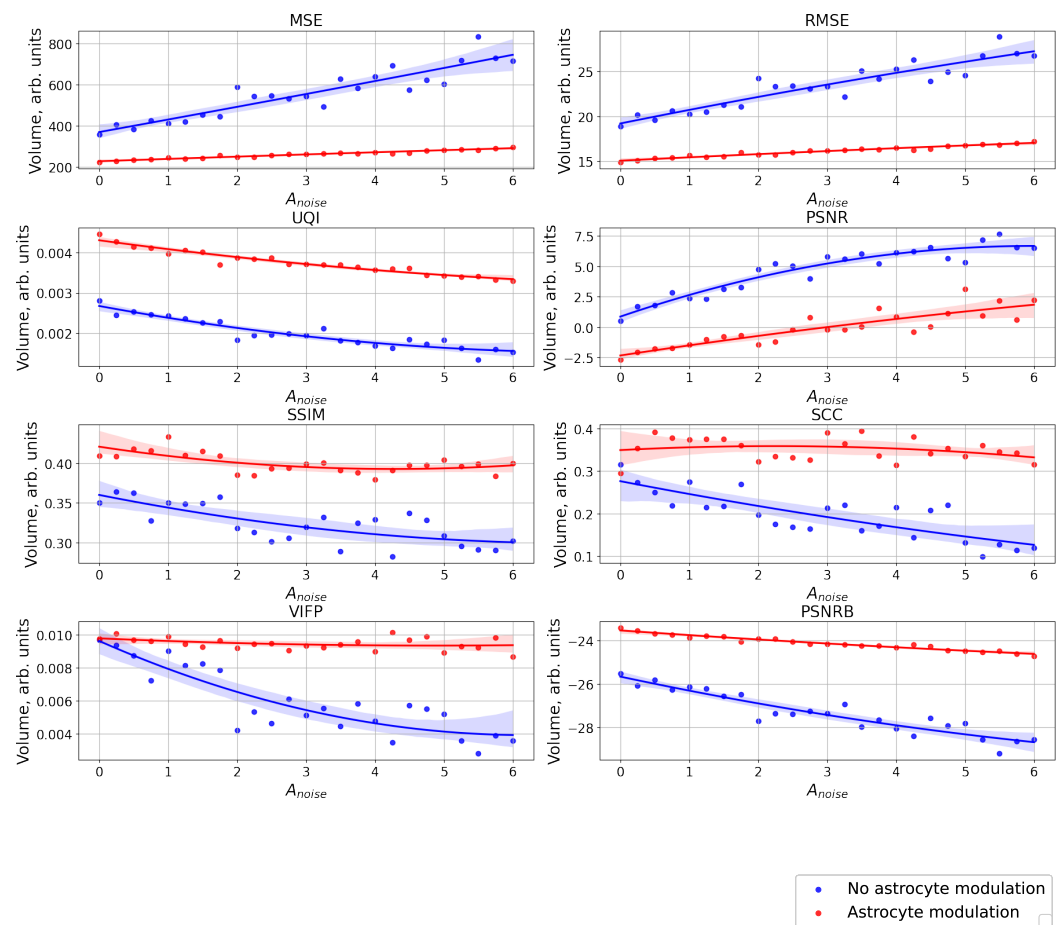


**Figure S54.** The case of using a quality metrics (MSE, RMSE, UQI, PSNR, SSIM, SCC, VIFP, PSNRB) for comparing raster diagrams of neural activity from Figure S49 and Figure S50 with an image category 9 from database Fashion-MNIST [2] fed to a spike neural network with an increase in the amplitude,  $A_{noise}$ , of the noise signal from 0 to 6 supplied to the neurons of the neural network without astrocytic modulation (blue dots and curve) and with astrocytic modulation (red dots and curve).

### S3. Cases with numbers from database SVHN

#### S3.1. Number 0 from database SVHN

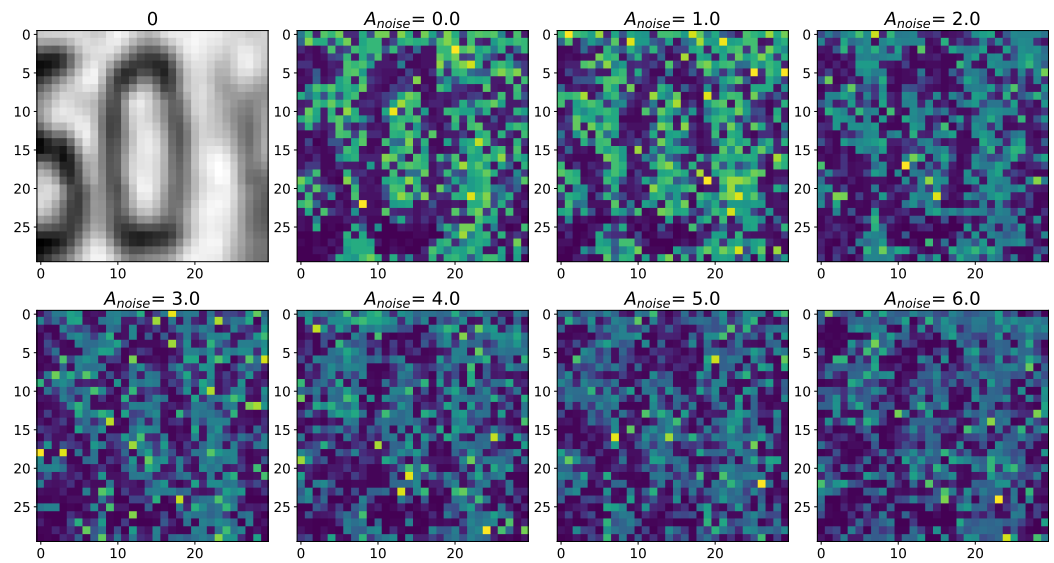


**Figure S55.** Changes in the spatial sweep of the spike neural network during the representation of the supplied image 0 from database SVHN [3] when the amplitude,  $A_{noise}$ , of the noise current,  $I_{noise}$ , changes from 0 to 6 without modulation of neuronal activity by astrocytes.

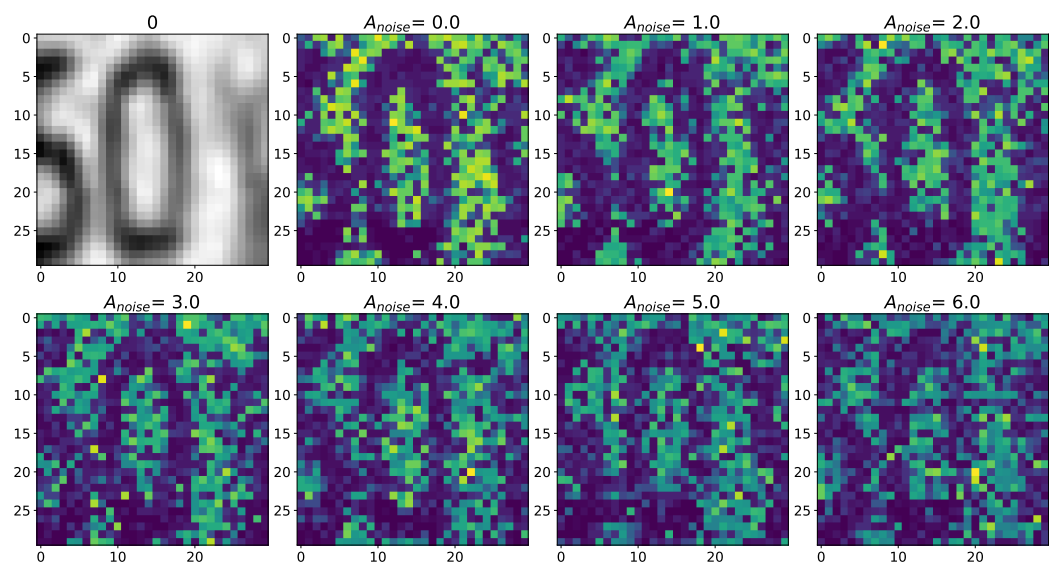


**Figure S56.** Changes in the spatial sweep of the spike neural network during the representation of the supplied image 0 from database SVHN [3] when the amplitude,  $A_{noise}$ , of the noise current,  $I_{noise}$ , changes from 0 to 6 with modulation of neuronal activity by astrocytes.

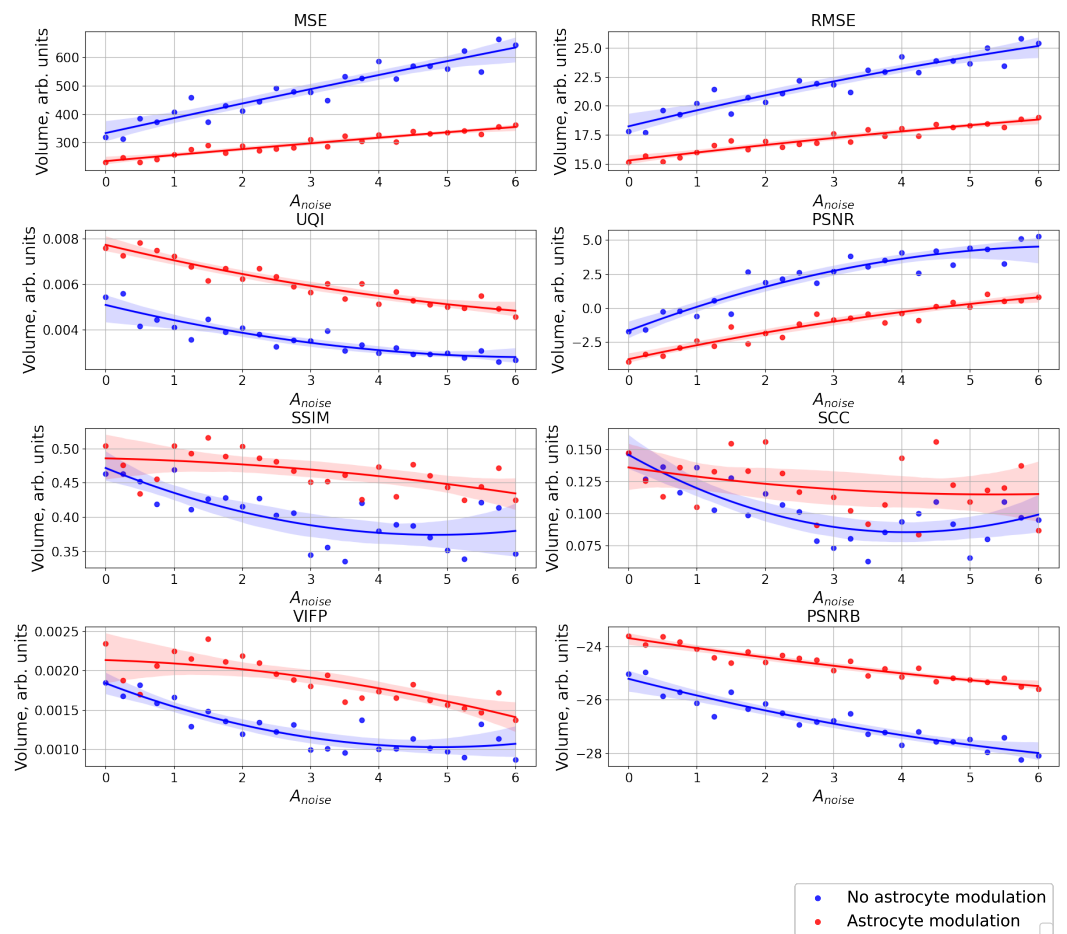


**Figure S57.** The case of using a quality metrics (MSE, RMSE, UQI, PSNR, SSIM, SCC, VIFP, PSNRB) for comparing raster diagrams of neural activity from Figure S55 and Figure S56 with an image 0 from database SVHN [3] fed to a spike neural network with an increase in the amplitude,  $A_{noise}$ , of the noise signal from 0 to 6 supplied to the neurons of the neural network without astrocytic modulation (blue dots and curve) and with astrocytic modulation (red dots and curve).

S3.2. Number 1 from database SVHN

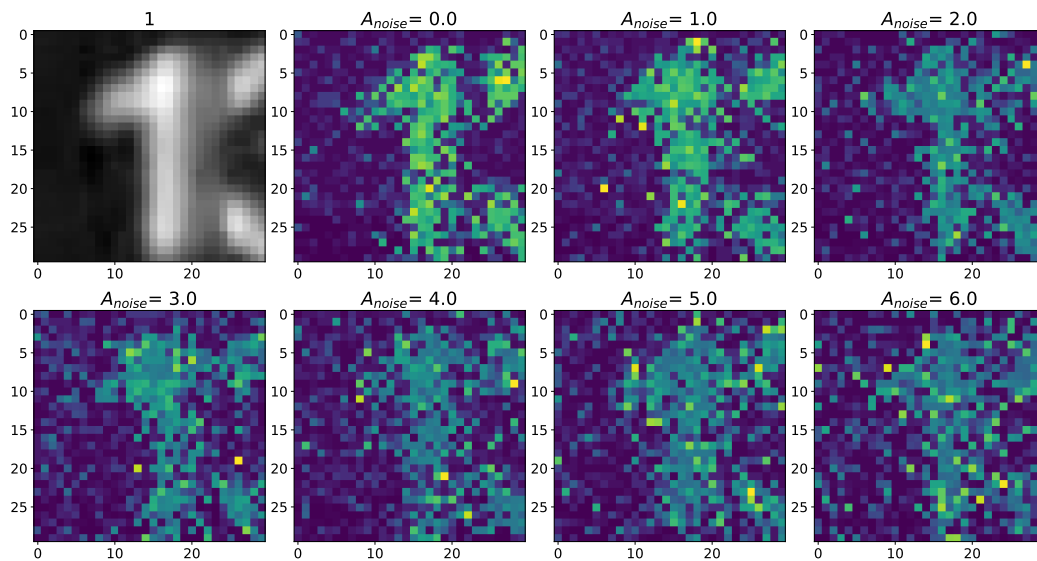


**Figure S58.** Changes in the spatial sweep of the spike neural network during the representation of the supplied image 1 from database SVHN [3] when the amplitude,  $A_{noise}$ , of the noise current,  $I_{noise}$ , changes from 0 to 6 without modulation of neuronal activity by astrocytes.

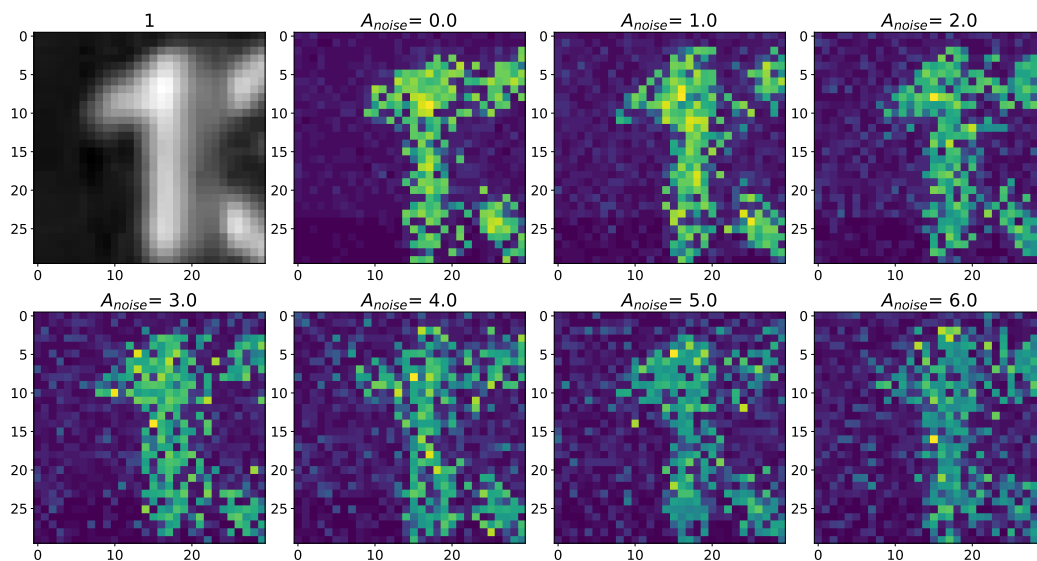


**Figure S59.** Changes in the spatial sweep of the spike neural network during the representation of the supplied image 1 from database SVHN [3] when the amplitude,  $A_{noise}$ , of the noise current,  $I_{noise}$ , changes from 0 to 6 with modulation of neuronal activity by astrocytes.

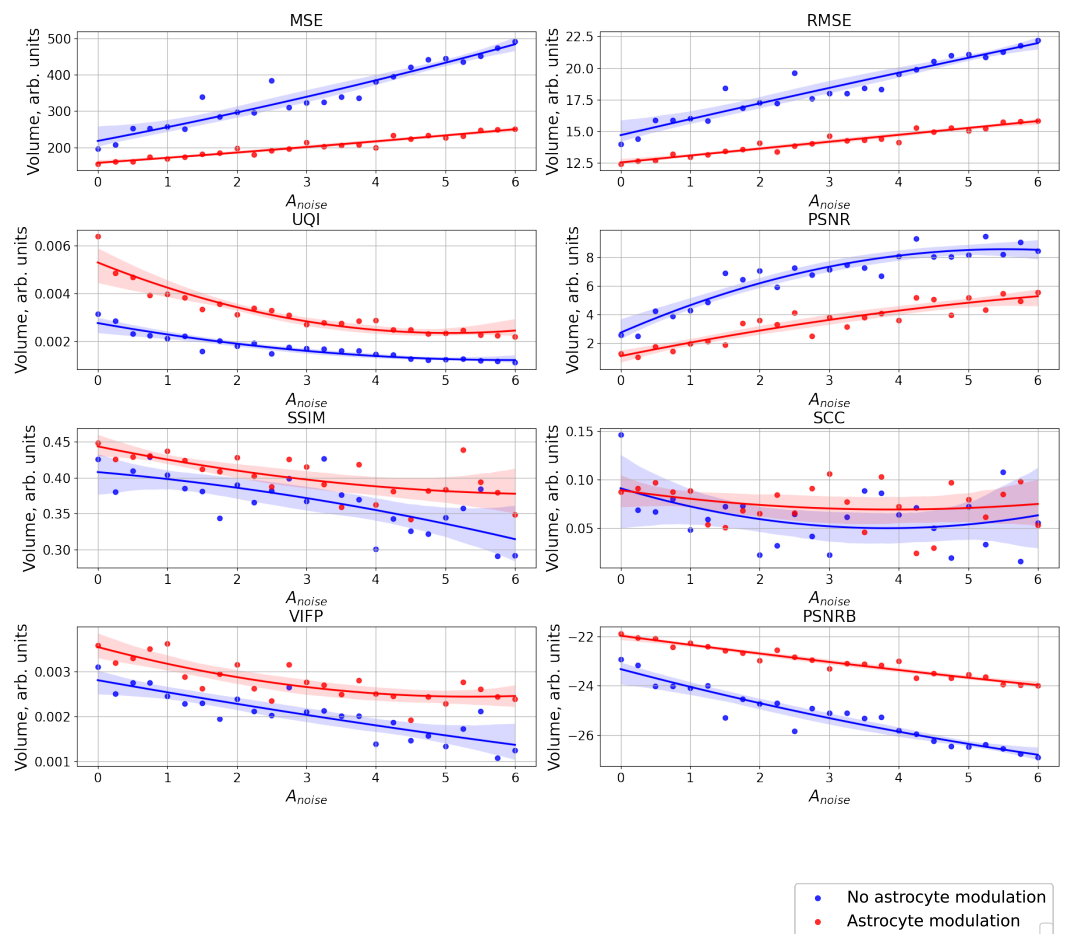


**Figure S60.** The case of using a quality metrics (MSE, RMSE, UQI, PSNR, SSIM, SCC, VIFP, PSNRB) for comparing raster diagrams of neural activity from Figure S58 and Figure S59 with an image 1 from database SVHN [3] fed to a spike neural network with an increase in the amplitude,  $A_{noise}$ , of the noise signal from 0 to 6 supplied to the neurons of the neural network without astrocytic modulation (blue dots and curve) and with astrocytic modulation (red dots and curve).

S3.3. Number 2 from database SVHN

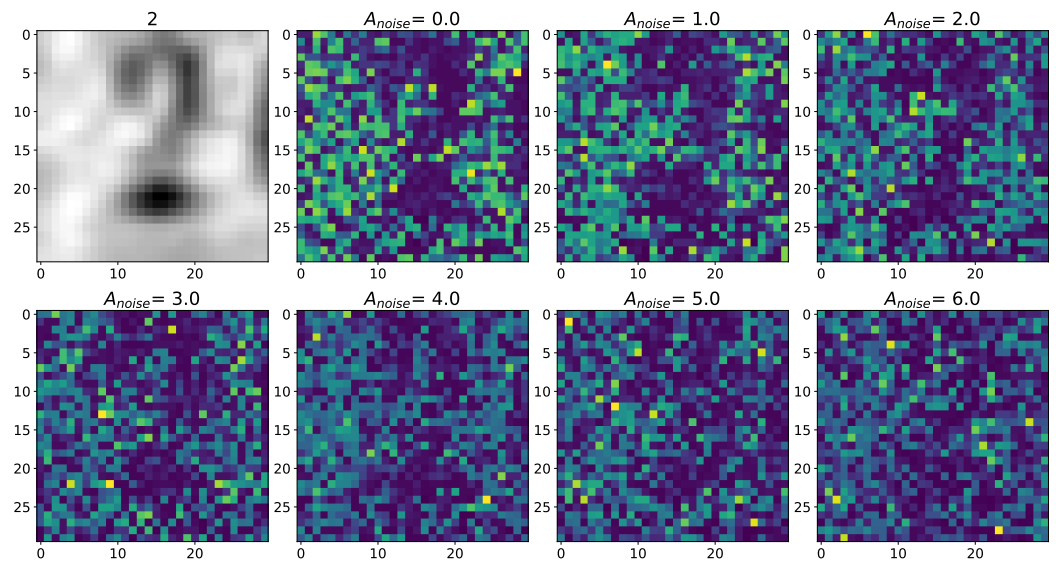


**Figure S61.** Changes in the spatial sweep of the spike neural network during the representation of the supplied image 2 from database SVHN [3] when the amplitude,  $A_{noise}$ , of the noise current,  $I_{noise}$ , changes from 0 to 6 without modulation of neuronal activity by astrocytes.

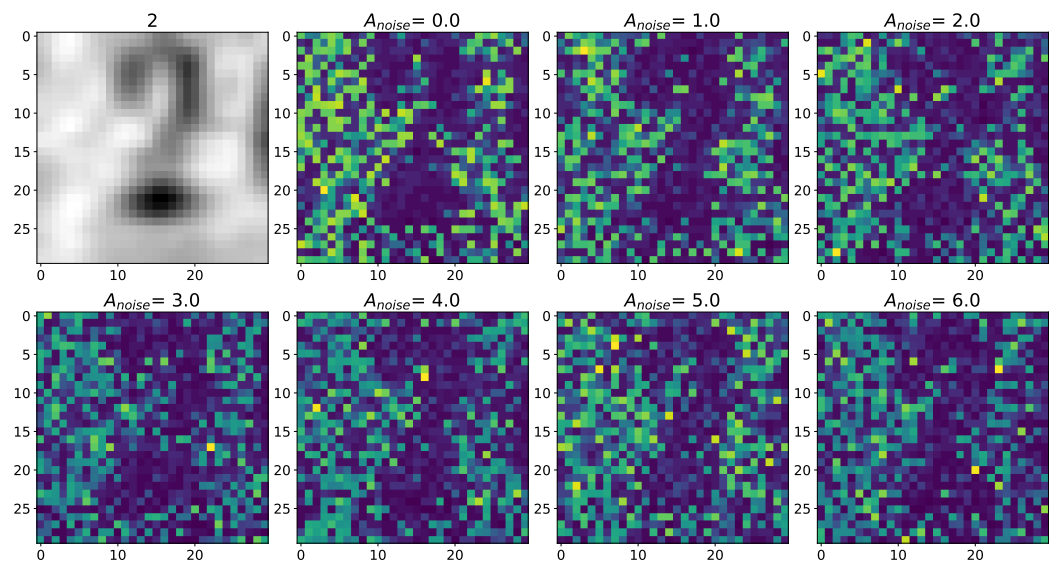


**Figure S62.** Changes in the spatial sweep of the spike neural network during the representation of the supplied image 2 from database SVHN [3] when the amplitude,  $A_{noise}$ , of the noise current,  $I_{noise}$ , changes from 0 to 6 with modulation of neuronal activity by astrocytes.

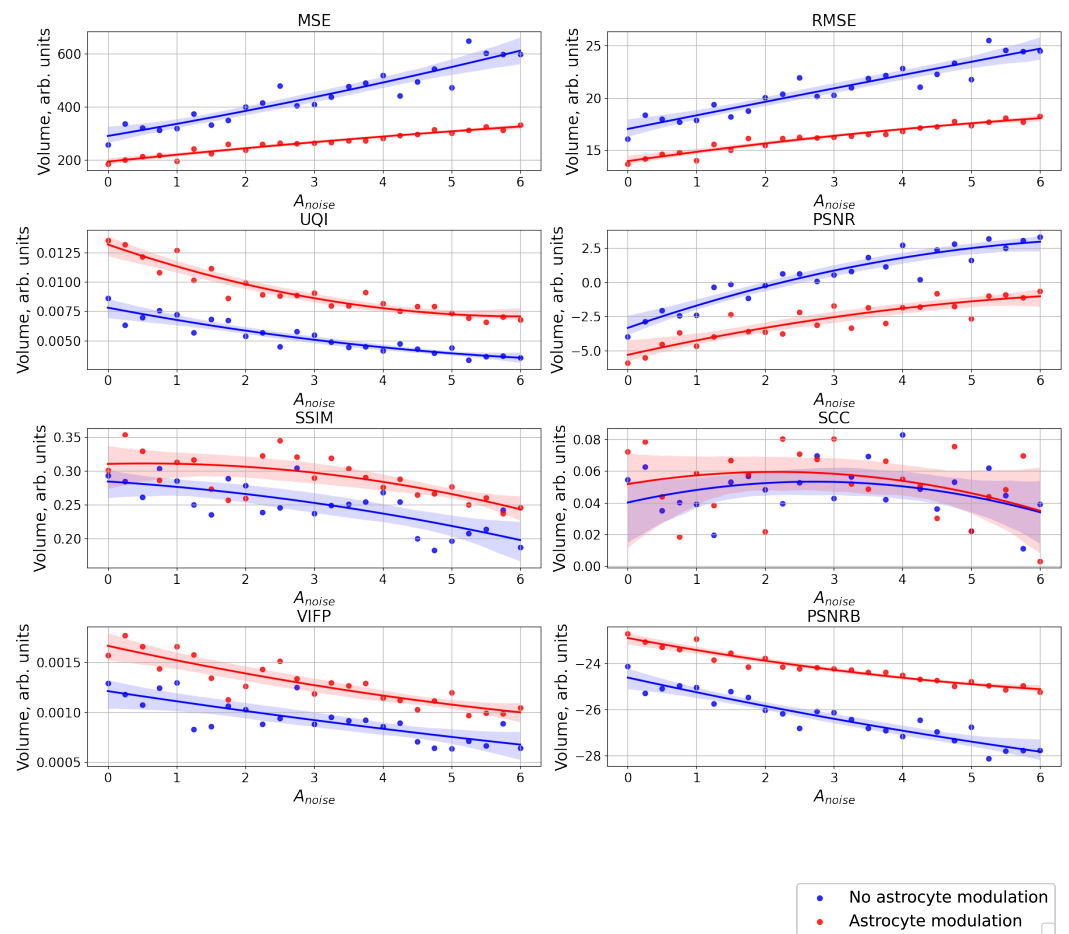


**Figure S63.** The case of using a quality metrics (MSE, RMSE, UQI, PSNR, SSIM, SCC, VIFP, PSNRB) for comparing raster diagrams of neural activity from Figure S61 and Figure S62 with an image 2 from database SVHN [3] fed to a spike neural network with an increase in the amplitude,  $A_{noise}$ , of the noise signal from 0 to 6 supplied to the neurons of the neural network without astrocytic modulation (blue dots and curve) and with astrocytic modulation (red dots and curve).

S3.4. Number 3 from database SVHN

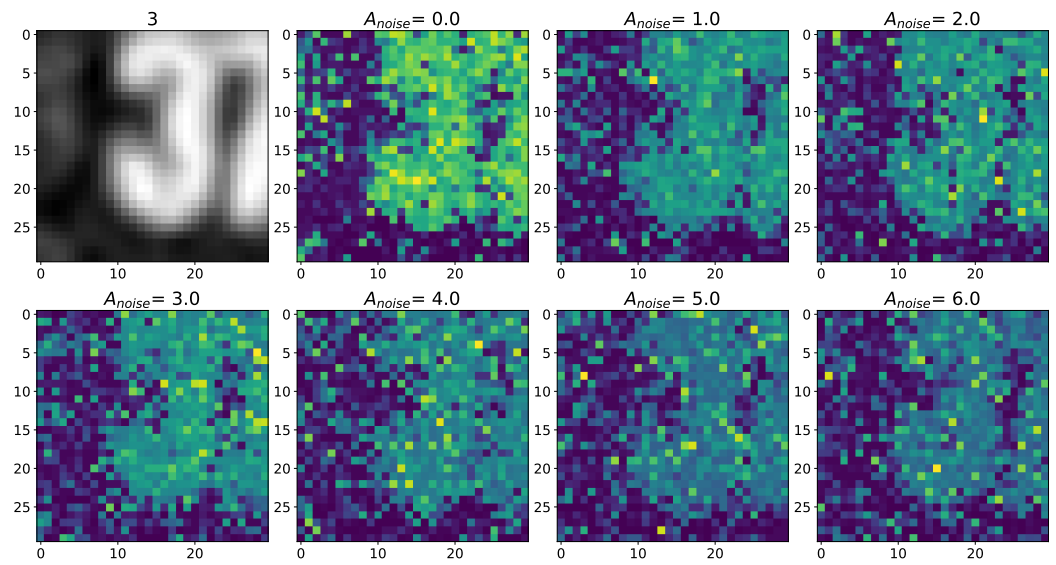


**Figure S64.** Changes in the spatial sweep of the spike neural network during the representation of the supplied image 3 from database SVHN [3] when the amplitude,  $A_{noise}$ , of the noise current,  $I_{noise}$ , changes from 0 to 6 without modulation of neuronal activity by astrocytes.

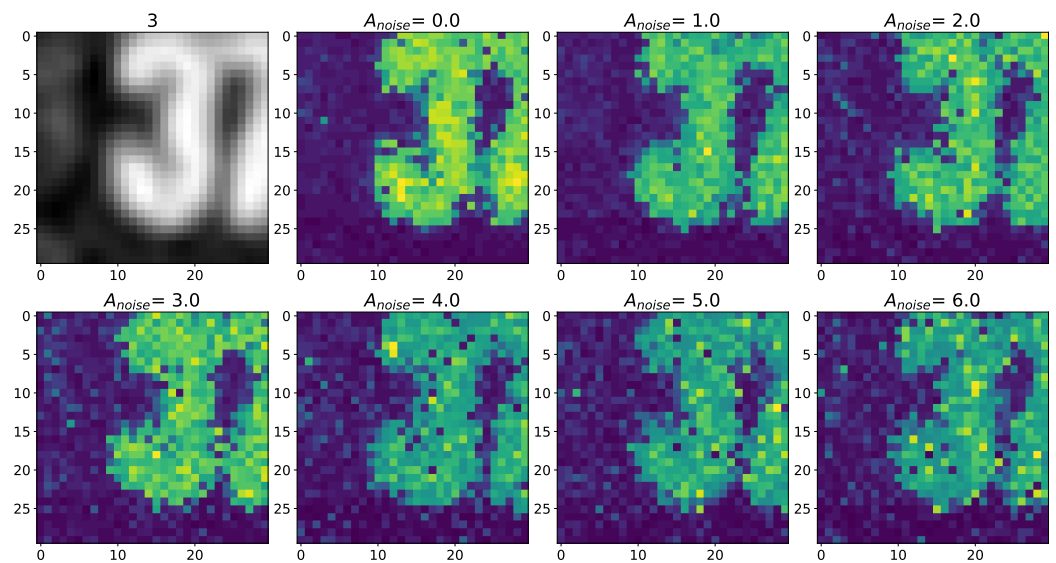


**Figure S65.** Changes in the spatial sweep of the spike neural network during the representation of the supplied image 3 from database SVHN [3] when the amplitude,  $A_{noise}$ , of the noise current,  $I_{noise}$ , changes from 0 to 6 with modulation of neuronal activity by astrocytes.

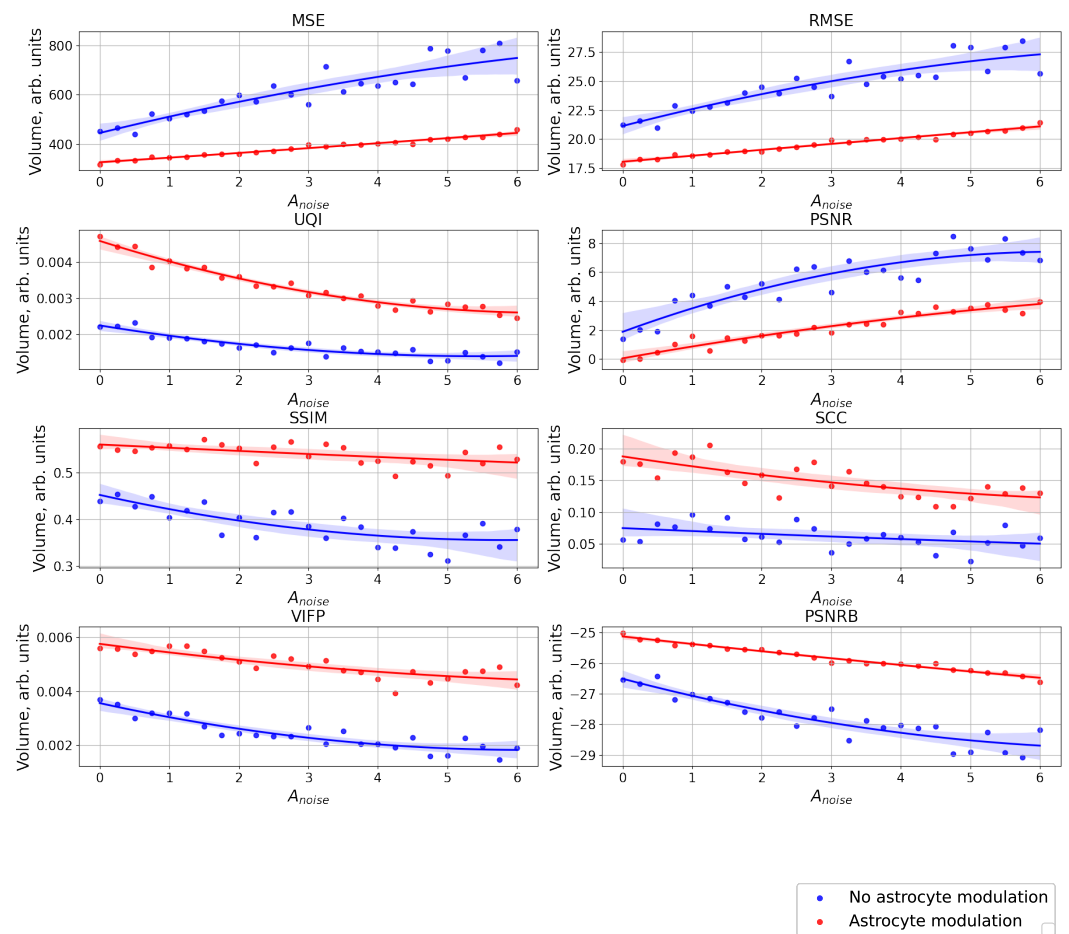


**Figure S66.** The case of using a quality metrics (MSE, RMSE, UQI, PSNR, SSIM, SCC, VIFP, PSNRB) for comparing raster diagrams of neural activity from Figure S64 and Figure S65 with an image 3 from database SVHN [3] fed to a spike neural network with an increase in the amplitude,  $A_{noise}$ , of the noise signal from 0 to 6 supplied to the neurons of the neural network without astrocytic modulation (blue dots and curve) and with astrocytic modulation (red dots and curve).

S3.5. Number 4 from database SVHN

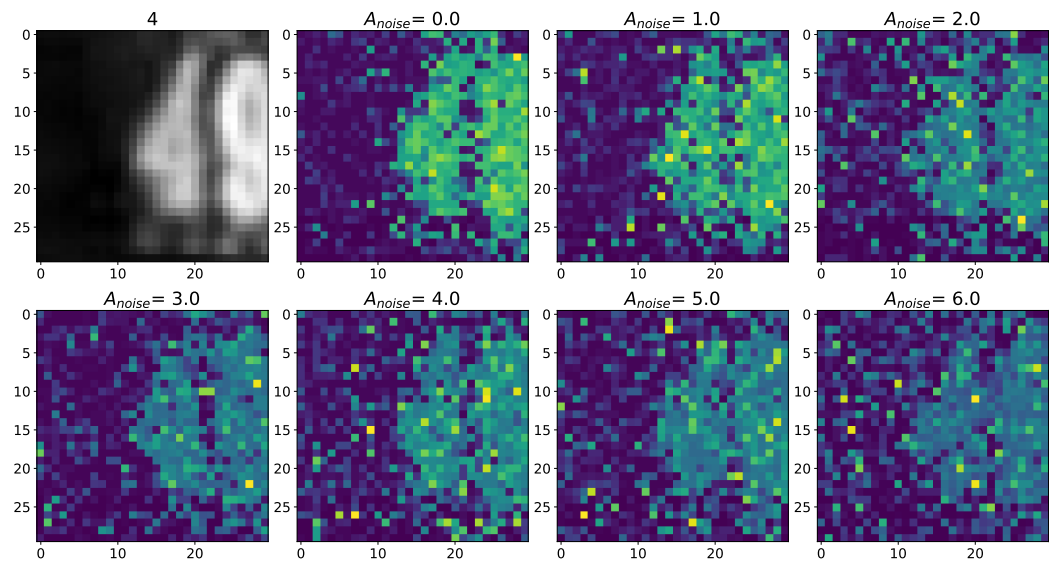


**Figure S67.** Changes in the spatial sweep of the spike neural network during the representation of the supplied image 4 from database SVHN [3] when the amplitude,  $A_{noise}$ , of the noise current,  $I_{noise}$ , changes from 0 to 6 without modulation of neuronal activity by astrocytes.

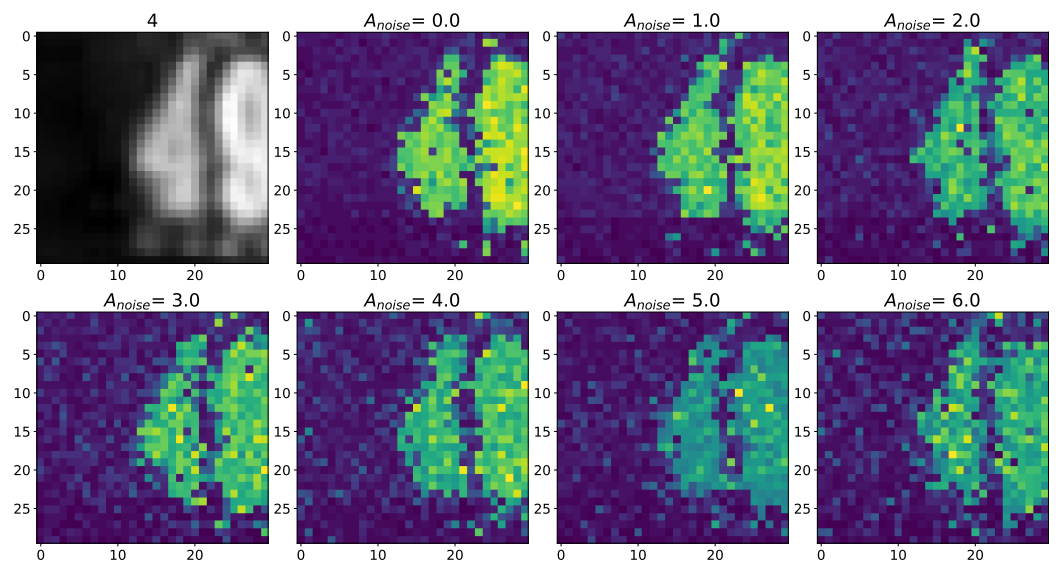


**Figure S68.** Changes in the spatial sweep of the spike neural network during the representation of the supplied image 4 from database SVHN [3] when the amplitude,  $A_{noise}$ , of the noise current,  $I_{noise}$ , changes from 0 to 6 with modulation of neuronal activity by astrocytes.

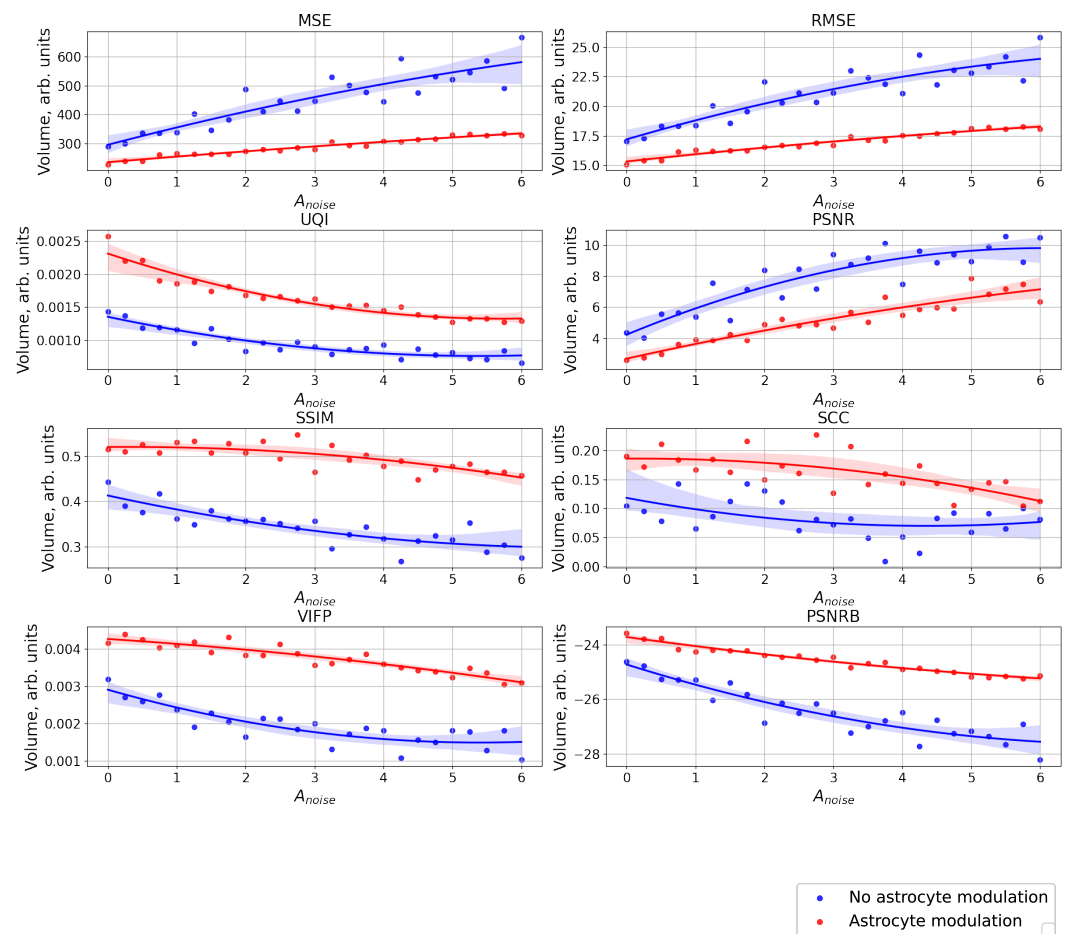


**Figure S69.** The case of using a quality metrics (MSE, RMSE, UQI, PSNR, SSIM, SCC, VIFP, PSNRB) for comparing raster diagrams of neural activity from Figure S67 and Figure S68 with an image 4 from database SVHN [3] fed to a spike neural network with an increase in the amplitude,  $A_{noise}$ , of the noise signal from 0 to 6 supplied to the neurons of the neural network without astrocytic modulation (blue dots and curve) and with astrocytic modulation (red dots and curve).

S3.6. Number 5 from database SVHN

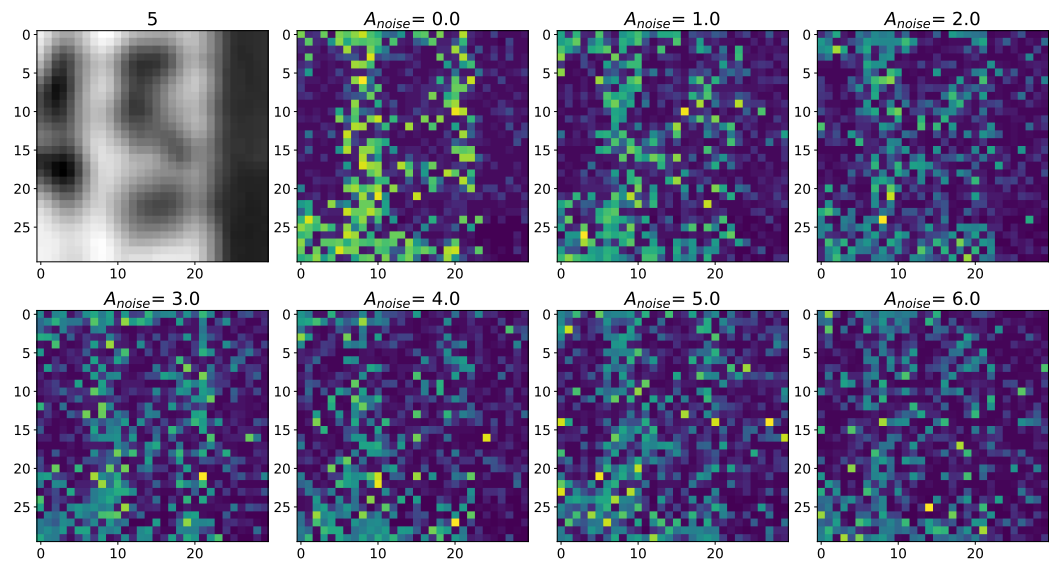


**Figure S70.** Changes in the spatial sweep of the spike neural network during the representation of the supplied image 5 from database SVHN [3] when the amplitude,  $A_{noise}$ , of the noise current,  $I_{noise}$ , changes from 0 to 6 without modulation of neuronal activity by astrocytes.

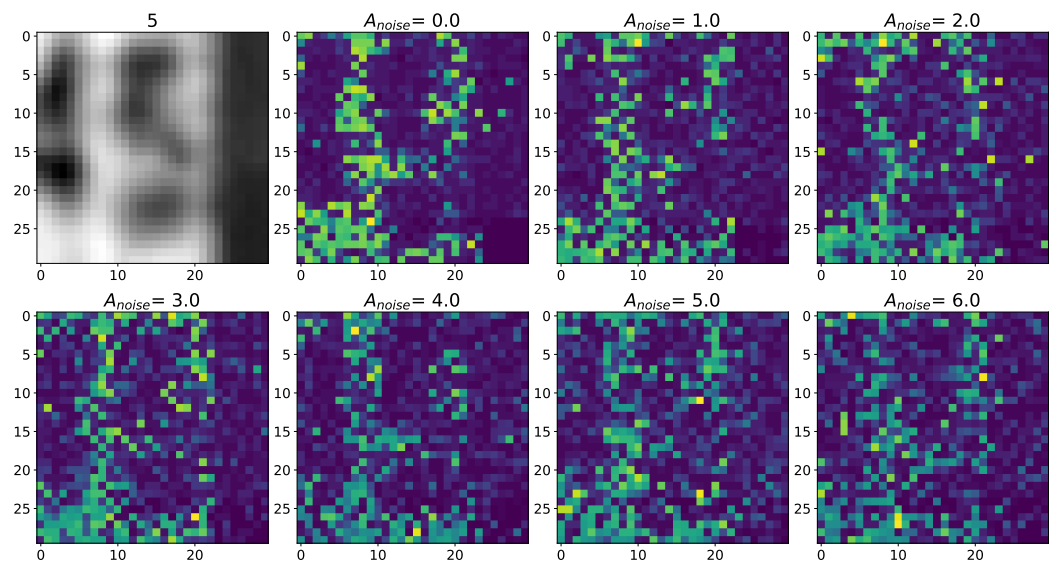


**Figure S71.** Changes in the spatial sweep of the spike neural network during the representation of the supplied image 5 from database SVHN [3] when the amplitude,  $A_{noise}$ , of the noise current,  $I_{noise}$ , changes from 0 to 6 with modulation of neuronal activity by astrocytes.

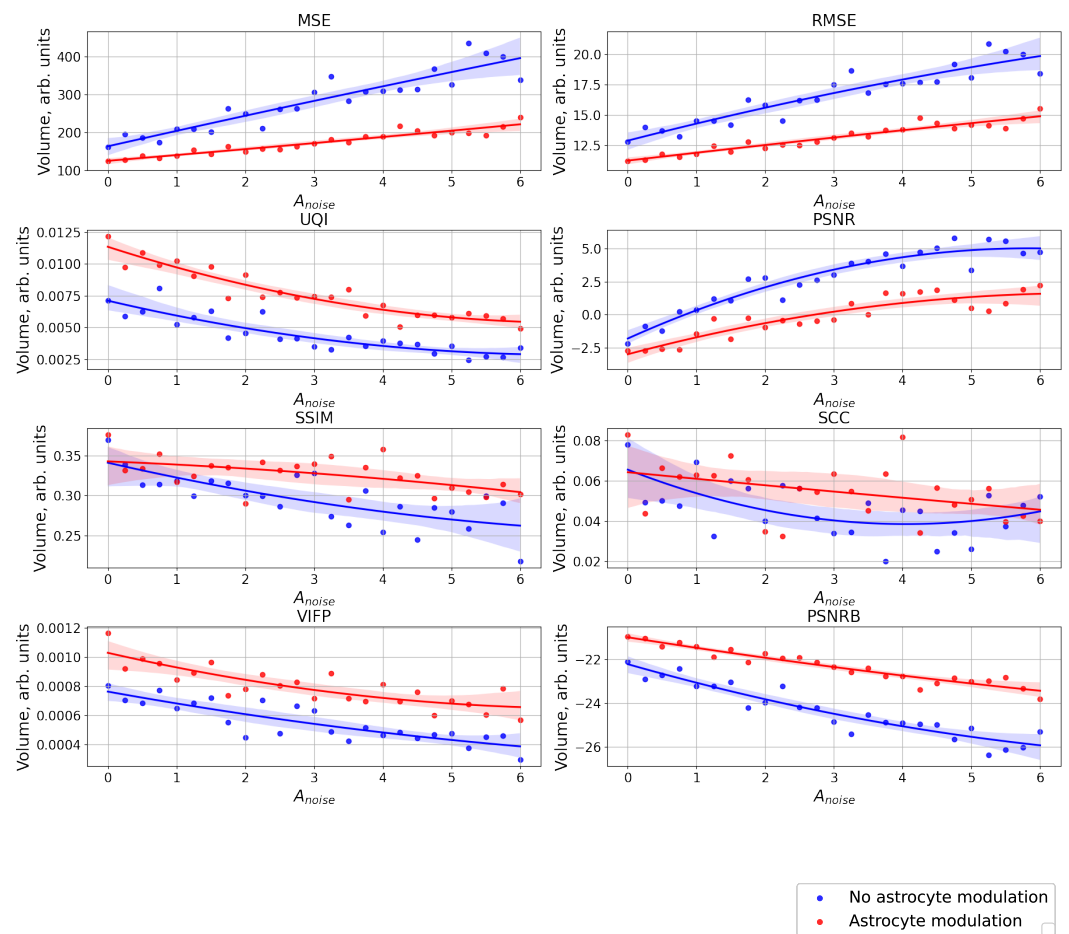


**Figure S72.** The case of using a quality metrics (MSE, RMSE, UQI, PSNR, SSIM, SCC, VIFP, PSNRB) for comparing raster diagrams of neural activity from Figure S70 and Figure S71 with an image 5 from database SVHN [3] fed to a spike neural network with an increase in the amplitude,  $A_{noise}$ , of the noise signal from 0 to 6 supplied to the neurons of the neural network without astrocytic modulation (blue dots and curve) and with astrocytic modulation (red dots and curve).

S3.7. Number 6 from database SVHN

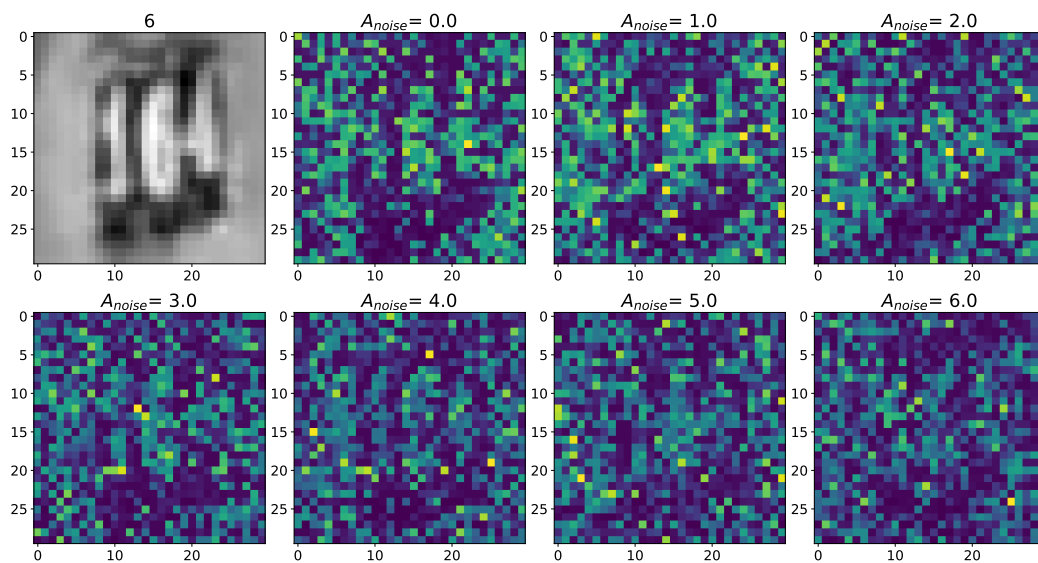


**Figure S73.** Changes in the spatial sweep of the spike neural network during the representation of the supplied image 6 from database SVHN [3] when the amplitude,  $A_{noise}$ , of the noise current,  $I_{noise}$ , changes from 0 to 6 without modulation of neuronal activity by astrocytes.

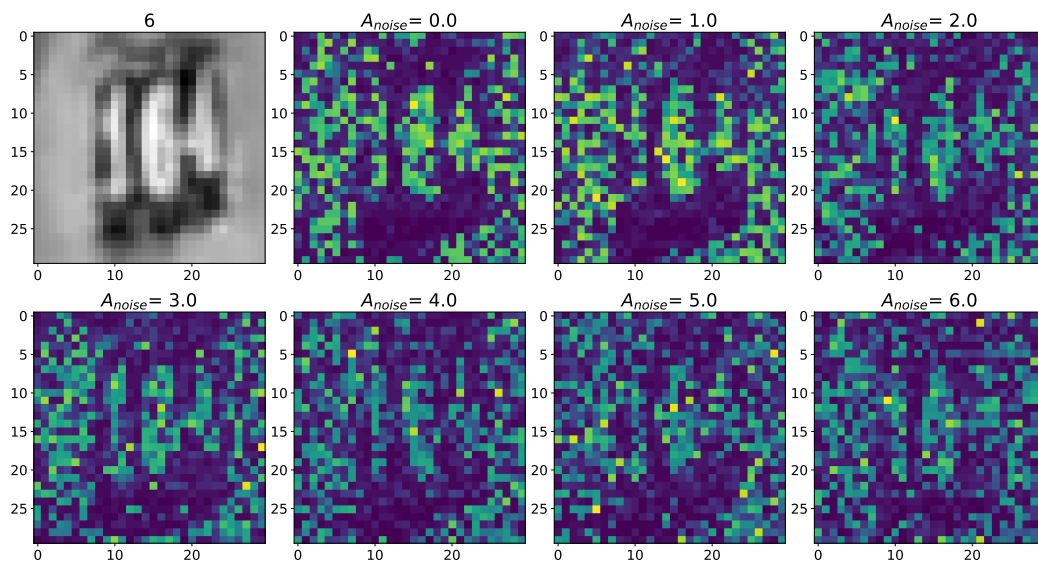


**Figure S74.** Changes in the spatial sweep of the spike neural network during the representation of the supplied image 6 from database SVHN [3] when the amplitude,  $A_{noise}$ , of the noise current,  $I_{noise}$ , changes from 0 to 6 with modulation of neuronal activity by astrocytes.

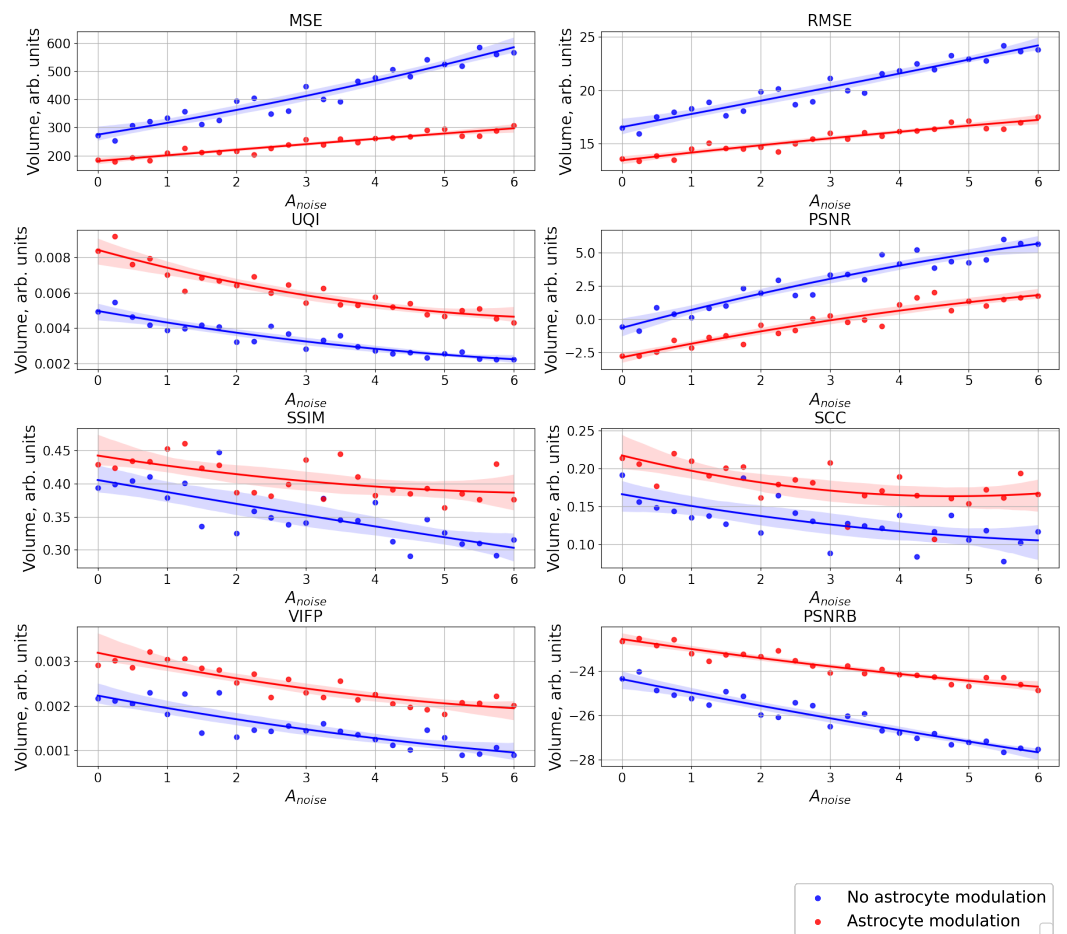


**Figure S75.** The case of using a quality metrics (MSE, RMSE, UQI, PSNR, SSIM, SCC, VIFP, PSNRB) for comparing raster diagrams of neural activity from Figure S73 and Figure S74 with an image 6 from database SVHN [3] fed to a spike neural network with an increase in the amplitude,  $A_{noise}$ , of the noise signal from 0 to 6 supplied to the neurons of the neural network without astrocytic modulation (blue dots and curve) and with astrocytic modulation (red dots and curve).

S3.8. Number 7 from database SVHN

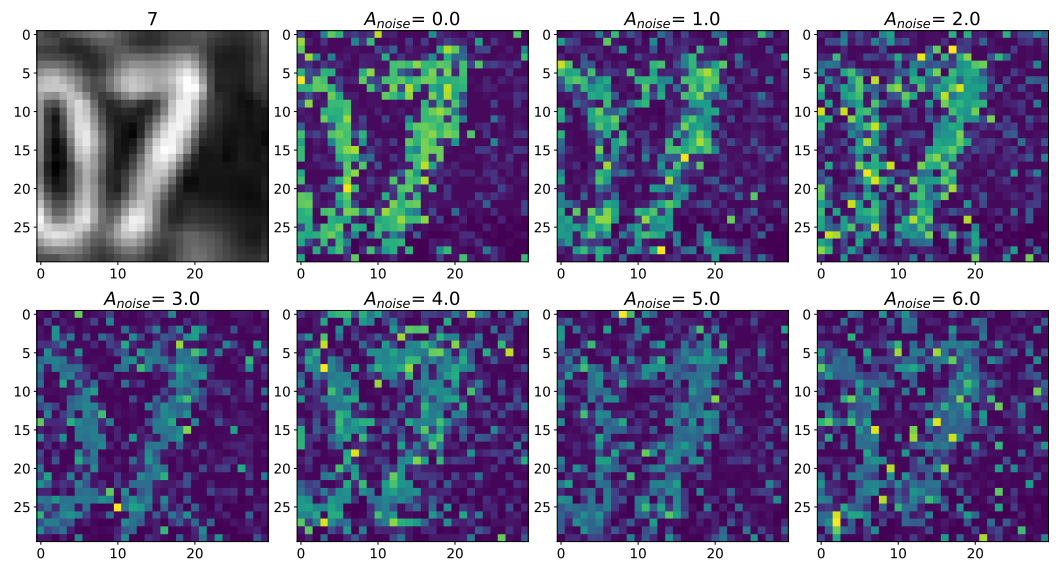


**Figure S76.** Changes in the spatial sweep of the spike neural network during the representation of the supplied image 7 from database SVHN [3] when the amplitude,  $A_{noise}$ , of the noise current,  $I_{noise}$ , changes from 0 to 6 without modulation of neuronal activity by astrocytes.

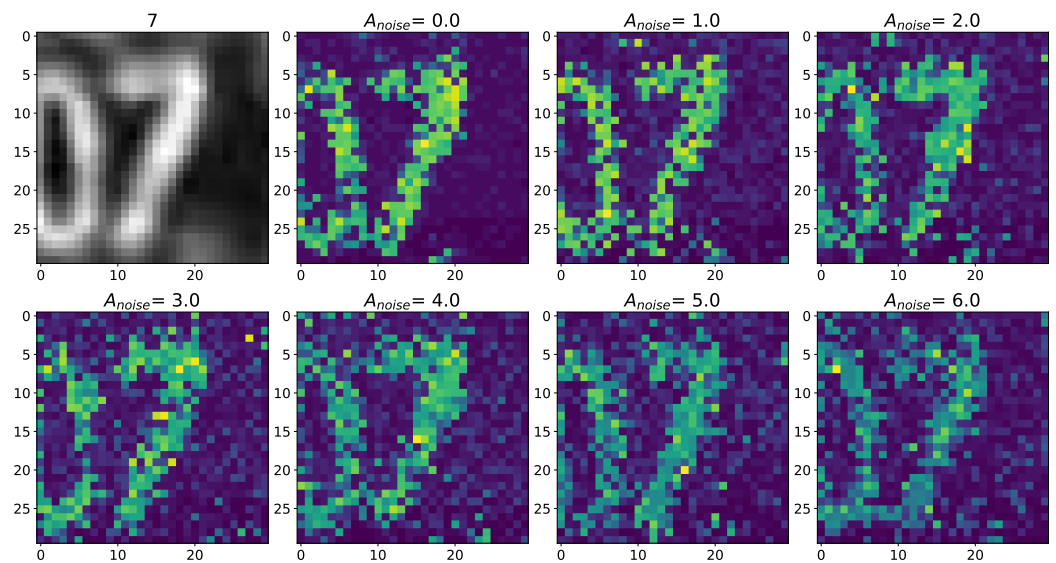


**Figure S77.** Changes in the spatial sweep of the spike neural network during the representation of the supplied image 7 from database SVHN [3] when the amplitude,  $A_{noise}$ , of the noise current,  $I_{noise}$ , changes from 0 to 6 with modulation of neuronal activity by astrocytes.

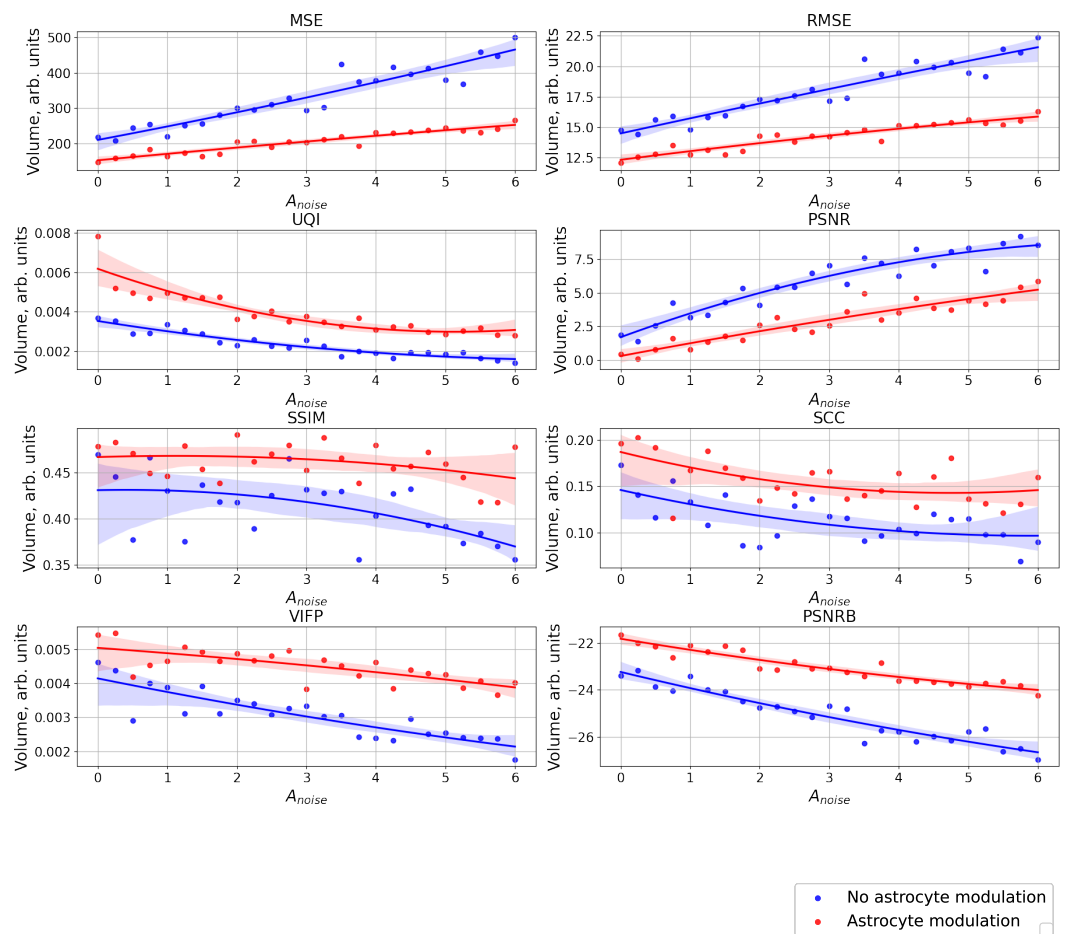


**Figure S78.** The case of using a quality metrics (MSE, RMSE, UQI, PSNR, SSIM, SCC, VIFP, PSNRB) for comparing raster diagrams of neural activity from Figure S76 and Figure ?? with an image 7 from database SVHN [3] fed to a spike neural network with an increase in the amplitude,  $A_{noise}$ , of the noise signal from 0 to 6 supplied to the neurons of the neural network without astrocytic modulation (blue dots and curve) and with astrocytic modulation (red dots and curve).

S3.9. Number 8 from database SVHN

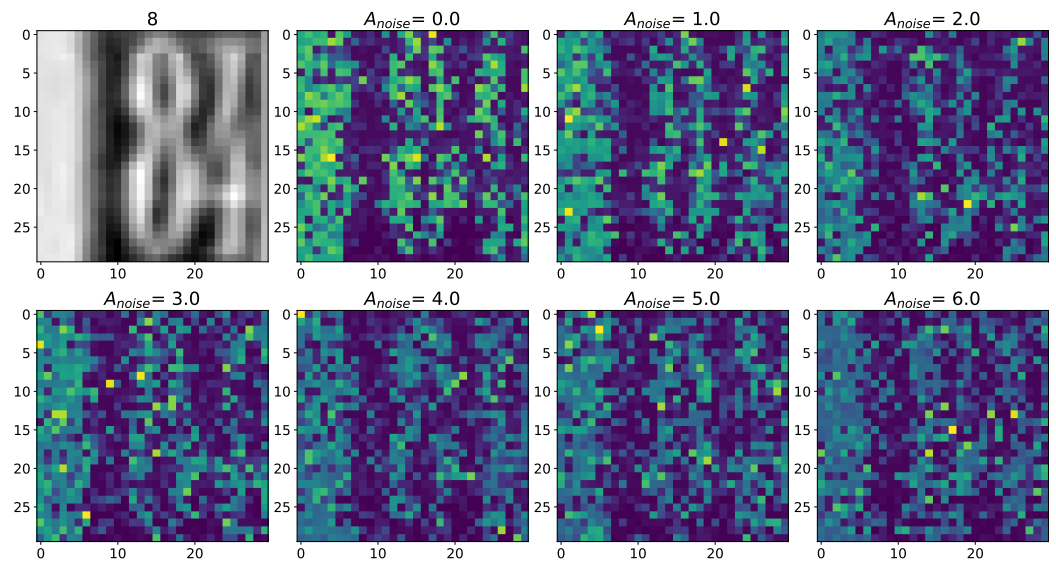


**Figure S79.** Changes in the spatial sweep of the spike neural network during the representation of the supplied image 8 from database SVHN [3] when the amplitude,  $A_{noise}$ , of the noise current,  $I_{noise}$ , changes from 0 to 6 without modulation of neuronal activity by astrocytes.

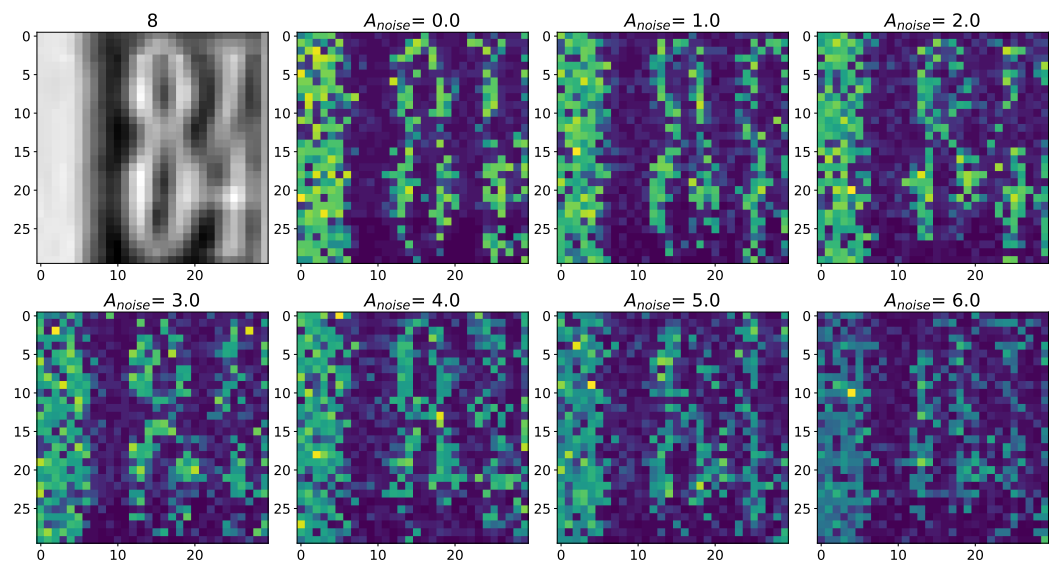


**Figure S80.** Changes in the spatial sweep of the spike neural network during the representation of the supplied image 8 from database SVHN [3] when the amplitude,  $A_{noise}$ , of the noise current,  $I_{noise}$ , changes from 0 to 6 with modulation of neuronal activity by astrocytes.

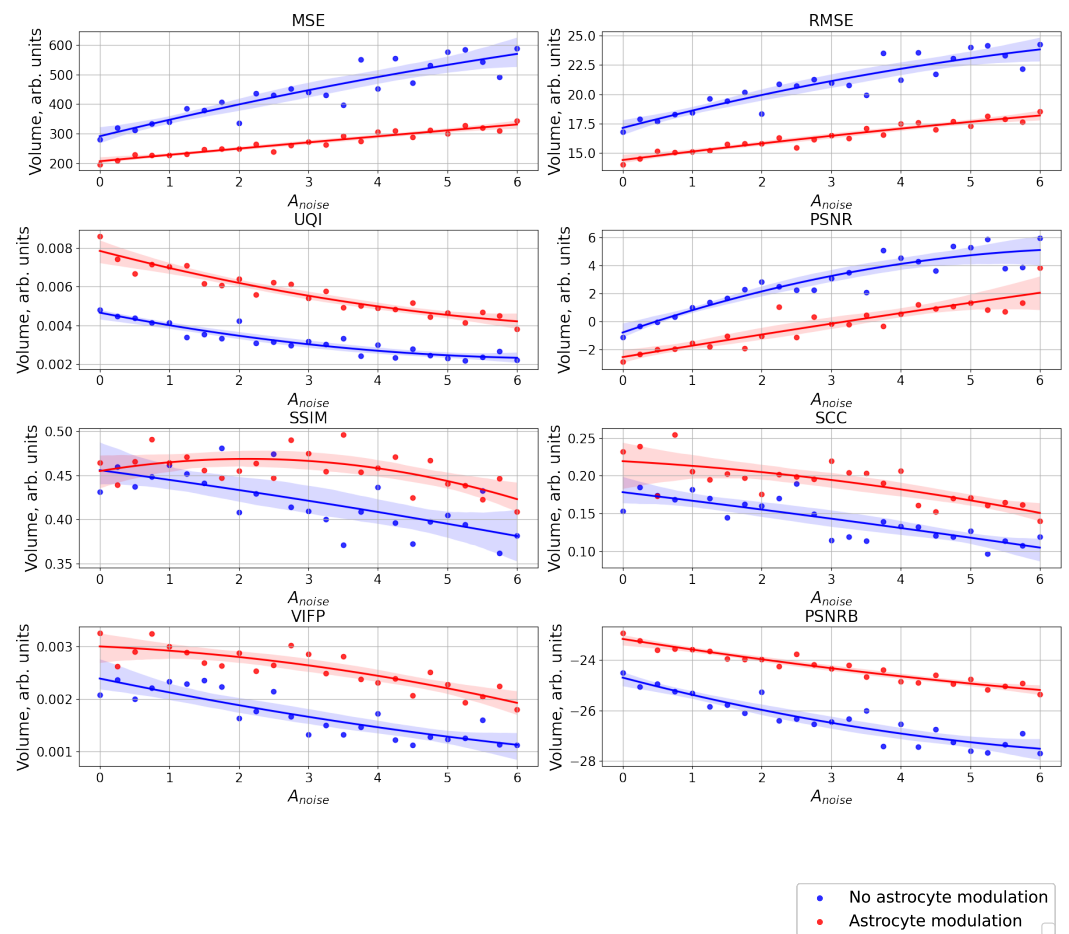


**Figure S81.** The case of using a quality metrics (MSE, RMSE, UQI, PSNR, SSIM, SCC, VIFP, PSNRB) for comparing raster diagrams of neural activity from Figure S79 and Figure S80 with an image 8 from database SVHN [3] fed to a spike neural network with an increase in the amplitude,  $A_{noise}$ , of the noise signal from 0 to 6 supplied to the neurons of the neural network without astrocytic modulation (blue dots and curve) and with astrocytic modulation (red dots and curve).

S3.10. Number 9 from database SVHN

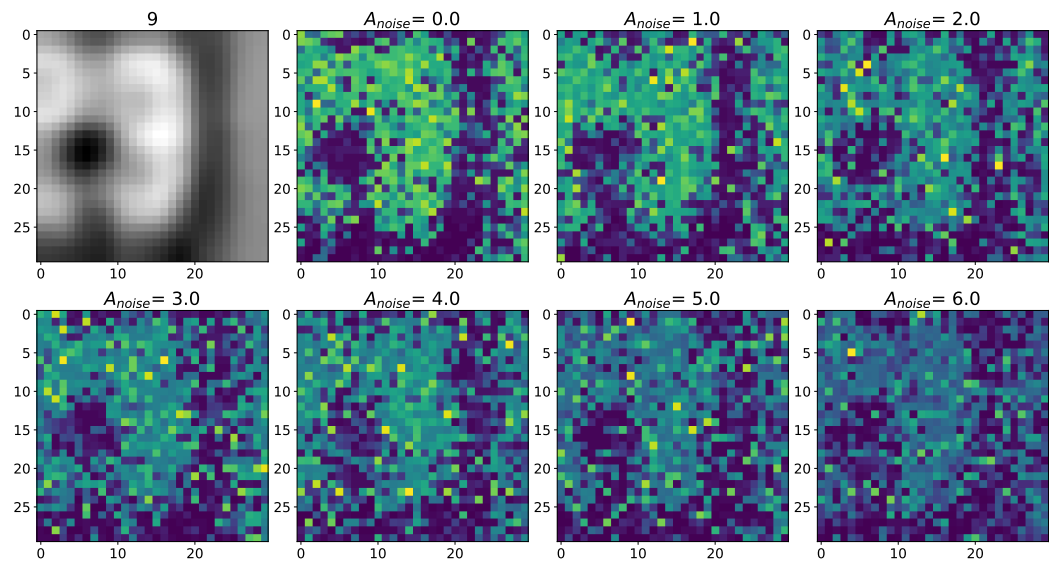


**Figure S82.** Changes in the spatial sweep of the spike neural network during the representation of the supplied image 9 from database SVHN [3] when the amplitude,  $A_{noise}$ , of the noise current,  $I_{noise}$ , changes from 0 to 6 without modulation of neuronal activity by astrocytes.

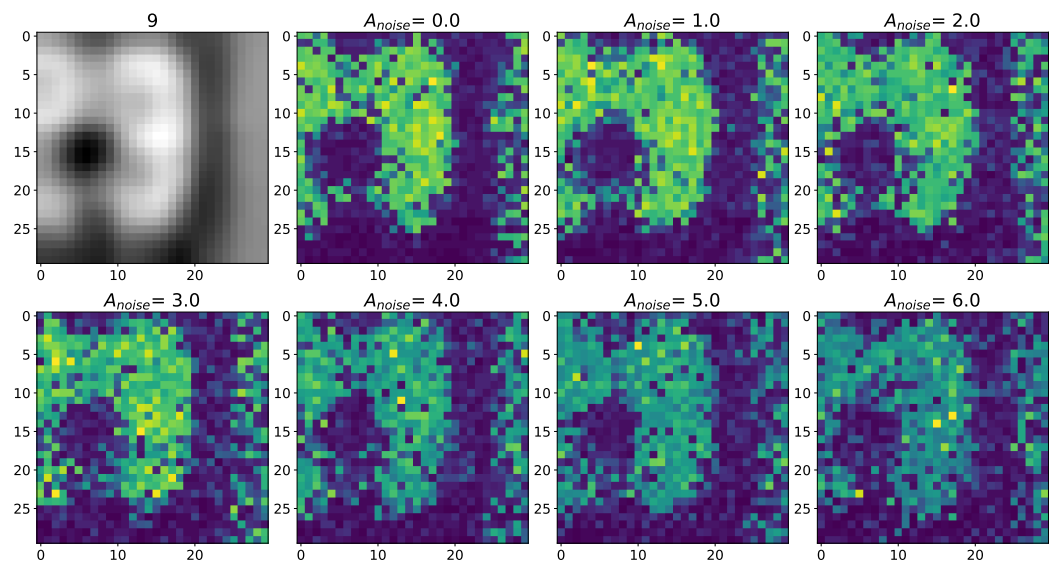


**Figure S83.** Changes in the spatial sweep of the spike neural network during the representation of the supplied image 9 from database SVHN [3] when the amplitude,  $A_{noise}$ , of the noise current,  $I_{noise}$ , changes from 0 to 6 with modulation of neuronal activity by astrocytes.

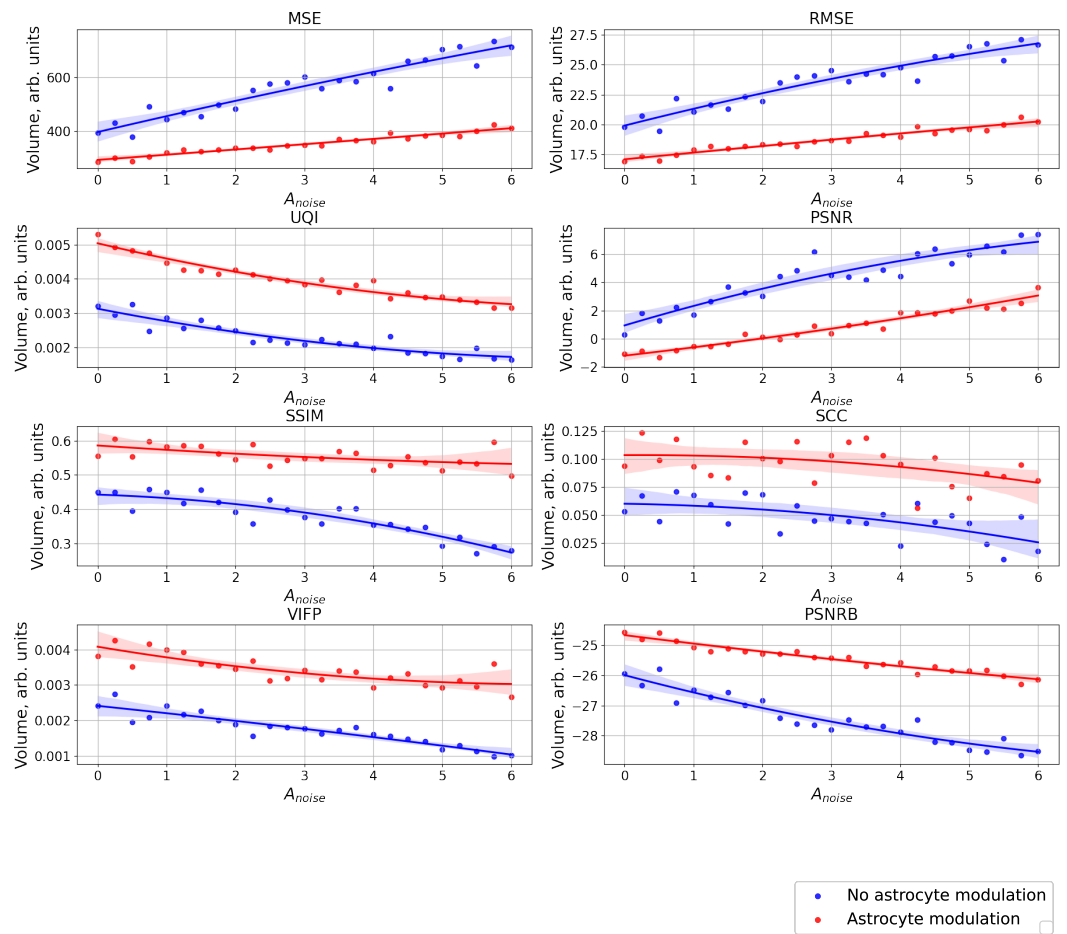


**Figure S84.** The case of using a quality metrics (MSE, RMSE, UQI, PSNR, SSIM, SCC, VIFP, PSNRB) for comparing raster diagrams of neural activity from Figure S82 and Figure S83 with an image 9 from database SVHN [3] fed to a spike neural network with an increase in the amplitude,  $A_{noise}$ , of the noise signal from 0 to 6 supplied to the neurons of the neural network without astrocytic modulation (blue dots and curve) and with astrocytic modulation (red dots and curve).

**References**

1. LeCun, Y.; Cortes, C.; Burges, C. MNIST Handwritten Digit Database. 2010. Available online: <http://yann.lecun.com/exdb/mnist> (accessed on 1 November 2022).
2. Xiao, H.; Rasul, K.; Vollgraf, R. Fashion-mnist: a novel image dataset for benchmarking machine learning algorithms. *arXiv* **2017**, arXiv:1708.07747.
3. Yang, R.; Deng, Y.; Zhu, A.; Tong, X.; Chen, Z. Few Shot Learning Based on the Street View House Numbers (SVHN) Dataset. In *International Conference on Edge Computing and IoT*; Springer: Cham, Switzerland, 2021; pp. 86–102.